



**Nuno Miguel Moura Espinha**

Degree in Biochemistry

**Bioprocess engineering of induced pluripotent stem cells for application in cell therapy and pre-clinical research**

Dissertation to obtain Master Degree in  
Biotechnology

Supervisor: Dr. Maria Margarida de Carvalho Negrão Serra,  
IBET/ITQB-UNL

Co-Supervisor: Dr. Ana Teresa de Carvalho Negrão Serra,  
IBET/ITQB-UNL

Jury:

President: Prof. Dr. Pedro Miguel Ribeiro Viana Baptista

Examiner: Prof. Dr. Maria Alexandra Nuncio de Carvalho Ramos Fernandes

Supervisor: Dr. Maria Margarida de Carvalho Negrão Serra



FAÇULDADE DE  
CIÊNCIAS E TECNOLOGIA  
UNIVERSIDADE NOVA DE LISBOA

January, 2014





**Nuno Miguel Moura Espinha**

Degree in Biochemistry

**Bioprocess engineering of induced pluripotent stem cells for application in cell therapy and pre-clinical research**

Dissertation to obtain Master Degree in  
Biotechnology

Supervisor: Dr. Maria Margarida de Carvalho Negrão Serra,  
IBET/ITQB-UNL

Co-Supervisor: Dr. Ana Teresa de Carvalho Negrão Serra,  
IBET/ITQB-UNL

Jury:

President: Prof. Dr. Pedro Miguel Ribeiro Viana Baptista

Examiner: Prof. Dr. Maria Alexandra Nuncio de Carvalho Ramos Fernandes

Supervisor: Dr. Maria Margarida de Carvalho Negrão Serra



FAÇULDADE DE  
CIÊNCIAS E TECNOLOGIA  
UNIVERSIDADE NOVA DE LISBOA

January, 2014



## **Copyright**

### **Bioprocess engineering of induced pluripotent stem cells for application in cell therapy and pre-clinical research**

Nuno Miguel Moura Espinha, FCT/UNL, UNL

A Faculdade de Ciências e Tecnologia e a Universidade Nova de Lisboa têm o direito, perpétuo e sem limites geográficos, de arquivar e publicar esta dissertação através de exemplares impressos reproduzidos em papel ou de forma digital, ou por qualquer outro meio conhecido ou que venha a ser inventado, e de a divulgar através de repositórios científicos e de admitir a sua cópia e distribuição com objetivos educacionais ou de investigação, não comerciais, desde que seja dado crédito ao autor e editor.



## Acknowledgements

I would like to acknowledge all the people directly or indirectly involved in this thesis.

To Dr. Paula Alves, for giving me the opportunity to do my master thesis at the Animal Cell Technology Unit at ITQB/IBET, for the good working conditions offered and for being a strong example of leadership and professionalism.

To Dr. Margarida Serra, for her guidance, constant encouragement and support. I am grateful to her for inspiring me with her persistence, critical thinking, perfectionism and the motivation demonstrated throughout this whole work. Also, I would like to thank the chance of having attended the international conference “Stem Cells for Drug Screening and Regenerative Medicine” that positively contributed to my scientific formation.

To Dr. Ana Teresa Serra, for her kindness, constant good mood and, most of all, for her guidance during the development of the cell-based cardiotoxicity and cardioprotective assays presented in this work.

To Dr. Tomo Saric and his group for providing the Murine transgenic  $\alpha$ PIG-iPS cell line, the starting point for this whole thesis, and for the support in RT-PCR and electrophysiology analysis. Also, I would like to thank Yuri Lages for his support during the perfusion bioreactors developed in this work.

To Marcos Sousa, for the constant availability, encouragement and all the advices with the environmentally controlled bioreactor processes. Also, to João Clemente, for his good mood and help during wave bioreactor cultures.

To Cláudia Correia, for having taught the majority of what I learned during this year and for always being there when it was most needed. A special thanks for her confidence, constant support, encouragement, scientific discussions and for being a good friend throughout the year.

To all the ACTU colleagues, for the good working environment, friendship and help during this year.

To my family, for all the support and understanding during all my academic formation. A special thanks to my mother for all the well prepared meals which I brought with me to work every day.

A special thanks to all my close friends and ITQB/IBET colleagues, for the hours of relaxation, and friendship. They were a huge support during this year.

And finally, to Joana, for all the waiting hours, for always being there for me, for the companionship, strength and motivation she gives me every day. Also, for her unconditional support, strong personality and for advising me whenever it is needed.





## Preface

This work was performed at the Animal Cell Technology Unit, IBET and ITQB-UNL, within the scope of the project “CAREMI - Cardio Repair European Multidisciplinary Initiative” (HEALTH-F5-2010-242038), funded by the European Union (EU).

Part of this work has been included in poster communications and a submitted article.

## Poster Communications

- Correia C, Serra M, Sousa M, Espinha N, Brito C, Burkert K, Fatima A, Hescheler J, Carrondo MJT, Saric T, Alves PM (2013). “Novel Scalable Platforms for the Production of iPSC-derived Cardiomyocytes”. 1st International Meeting on Stem Cells for Regenerative Medicine and Drug Screening, Cantanhede, Portugal.
- Correia C, Serra M, Sousa M, Espinha N, Brito C, Burkert K, Fatima A, Hescheler J, Carrondo MJT, Saric T, Alves PM (2013). “Novel Scalable Platforms for the Production of pure Cardiomyocytes derived from iPSC”. ESACT Meeting in Lille, France.
- Correia C, Serra M, Sousa M, Espinha N, Brito C, Burkert K, Fatima A, Hescheler J, Carrondo MJT, Saric T, Alves PM (2013). “Improving the Production of Cardiomyocytes derived from iPSC for cardiac cell-based therapies”. Cardiac Biology - From Development to Regenerative Medicine Symposium. EMBL Heidelberg, Germany.
- Correia C, Serra M, Sousa M, Espinha N, Brito C, Burkert K, Fatima A, Hescheler J, Carrondo MJT, Saric T, Alves PM (2013). “Novel Scalable Platforms for the Production of pure Cardiomyocytes derived from iPSC”. 8th International Meeting of the Portuguese Society for Stem Cells and Cell Therapies, Faro, Portugal.
- Correia C, Serra M, Espinha N, Sousa M, Brito C, Burkert K, Fatima A, Hescheler J, Carrondo MJT, Saric T, Alves PM (2014). Towards Scalable Production and Cryopreservation of Functional iPSC-derived Cardiomyocytes. Scale-up and Manufacturing of Cell-based Therapies III, San Diego, California, USA.

## Submitted Article

Article submitted to Stem Cell Reviews and Reports (January, 2014)

- Cláudia Correia, Margarida Serra, Nuno Espinha, Marcos Sousa, Catarina Brito, Karsten Burkert, Yunjie Zheng, Jürgen Hescheler, Manuel J.T. Carrondo, Tomo Šarić, Paula M. Alves. “Combining hypoxia with a cyclic strain-rich environment in bioreactors boosts induced pluripotent stem differentiation towards the cardiomyocyte lineage”



## Abstract

The production of cardiomyocytes (CMs) from induced pluripotent stem cells (iPSCs) presents great potential for patient-specific regenerative therapies and cardiotoxicity drug evaluation. The successful translation of iPSCs to these fields requires the development of robust bioprocesses capable of producing CMs in high quality, quantity and purity. Traditional protocols for CM differentiation of iPSCs lack control and robustness and are thus inefficient. Furthermore, efficient cryopreservation and hypothermic storage strategies are a demand, as cell banking and transport is a prerequisite for clinical and industrial applications. The main aim of this thesis was the evaluation of different bioreactor systems for the production and purification of miPSC-derived CMs. Novel strategies for CM cryopreservation were tested. Also, CMs were used to study the cardioprotective effect of antioxidant compounds.

The wave bioreactor was the most suitable system for CM differentiation, allowing high differentiation yields (60 CMs/input of miPSC) and the production of clinically relevant numbers of CMs ( $2.3 \times 10^9$  CMs), simultaneously reducing bioprocess duration when compared to stirred tank bioreactors. Produced CMs presented typical structural and functional features. Moreover, CryoStor™CS10 and FBS+10%DMSO (with ROCKi pretreatment) revealed to be suitable solutions for cryopreservation of miPSC-derived CMs, achieving high cell recoveries after thawing. In addition, HypoThermosol®-FRS enabled hypothermic storage of CMs for up to 7 days. Finally, it was shown that CMs derived from miPSCs present potential to be used in the development of cardioprotective assays.

This work demonstrates the establishment of a fully integrated bioprocess, capable of producing high quality miPSC-derived CMs in environmentally controlled bioreactors and ensuring efficient cryopreservation and storage of the produced cells. Hopefully, the knowledge acquired with this work can be translated to human iPSCs, presenting a relevant step forward towards the application of human CMs to clinical and industrial applications, such as cardiac regeneration, disease modeling and cardiotoxicity and cardioprotective cell-based assays.

**Key Words:** induced Pluripotent Stem Cells (iPSCs); cardiomyocyte differentiation; 3D culture; environmentally controlled bioreactors; cryopreservation; cardioprotection cell-based assays



## Resumo

A produção de cardiomiócitos (CMs) derivados de células estaminais pluripotentes induzidas (iPSCs) apresenta grande potencial para terapias regenerativas e avaliação de drogas cardiotoxícas. A transferência de iPSCs para estas aplicações necessita do desenvolvimento de bioprocessos robustos e capazes de produzir CMs de elevada qualidade, quantidade e pureza. Protocolos tradicionais para diferenciação de iPSCs em CMs revelam falta de controlo e robustez sendo inefficientes. Além disso, são necessárias estratégias efficientes de criopreservação e armazenamento hipotérmico, sendo que a formação de bancos de células e transporte é um pré-requisito para aplicações clínicas e industriais. O principal objetivo desta tese foi a avaliação de diferentes sistemas de biorreatores para a produção e purificação de CMs derivados de miPSCs. Foram avaliadas novas estratégias para criopreservação de CMs. Ainda, CMs foram utilizados para estudar o efeito cardioprotector de compostos antioxidantes.

O biorreator wave foi o sistema mais apropriado para a diferenciação de CMs, permitindo elevados rendimentos de diferenciação (60 CMs/miPSCs) e a produção de números clinicamente relevantes de CMs ( $2.3 \times 10^9$  CMs), simultaneamente reduzindo a duração do bioprocessos quando comparado a biorreatores de tanque agitado. Os CMs produzidos apresentavam estrutura e funcionalidades típicas. Além disso, Cryostor™CS10 e FBS+10%DMSO (pre-tratado com ROCKi) revelaram ser soluções adequadas para a criopreservação de CMs, atingindo recuperações celulares elevadas após descongelamento. Ainda, HypoThermosol®FRS permitiu um armazenamento hipotérmico de CMs até 7 dias. Por último, foi demonstrado que CMs derivados de miPSCs apresentam potencial para serem usados no desenvolvimento de ensaios cardioprotectores.

Este trabalho demonstrou o estabelecimento de um bioprocessos integrado, capaz de produzir elevadas quantidades de CMs derivados de miPSCs em biorreatores controlados e assegurando criopreservação e armazenamento eficazes das células produzidas. Esperançosamente, o conhecimento adquirido neste trabalho pode ser transferido para iPSCs humanas, sendo um passo relevante para a utilização de CMs humanos para aplicações clínicas ou industriais, tais como, regeneração cardíaca, modelos de doenças e ensaios celulares de cardiotoxicidade e cardioprotecção.

**Palavras-chave:** células estaminais pluripotentes induzidas (iPSCs); diferenciação de cardiomiócitos; cultura 3D; biorreatores; criopreservação; ensaios celulares de cardioprotecção.



## List of Abbreviations

<b>AFP</b>	Alpha-fetoprotein
<b>ALCAM</b>	Activated leukocyte cell adhesion molecule
<b>ANP</b>	Atrial natriuretic peptide
<b>AP</b>	Alkaline phosphatase
<b>AP</b>	Action potential
<b>bFGF</b>	basic fibroblast growth factor
<b>BMP</b>	Bone morphogenic protein
<b>BR</b>	Bioreactor
<b>BSA</b>	Bovine serum albumin
<b>Cch</b>	Carbachol
<b>CCD</b>	Charged-coupled device
<b>cDNA</b>	complementary deoxyribonucleic acid
<b>CMs</b>	Cardiomyocytes
<b>CPA</b>	Cryoprotective agents
<b>CS10</b>	Cryostor CS10 solution
<b>cTnT</b>	cardiac troponin T
<b>Ct's</b>	Cycle threshold
<b>CVD</b>	Cardiovascular diseases
<b>DMEM</b>	Dulbecco modified Eagle medium
<b>DMSO</b>	Dimethyl sulfoxide
<b>DO</b>	Dissolved oxygen
<b>DKK1</b>	Dickkopf homolog 1
<b>EB</b>	Embryoid body
<b>ECM</b>	Extracellular matrix
<b>EDTA</b>	Ethylenediamine tetraacetic acid
<b>eGFP</b>	enhanced green fluorescent protein
<b>ESCs</b>	Embryonic stem cells
<b>FACS</b>	Fluorescence-activated cell sorting
<b>FBS</b>	Fetal bovine serum
<b>FDA</b>	Fluorescein diacetate
<b>FDA</b>	Food and Drug Administration
<b>FGFs</b>	Fibroblast growth factors
<b>FI</b>	Fold increase
<b>GAPDH</b>	Glyceraldehyde-3-Phosphate Dehydrogenase
<b>GFP</b>	Green fluorescent protein
<b>GMP</b>	Good manufacturing practices
<b>HCN4</b>	Hyperpolarization activated cyclic nucleotide-gated potassium channel 4
<b>HTS</b>	HypoThermosol solution
<b>IgG</b>	Immunoglobulin G
<b>IgM</b>	Immunoglobulin M
<b>IMDM</b>	Iscove's modified Dulbecco's medium
<b>iPSCs</b>	induced pluripotent stem cells
<b>Iso</b>	Isoproterenol

<b>LDH</b>	Lactate dehydrogenase
<b>LDS</b>	Late development stage
<b>LIF</b>	Leukemia inhibitory factor
<b>LN<sub>2</sub></b>	Liquid nitrogen
<b>MACS</b>	Magnetic-assisted cell separation
<b>MDP</b>	Maximum diastolic potential
<b>MEFs</b>	Murine embryonic fibroblasts
<b>MEM- NEAA</b>	Minimum essential medium – non-essential amino acids
<b>MI</b>	Myocardial infarction
<b>miPSCs</b>	murine induced pluripotent stem cells
<b>Myl2</b>	Myosin light chain, ventricular isoform
<b>Myl7</b>	Myosin light chain, atrial isoform
<b>NADH</b>	Nicotinamide adenine dinucleotide
<b>Nkx2.5</b>	Nk2 transcription factor related locus 5
<b>Oct-4</b>	Octamer-4 transcription factor
<b>PBS</b>	Phosphate buffered saline
<b>PBS</b>	Pneumatic Bioreactor System
<b>Pen/Strep</b>	Penicillin-streptomycin
<b>PFA</b>	Paraformaldehyde
<b>PGI<sub>2</sub></b>	Prostaglandin I <sub>2</sub>
<b>PI</b>	Propidium iodide
<b>PSCs</b>	Pluripotent stem cells
<b>RNA</b>	Ribonucleic acid
<b>ROCKi</b>	Rho-associated kinase inhibitor
<b>ROS</b>	Reactive oxygen species
<b>RT-PCR</b>	Real time-polymerase chain reaction
<b>RT-qPCR</b>	Real time-quantitative polymerase chain reaction
<b>SIRPA</b>	Signal-regulatory protein alpha
<b>SSEA-1</b>	Stage-specific embryonic antigen-1
<b>T-Bra</b>	T Brachyury
<b>TGF-<math>\beta</math></b>	Transforming growth factor $\beta$
<b>TMRM</b>	Tetramethylrhodamine methyl ester perchlorate
<b>VCAM1</b>	Vascular adhesion molecule 1
<b>Vdd</b>	Velocity of diastolic depolarization
<b>VEGF</b>	Vascular endothelial growth factor
<b>Vmax</b>	Maximum velocity of depolarization
<b>Vvm</b>	Volume of gas flow per volume of culture medium per minute
<b>WB</b>	Washing buffer
<b>WNT</b>	Wingless/INT
<b><math>\alpha</math>-MHC</b>	$\alpha$ -myosin heavy chain
<b>2D</b>	Two-dimensional
<b>3D</b>	Three-dimensional



## Table of Contents

1. Introduction.....	1
1.1 Stem cell-based therapies for cardiac repair .....	1
1.1.1 Pluripotent stem cells: ESCs vs iPSCs.....	2
1.2 Cardiomyocyte differentiation.....	5
1.2.1 Understanding cardiac differentiation.....	5
1.2.2 Embryoid body formation.....	7
1.2.3 Co-culture of PSCs with END2 cells.....	8
1.2.4 Guided differentiation with growth factors and small molecules.....	9
1.2.5 Guided differentiation promoted by cyclic strains & oxygen.....	10
1.2.6 Scalable production of cardiomyocytes derived from PSCs .....	11
1.3 Purification of iPSC-derived cardiomyocytes .....	16
1.3.1 Genetic selection of cardiomyocytes.....	16
1.3.2 Non-genetic purification of cardiomyocytes .....	17
1.4 Characterization of cardiomyocytes .....	18
1.5 Cryopreservation and storage of PSC-derived cardiomyocytes.....	20
1.6 PSC-derived cardiomyocytes as promising cell models for cardiotoxicity assays .....	22
2. Aim of the thesis .....	25
3. Materials and Methods.....	27
3.1 miPSC culture on feeder layers.....	27
3.2 miPSC differentiation in fully controlled bioreactors .....	27
3.2.1 miPSC differentiation in stirred tank bioreactor.....	27
3.2.2 Disposable single-use bioreactors.....	29
3.3 Cryopreservation and hypothermic storage of CMs derived from miPSC.....	30
3.3.1 Cryopreservation of 2D monolayers .....	31
3.3.2 Cryopreservation of 3D aggregates .....	31
3.3.3 Hypothermic storage of CMs derived from miPSC .....	31
3.3.4 Assessment of cell recovery of CMs .....	31
3.4 Cardiotoxicity and cardioprotective assays.....	32
3.5 Cell viability evaluation .....	32
3.6 Evaluation of aggregate concentration and size.....	33
3.7 Culture yields determination.....	33
3.8 Characterization of miPSCs and miPSC-derived CMs .....	34
3.8.1 Structural characterization.....	34
3.8.2 Functional characterization.....	36

3.9 Statistical analysis .....	36
4. Results and Discussion .....	37
4.1 Bioprocess engineering of miPSCs .....	37
4.1.1 Production of miPSC-derived CMs in fully controlled bioreactors.....	37
4.1.2 Development of a perfusion strategy in a stirred tank bioreactor .....	45
4.1.3 Structural and functional characterization of miPSC-derived CMs.....	48
4.2 Cryopreservation and hypothermic storage of miPSC-derived CMs.....	52
4.2.1 Cryopreservation of CMs as monolayers and aggregates .....	53
4.2.2 Hypothermic storage of CMs as monolayers and aggregates.....	58
4.2.3 Characterization of cryopreserved and hypothermically stored CM monolayers.....	59
4.3 Evaluation of the potential of miPSC-derived CMs to be used in the development of cardioprotective cell-based assays.....	60
5. Conclusion .....	63
6. References .....	65
7. Annexes.....	77

## List of Figures

<b>Figure 1.1:</b> Causes of death in Europe, 2011 (adapted from [2]) .....	1
<b>Figure 1.2:</b> Stem cell sources, pluripotency potential and generation of iPSCs .....	3
<b>Figure 1.3:</b> Schematic representation depicting sequential steps required for obtaining PSC-derived cardiomyocytes .....	6
<b>Figure 1.4:</b> Current methods for cardiac differentiation of human PSCs .....	7
<b>Figure 1.5:</b> 2D and 3D strategies for cultivation of PSCs (adapted from [15]) .....	12
<b>Figure 1.6:</b> Examples of different bioreactor designs used for stem cell bioprocessing.....	13
<b>Figure 1.7:</b> Basic characterization of PSC-derived cardiomyocytes.....	19
<b>Figure 1.8:</b> Main steps composing common cryopreservation procedure for mammalian cells.....	21
<b>Figure 2.1:</b> Thesis rational.....	25
<b>Figure 3.1:</b> Perfusion apparatus used in continuous perfusion experiments .....	29
<b>Figure 4.1:</b> Characterization of miPSCs.....	37
<b>Figure 4.2:</b> miPSCs aggregation step .....	39
<b>Figure 4.3:</b> miPSC differentiation into CMs using different bioreactor systems.....	39
<b>Figure 4.4:</b> Production of miPSC-derived CMs using fully controlled bioreactors .....	41
<b>Figure 4.5:</b> Evaluation of gene expression and levels of eGFP positive cells during CM production in Stirred Tank and Wave BRs.....	43
<b>Figure 4.6:</b> Production of miPSC-derived CMs using a continuous perfusion strategy .....	46
<b>Figure 4.7:</b> Structural characterization of miPSC-derived CMs produced in Stirred Tank and Wave BRs. .	48
<b>Figure 4.8:</b> Functional characterization of miPSC-derived CMs produced in Stirred Tank and Wave BRs. .	49
<b>Figure 4.9:</b> Effect of cryopreservation medium on miPSC-derived CM viability after cryopreservation of CM monolayers.....	53
<b>Figure 4.10:</b> Effect of cryopreservation medium on miPSC-derived CM viability after cryopreservation of cardiospheres.....	55
<b>Figure 4.11:</b> Hypothermic storage of miPSC-derived CMs as monolayers and cardiospheres.....	58
<b>Figure 4.12:</b> Structural characterization of cryopreserved and hypothermically stored CM monolayers..	59
<b>Figure 4.13:</b> Effect of oxidative stress and antioxidant pretreatment on CMs .....	60
<b>Figure 7.1:</b> Bioreactor design adverse effects of miPSC aggregate culture .....	78



## List of Tables

<b>Table 1.1:</b> Major challenges and potential solutions facing the use of iPSCs for cardiac repair (adapted from [4]) .....	5
<b>Table 1.2:</b> Studies involving cultivation of mESCs in scalable 3D approaches involving expansion and differentiation into cardiomyocytes. ....	16
<b>Table 1.3:</b> Cardiac markers used for the characterization of cardiomyocytes (adapted from [54]).....	18
<b>Table 3.1:</b> Dilution rates tested in the continuous perfusion system approach. ....	29
<b>Table 4.1:</b> Quantitative characterization of CM production derived from miPSCs using environmentally controlled bioreactors.....	44
<b>Table 4.2:</b> Action potential parameters for CMs obtained from Stirred Tank and Wave BRs.....	50
<b>Table 7.1:</b> List of primers used for semiquantitative and quantitative RT-PCR analysis.....	77



## 1. Introduction

### 1.1 Stem cell-based therapies for cardiac repair

Cardiovascular diseases (CVD) are one of the major causes of death worldwide, accounting for 17.3 million deaths per year [1]. In Europe, they are responsible for 47% of all deaths issues (Figure 1.1) [2]. In particular, myocardial infarction (MI) results in massive cardiac loss, where up to a billion cardiomyocytes (CMs) die resulting in loss of contractility and decreased heart function [3]. Upon injury, the adult heart is endowed of some endogenous regenerative capacity, provided by resident cardiac stem cells. However this endogenous regenerative capacity is limited as fully differentiated cardiomyocytes can no longer proliferate and replace degenerated tissue [4].

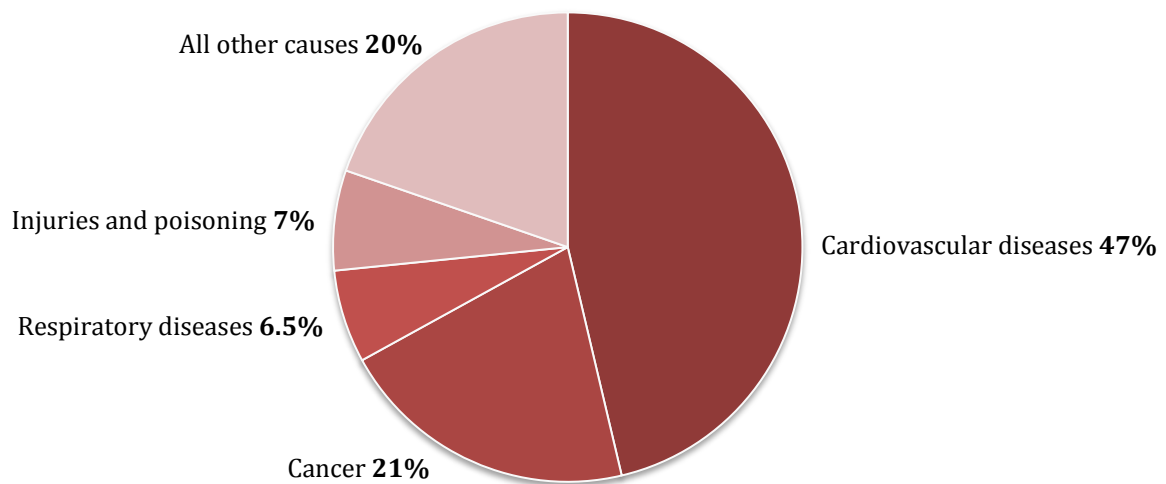


**Figure 1.1: Causes of death in Europe, 2011 (adapted from [2]).**

Cardiac repair (replacement, restoration and regeneration) is thus essential to restore heart function following MI [5]. Heart transplantation remains as the only long term treatment available, even though limited due to high costs, shortage of donor organs and possible immunological rejection [6, 7]. As new therapies are still a need, emerging technologies such as cell-based therapies intend to restore heart function by two experimental approaches: enhancement of endogenous heart regeneration [8] and transplantation of exogenous cells to repopulate the heart [9]. Notably, combining both strategies would certainly provide a better alternative for therapies aiming at restoring heart function [3].

Many cell types have been examined as potential cell sources for cell therapy such as endothelial progenitor cells, cardiac progenitor cells, mesenchymal stem cells derived from bone marrow and pluripotent stem cells (PSCs) (reviewed in [10]). The majority of stem cell therapies in cardiac disease involve bone-marrow derived cells. Currently, companies such as

Baxter, Cardio3 Biosciences or Mesoblast are using this cell source in advanced stages of clinical trials (phase 3) [11]. Most candidate cell types improve ventricular function, however show limited or no potential to produce cardiomyocytes [4]. The ideal cell source for heart transplantation would be a proliferative cell with potential to generate all the different cells of the heart [3]. PSCs meet these standards, proliferate indefinitely and differentiate into all cell types of the body (except for extra-embryonic tissues), thus being a potential candidate for stem cell therapies in cardiac repair [3].

### 1.1.1 Pluripotent stem cells: ESCs vs iPSCs

Murine embryonic stem cells (ESCs) were first isolated in 1981 [12] and their human counterparts were derived by Thomson in 1998 [13]. ESCs were isolated from the inner cell mass of blastocysts, pre-implanted embryos at day 5 of embryonic development (Figure 1.2). Blastocysts comprise an outer layer of cells (trophoectoderm) and an inner cell mass. ESCs are derived by removing the outer layer and isolating the inner cell mass [14].

ESCs can give rise to all cell types of the body, i.e. all three germ layers: endoderm, ectoderm and mesoderm, and are thus called pluripotent. These cells present high self-renewal capacity as they can proliferate continuously giving rise to undifferentiated cells [15]. ESCs were the first stem cell source that could reliably give rise to cardiomyocytes *in vitro* (reviewed in [4]). Despite their enormous potential for cell-based therapies, ESCs are inevitably associated with ethical considerations due to the manipulation of embryos, are technically difficult to derive and still present limitations for clinical applications, such as immune rejection and possible teratoma formation (cell tumor containing tissue components of the three germ layers) (reviewed in [3]).

Cell differentiation was recently shown to be a dynamic reversible process. In 2006, Yamanaka and co-workers were able to reprogram mature cells to a pluripotent state [16]. The reverted cells were called induced pluripotent stem cells (iPSCs) and are generated by reversing somatic cells to a state of pluripotency (embryonic-like state) by the induced expression of specific reprogramming factors [17]. This insight has influenced all areas of medicine and physiology, and was awarded the Nobel Prize in Physiology or Medicine in 2012 (to Dr. John B. Gurdon and Dr. Shinya Yamanaka) for the discovery that mature, differentiated cells can be reprogrammed to a pluripotent stem cell state.

As mentioned above, the first study on derivation of iPSCs from murine fibroblast was reported by Takahashi and Yamanaka in 2006, [16]. In this study, 4 transcription factors (*Oct-4*, *Sox2*, *Klf4* and *c-Myc*) were stated as being the minimal required for maintenance of pluripotency and capable of yielding cells with characteristics similar to ESCs. After iPSC formation, reprogramming factors are usually inactivated. Occasional reactivation of specific



factors can give rise to tumor formation after transplantation [18]. Therefore, in a later study reported by Thomson and co-workers, *c-Myc* and *Klf4*, well known proto-oncogenes, were replaced by *Nanog* and *Lin28* [19]. It has also been shown that combinations of all these 6 factors are also able to generate iPSCs [7, 19].

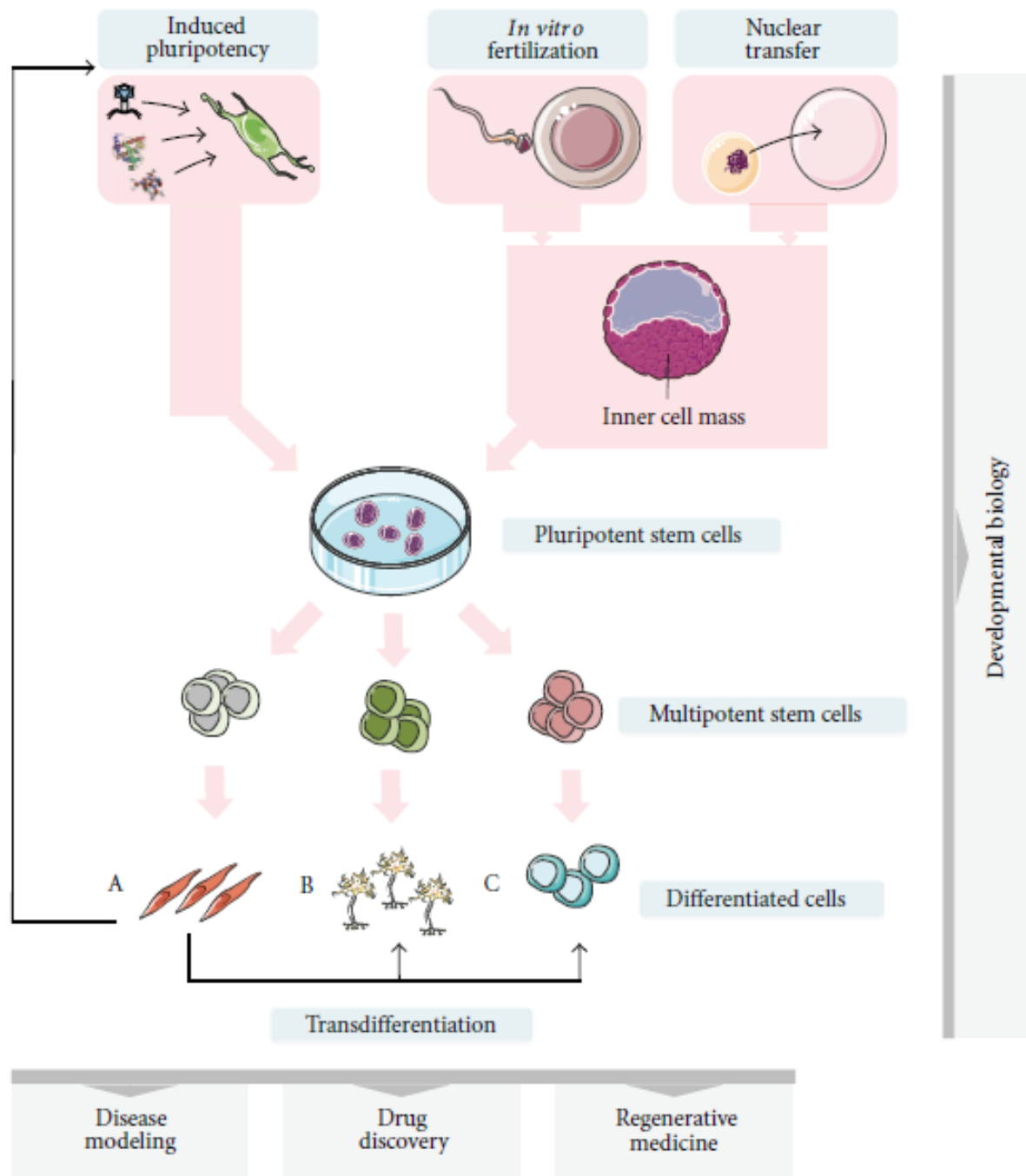


**Figure 1.2: Stem cell sources, pluripotency potential and generation of iPSCs.** ESCs are isolated from early embryos obtained by *in vitro* fertilization or nuclear transfer, and generating more specialized cells (pink arrows). Reprogramming technologies allow generation of iPSCs from mature cells, or lineage conversion between differentiated cell types (black arrows). Stem cells and their differentiated progeny are used in a variety of applications, such as disease modeling, drug discovery, and regenerative medicine [20].

The first reprogramming protocols relied on the use of integrating vectors to deliver desired transgenes into the genome of somatic cells. These integrating vectors were mainly retroviral or lentiviral [21, 22]. Even though reprogramming was possible, random transgene insertion could interrupt existing genes causing tumor formation (after transplantation) and disturb the maintenance of the cells undifferentiated state. This approach presents other drawbacks such as low stability, difficult cellular targeting and possible insertion of mutagenesis [23]. To overcome these limitations and establish safer iPSC lines, - methods that allow the expression of pluripotency genes without integrating host genome are currently being explored. For example, non-integrated virus (e.g. adenoviruses, baculoviruses) have been used, despite suffering from low efficiencies [21]. Virus-free reprogramming can also be achieved by using episomal vectors or excisable transposon systems (e.g. PiggyBac or Cre/*loxP* systems), which integrate the cells but can be removed by transposase, without leaving genetic material behind (reviewed in [21, 24]). Other techniques for the generation of safer iPSC lines include the use of exogenous plasmids, protein factors, small molecules and microRNAs. Nuclear reprogramming has been shown to be an inefficient process. However, a novel method for reprogramming is able to successfully revert cells to a pluripotent state, by deleting the *Mbd3* gene, which is an important epigenetic regulator that restricts expression of pluripotency genes. This method shows reprogramming efficiencies near 100% for mouse and human cells [25].

In the last few years, iPSCs are boosting the field of regenerative medicine, offering numerous advantages over adult stem cells and ESCs [3]. iPSCs can circumvent the need for embryo use, being ethically less controversial, and thereby could potentially replace ESCs. Also, differentiated cells derived from iPSCs have recently been shown to present limited immunogenicity and could therefore be used in autologous [26] (patient specific) or allogeneic therapies (universal donor-derived cells). iPSC-derived cardiomyocytes have tremendous potential to be used in cardiac repair strategies.

Although recent approaches have proved promising, there are still challenges to overcome in order to transfer PSCs to clinical applications. Selection of the adequate cell source is crucial, namely whether to use autologous or allogenic therapies. Quantity and purity of cells are essential for successful therapies, minimizing tumorigenic potential of transplantation. Also, quality is a requirement, assuring the desired phenotype and potency of the chosen cell source (reviewed in [15]).

Table 1.1 summarizes the major challenges and solutions facing the use of iPSCs in cardiac repair.

**Table 1.1: Major challenges and potential solutions facing the use of iPSCs for cardiac repair (adapted from [4])**

Hurdles	Possible solutions
Heterogeneous population of differentiated cells	- Directed cardiac differentiation - Specific selection of cardiomyocytes
Low cardiomyocyte yield	- Directed cardiac differentiation - Upscaling differentiation process
Survival, integration and maturation of cell-grafts <i>in vivo</i>	- Cell delivery approaches - Tissue engineering strategies - Genetic modifications
Tumorigenic potential	- Integration-free iPSCs generation - c-Myc-free reprogramming strategies - Appropriate selection process
Risk of genetic modifications	- Genetic screening of undifferentiated iPSCs

## 1.2 Cardiomyocyte differentiation

### 1.2.1 Understanding cardiac differentiation

Cardiomyocyte differentiation of stem cells recapitulates aspects of cardiogenesis *in vivo*, which involves complex processes highly controlled by positive and negative molecular signals that guide stem cells towards cardiac fate [27]. As molecular mechanisms in human cardiogenesis are still not thoroughly known, cardiac development in animal models (e.g. mouse) has provided valuable information to improve *in vitro* cardiomyocyte differentiation protocols (reviewed in [28]). Understanding how the cardiac lineage is established in these models is crucial for developing efficient differentiation protocols. Cardiomyocyte differentiation of murine iPSCs (miPSCs) was first described by Mauritz et al. [29] who utilized the embryoid body (EB) system to obtain cardiomyocytes.

The mammalian heart is the first organ developed in embryogenesis and consists of three mesodermal cell types: endothelial cells, vascular smooth muscle cells and cardiomyocytes [30]. Cardiomyogenesis consists of four consecutive steps: i) mesoderm formation, ii) mesoderm patterning toward anterior mesoderm or cardiogenic mesoderm, iii) cardiac mesoderm formation and iv) cardiomyocyte maturation [31]. Cardiac development is a dynamic process controlled by sequential expression of multiple signal transduction proteins and transcription factors. Major signaling pathways have been implicated with cardiac subtypes development, such as wingless/INT (WNTs) [32], nodal ([33]), bone morphogenic proteins (BMPs) [34] and fibroblast growth factors (FGFs) [35]. During

gastrulation (formation of gastrula in early embryonic development) signals mediated through WNT/ $\beta$ -catenin and transcription growth factor  $\beta$  (TGF- $\beta$ ) family members promote differentiation of ESCs into mesoderm (reviewed in [36]). However, following mesodermal induction, WNT/ $\beta$ -catenin signaling inhibits cardiac differentiation and may redirect cells to alternate mesodermal fates. This signaling pathway has a biphasic role during cardiac differentiation in mouse ESCs, being procardiac prior to primitive streak formation and presenting an antagonizing role thereafter (reviewed in [36]). Due to this biphasic effect during cardiac differentiation, the timing of the addition of specific cardiac factors is crucial and must be carefully optimized in order to efficiently drive PSCs to a cardiac cell fate. Figure 1.3 presents a schematic overview of the steps required for obtaining PSC-derived cardiomyocytes and typical markers expressed in each phase.

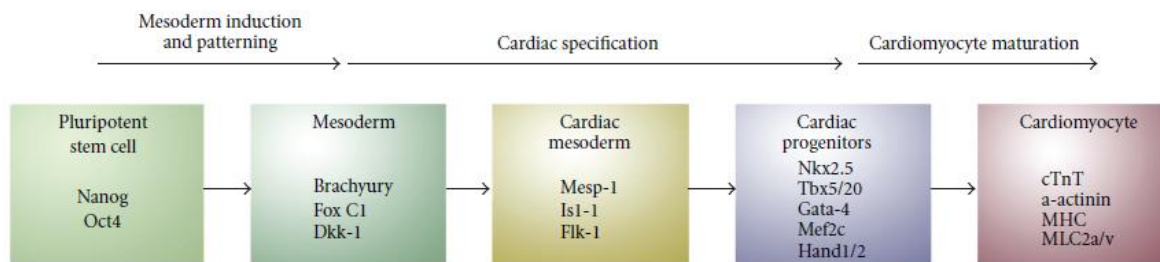


**Figure 1.3: Schematic representation depicting sequential steps required for obtaining PSC-derived cardiomyocytes.** Early mesoderm differentiates via cardiac mesoderm and committed cardiac progenitors to functional beating cardiomyocytes. Typical markers for each step are also indicated [37].

Currently, the main approaches for cardiomyocyte differentiation of PSCs are spontaneous differentiation through embryoid body (EB) formation, co-culture with cells presenting cardiac inductive activity and guided differentiation strategies (induced by environmental factors) (reviewed in [3]). Figure 1.4 presents a schematic overview of current differentiation methods used for generating PSC-derived cardiomyocytes.

Monolayers-based methods are the simplest approach for cardiomyocyte differentiation. PSCs are plated on an extracellular matrix (ECM) or on a top of a monolayer of feeder cells. These methods are focused primarily on the timing of application and concentration of specific cardiac inductive growth factors (e.g. activin A and BMP4) (reviewed in [3]). Other monolayer-based methods have focused on overlaying PSCs with hydrogels or specific matrices [38], also called the matrix sandwich method. When combined with sequential application of growth factors, this approach has been reported to generate cardiomyocytes with high purity (up to 98%) [38]. Despite the increased efficiency of these protocols, cell-cell interactions in EBs can stimulate the expression of early cardiac markers (reviewed in [39]), which favors the use of 3D structures for cardiac differentiation, as described in the following section.

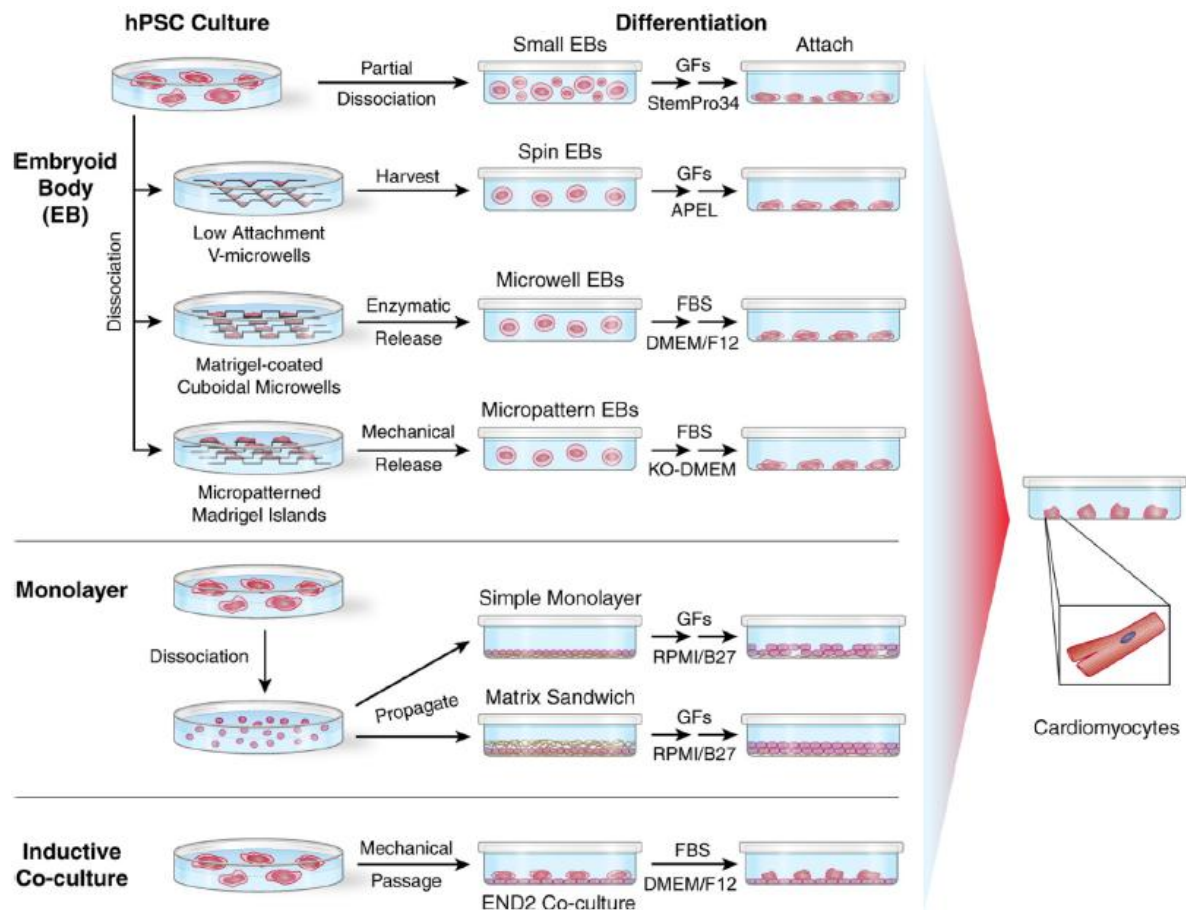


**Figure 1.4: Current methods for cardiac differentiation of human PSCs.** The 3 major approaches for differentiation of PSCs to cardiomyocytes are summarized: Embryoid bodies, monolayer cultures and inductive co-culture. StemPro34, APEL, DMEM/F12, KO-DMEM and RPMI/B27 are abbreviations of common culture medium formulations used for human PSC cultivation [40].

### 1.2.2 Embryoid body formation

When cultivated in non-adherent conditions (e.g. hanging drops, ultra low adherence culture plates) cells assembled into spheroids, capable of differentiating into derivatives of all three germ layers [41]. These three-dimensional (3D) aggregates are called embryoid bodies (EBs), because of their ability to recapitulate the early events of embryogenesis [42, 43]. EBs can spontaneously differentiate into contracting cardiomyocytes [44]. Early studies identified critical culture parameters to optimize *in vitro* cardiogenesis such as cell inoculum concentration, culture medium formulation (addition of serum or growth factors), culture strategy and time [45]. Spontaneous differentiation of PSC-derived cardiomyocytes in EBs is also highly dependent on cell line and is rather inefficient, usually yielding 10% of cardiomyocytes exhibiting beating areas [41, 46]. Regardless of these issues, this method is widely used for being simple and cost-effective [21].

Recent studies have shown that aggregate heterogeneity leads to adverse effects on differentiation efficiency and reproducibility [47]. To overcome this limitation, forced

aggregation methods have been one of the most used strategies to control EB formation and size. In this method, defined numbers of PSCs are centrifugated into U- or V-bottomed wells (Figure 1.4), leading to the formation of aggregates (also called spin EBs) with the same size in each well. Varying the number of cells per well allows the control of aggregate size with precision [48, 49]. This method is practical, reproducible and efficient. Engineered microwells (Figure 1.4) have also been used to form size-uniform EBs. It involves the microfabrication of microwells with defined sizes that are coated with an extracellular matrix, such as Matrigel, where cells attach and grow to fill the microwells. Removal of cell colonies from microwells results in cell aggregates (also called Microwell EBs) with defined sizes [50, 51]. However, microwells present reduced potential for scaling-up, requires appropriate and specialized technology and are currently not commercially available (reviewed in [40]). An alternative engineering approach is the use of micropatterned surfaces (Figure 1.4). In this approach, cells are cultivated on a micropatterned ECM (e.g. Matrigel) islands. Size of the colonies can be controlled by varying the size of these islands (e.g. 200 $\mu$ M, 400 $\mu$ M and 800 $\mu$ M) [47, 52]. Size-controlled EBs (Micropattern EBs) can be achieved after mechanical dissociation of colonies. Protocols for spontaneous differentiation of PSC via EB formation have been optimized aiming at improving cardiomyocyte differentiation yields, by adding specific growth factors in combination with defined medium formulations [40].

### **1.2.3 Co-culture of PSCs with END2 cells**

Another method for cardiomyocyte differentiation of stem cells is the co-culture of PSCs with a visceral endoderm-like cell line (END-2) derived from mouse P19 embryonal carcinoma cells [53]. This method was developed based on the discovery of cardiac inductive activity of endoderm in early embryonic studies (reviewed in [54]). The inductive effect of END-2 cells is not dependent on cell-cell contact, as studies have shown that conditioned media derived from END-2 culture is sufficient to induce cardiac differentiation of human ESCs (>10% cardiomyocytes) [55]. The presence of END-2 cells in culture causes rapid depletion of insulin, a common media supplement that inhibits cardiogenesis [56]. END-2 cells also produce significantly higher levels of prostaglandin I<sub>2</sub> (PGI<sub>2</sub>), a lipid molecule that enhances cardiac induction [56]. Co-culture of PSCs with END-2 cells is a simple and rapid protocol to differentiate hPSC into cardiomyocytes, as it requires few cells and generates cardiomyocytes in sufficient quantity and quality to detect visible beating areas and identify sarcomere structures [40]. Despite being a protocol with very low differentiation efficiency (5-20% cardiomyocytes), optimization with serum- and insulin- free protocols results in higher differentiation efficiencies [55].

### 1.2.4 Guided differentiation with growth factors and small molecules

Many growth factors are used to enhance mesoderm formation and cardiomyogenesis in cultures of PSC, as described above (Section 1.2.1). BMPs, members of the TGF- $\beta$  family, play a key role in promoting mesoderm formation and specifying myocardial lineage commitment during differentiation [57, 58]. Activin A, also a member of TGF- $\beta$ , has been demonstrated to promote cardiomyogenesis in PSCs (reviewed in [57]). It has been shown that sequential addition of these two growth factors (at specific concentrations) can generate spontaneous contracting areas within 10 days and 30% of differentiated cardiomyocytes within three weeks, under feeder-free and serum-free culture conditions [59]. The WNT family, specially the WNT/ $\beta$ -catenin pathway, has stage dependent effects on cardiac differentiation. Activation of this pathway at the beginning of differentiation (prior to gastrulation) enhances cardiomyogenesis, but in later stages, after mesoderm formation, inhibitory effects of cardiomyogenesis are observed [60]. FGFs have also been described to influence survival and proliferation of cardiac precursors [27]. More specifically, FGFs cooperate with BMPs to further induce cardiomyogenesis; this cooperation was demonstrated in chick embryos, as FGF2 and FGF4 induce cardiomyogenesis in non-precardiac mesoderm, but differentiation is more efficient in the presence of BMP2 or BMP4 [61]. Efficient cardiomyocyte differentiation has also been verified when combining different types of growth factors added into culture medium at specific time points [54]. As an example, it was shown that the sequential addition of activin A, BMP4, basic fibroblast growth factor (bFGF), Dickkopf homolog 1 (DKK1) and Vascular Endothelial Growth Factor (VEGF) yields 40%-50% of cardiomyocytes [62, 63]. Indeed, guided differentiation protocols, through addition of growth factors, usually assure higher yields of cardiomyocyte differentiation. However, the high costs associated to the use of growth factors and their low stability compromise scalability and reproducibility of differentiation protocols [40].

With the advent of high-throughput screening technologies, small molecule libraries have been screened to identify molecular interactions leading to a particular stem cell fate [40, 54]. The use of small molecules in guided differentiation protocols offer two major advantages over growth factors and recombinant protein based methods. First, small molecules can diffuse more efficiently throughout multiple cell layers within EBs to modulate signaling, thus yielding more consistent results, whereas much larger proteins may not be able to access the target cells. Second, a significant advantage of small molecules is that they are less expensive than growth factors, offering greater flexibility and scale-up prospects to guided differentiation protocols [64]. Several small molecules with potential to enhance cardiomyogenesis have been identified (reviewed in [54]). Ascorbic acid, one form of vitamin C, has been shown to consistently and robustly enhance differentiation of iPSCs into

cardiomyocytes [65]. More specifically, the addition of ascorbic acid at early stages of culture (between days 2 and 6) improves by 7.3-fold and 30.2-fold the yields of cardiomyocytes derived from mouse and human iPSC, respectively. Ascorbic acid promotes cardiomyocyte differentiation by increasing collagen synthesis, enhancing proliferation of cardiac progenitor cells and upregulating late stage markers of cardiomyogenesis (e.g. cardiac troponin T, sarcomeric myosin heavy chain,  $\alpha$ -actinin) [65, 66]. Moreover, ascorbic acid induced cardiomyocytes showed better sarcomeric organization and enhanced responses of action potentials and calcium transients during electrophysiological assays when compared to cardiomyocytes differentiated in the absence of ascorbic acid. Like ascorbic acid, other small molecules like 5-azacytidine (demethylating agent) or cyclosporin-A have been reported to possess pro-cardiogenesis effects (reviewed in [54]).

### **1.2.5 Guided differentiation promoted by cyclic strains & oxygen**

Stem cell fate is highly dependent on stimuli that lie in the extracellular environment that drive specific cellular fates. Substantial effort has been made to identify relevant cues governing stem cell fate. As mentioned above (Section 1.2.2-4) cell-cell interactions, the extracellular matrix and soluble factors have impact on differentiation of stem cells into cardiomyocytes. Stem cell fate can also be influenced by other extrinsic factors such as physicochemical environment and physical forces. Since cardiomyocytes are exposed to dynamic environments *in vivo*, these stimuli have potential to further drive differentiation *in vitro*.

Physicochemical parameters such as dissolved oxygen concentration have tremendous influence on cell cultures. Recent studies have shown that low oxygen tensions (2-5%) enhance PSC proliferation [67, 68]. Also, during cardiomyogenesis, many cues and processes are influenced by hypoxia conditions [69, 70].

Mechanical stimuli are translated into biological signals that mediate cell structure, survival, proliferation and differentiation [71]. Advances in mechanical stimulation have shown that fluid shear stress, cyclic strains and magnetically mediated strains present potential to drive differentiation of cells that reside in mechanically dynamic environments, such as cardiomyocytes [71], vascular smooth muscle cells [72] and endothelial cells [73]. Cardiomyocytes in the body are subjected to cyclic mechanical strain induced by the rhythmic heart beating [74]. Thus, with the hypothesis that mechanical loading promotes cardiomyogenesis of ESCs, a recent study has reported ESCs subjected to mechanical stimuli demonstrated commitment towards cardiomyocyte lineage [75].



### **1.2.6 Scalable production of cardiomyocytes derived from PSCs**

As mentioned before, PSC-derived cardiomyocytes are powerful cells for cell replacement therapies, tissue engineering, drug discovery and *in vitro* toxicology applications. Cell-based therapies may require  $10^8$  to  $10^9$  hPSCs derived cardiomyocytes per patient, reflecting the amount of working myocardial lost in myocardial infarction. Large numbers of cardiomyocytes are also needed for drug screening pipelines and *in vitro* toxicology tests (reviewed in [40]). To facilitate the implementation of these cells in clinic and industry, there is a need to translate culture protocols developed at research laboratories into validated bioprocesses that can guarantee reproducibility, scalability, standardization, robustness and safety. The most attractive strategy for manufacturing cardiomyocytes derived from PSCs consists in engineering stem cell niches by identifying key factors inducing cardiomyocyte differentiation of PSC (as described above – Section 1.2.5) and creating culture approaches that allow 3D cell organization in a bioreactor-based system where key environmental conditions are finely controlled.

#### **3D cell culture strategies**

In the last years, several two-dimensional (2D) monolayer protocols were described for the differentiation of PSCs into functional cardiomyocytes (as described above – Section 1.2.1). However, 2D culture systems inappropriately resemble the *in vivo* microenvironment, mislead in regards to cell-cell or cell-matrix interaction, tissue architecture and biochemical signals [15, 76]. These systems also inherit uncontrollability, present low scalability and low differentiation yields, making them unattractive and unsuitable for clinical and industrial applications [15].

Transition from 2D cell monolayers to a 3D cell culturing approach is imperative to fully enhance cell performance and potential. 3D culture systems can improve cell viability, functionality and also offer higher degree of efficiency, robustness and predictability to manufacturing platforms [77–79].

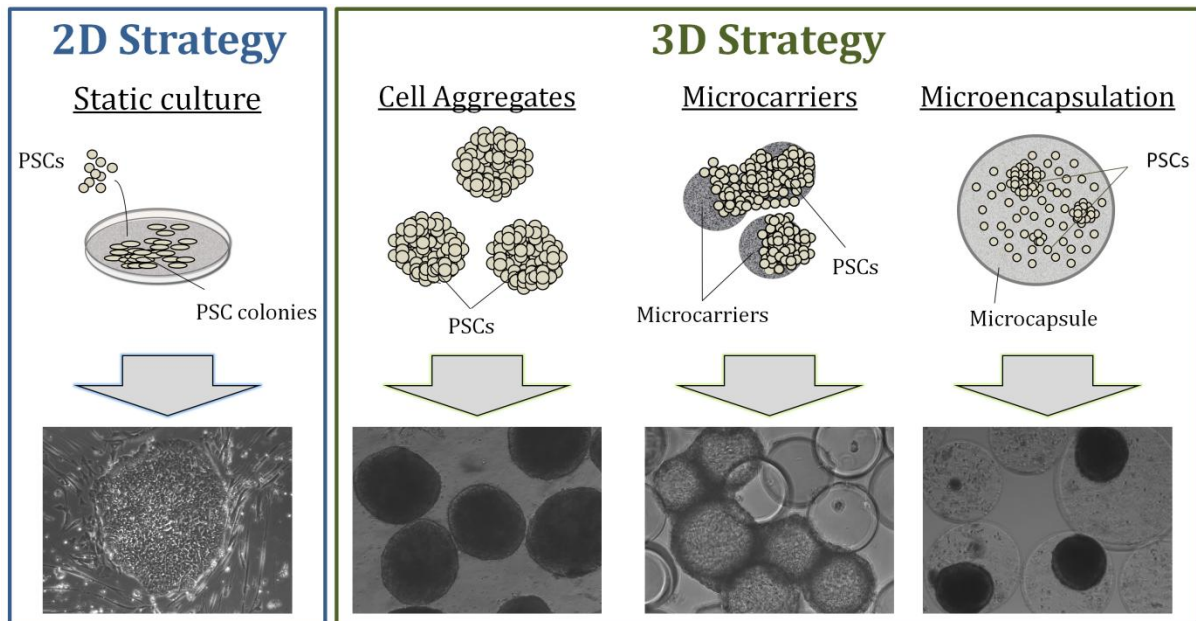


**Figure 1.5: 2D and 3D strategies for cultivation of PSCs (adapted from [15]).**

Formation of cell aggregates is one of the most common 3D cell culture strategies used in stem cell bioprocessing (Figure 1.5). When cultured as aggregates, cells re-establish mutual contacts allowing them to express a tissue-like structure, enhancing cell differentiation and functionality [79, 80]. Cell aggregates offer easy handling, scalable and reproducible opportunities to process development. The main limitation of this approach is the need to control aggregate size, avoiding diffusion gradients inside the aggregate that lead to necrotic centers and/or spontaneous differentiation [15]. Cell harvesting is also an issue as dissociation of aggregates can compromise cell viability [81]. This approach has been widely used for cardiac differentiation [69, 82]

One method for controlling cellular aggregation in suspension conditions is the use of microcarriers (Figure 1.5). A microcarrier is a support matrix that allows the growth of anchorage-dependent cells in suspension systems. A wide range of microcarrier types have been proposed for the cultivation of PSCs (porous, non-porous, composed by gelatin, glass, collagen, cellulose) presenting dimensions within the range of 10–200  $\mu\text{m}$ . A major advantage of microcarrier technology in PSC bioprocessing is the flexibility to easily adjust the area available for cell growth, further facilitating the process scale-up. From clinical/industrial perspectives, this attribute has a tremendous impact on reducing the costs of cell manufacturing (reviewed in [15]). However, this approach presents disadvantages such as microcarrier clumping [83] and harmful shear stress effects (cell damage due to physical forces). Microcarrier technology has also been used for differentiation towards cardiomyocyte lineage [84, 85].

Cell microencapsulation in hydrogels (Figure 1.5) ensures an environment free of shear stress while avoiding cell clumping [83]. The main benefit of cell microencapsulation technology is the possibility of designing the scaffold environment with specific biomaterials that exhibit a wide range of mechanical/chemical properties, correlating to the properties of native tissues. Nonetheless, microencapsulation also presents drawbacks such as additional costs associated to the use of hydrogels and other materials, limited gas and mass diffusion inside the capsule pores and difficult culture monitoring (reviewed in [15]). Studies have shown that PSC-derived cardiomyocytes can be obtained using cell microencapsulation [86]

### **Bioreactors for PSCs cultivation**

One of the most used strategies for scaling-up the production of PSC derivatives consists in cultivating cells using dynamic culture systems [40]. Spinner flasks (Figure 1.6A) have been widely used for PSCs expansion [83] and differentiation into cardiomyocytes [87]. However this culture system lacks culture control over parameters like temperature, pH or gas exchanges (e.g. oxygen).

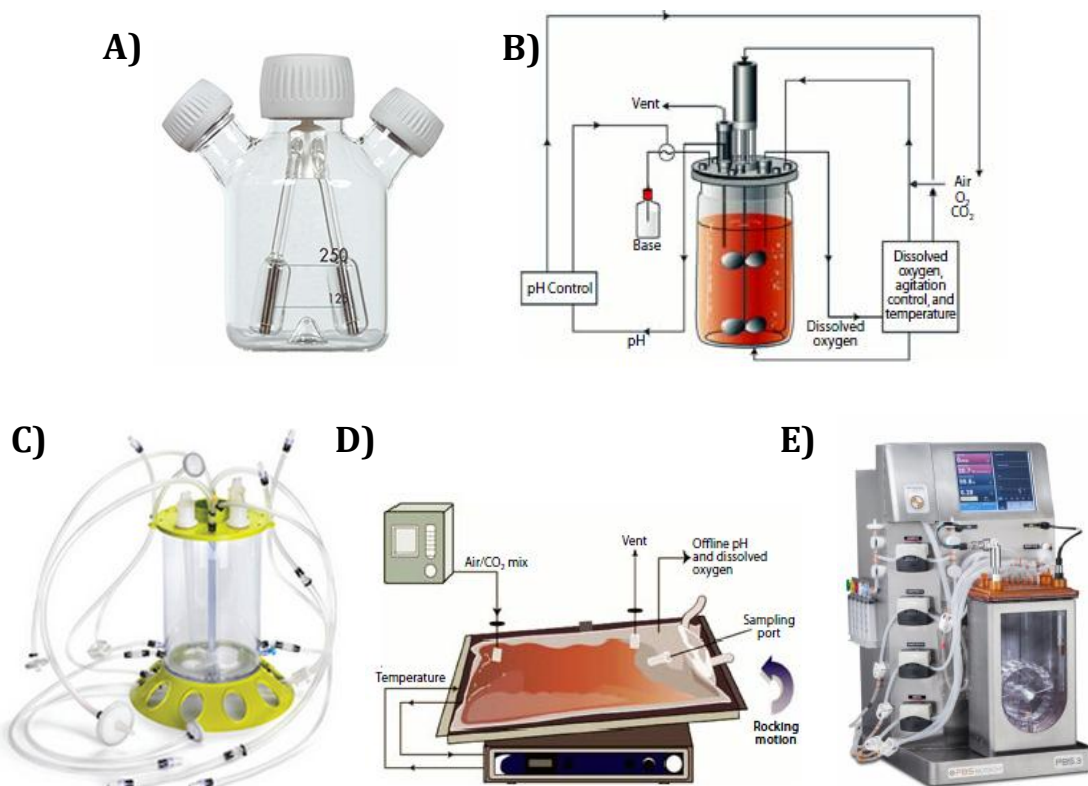


**Figure 1.6: Examples of different bioreactor designs used for stem cell bioprocessing. A)** Spinner flask. **B)** Stirred tank bioreactor [88]. Single-use disposable bioreactors: **C)** Single-use stirred tank bioreactor (Mobius CellReady, Millipore) ([www.millipore.com](http://www.millipore.com)). **D)** Wave induced bioreactor (WAVE Bioreactor, GE Healthcare) [88]. **E)** Pneumatically mixed bioreactor (PBS 3, PBS Biotech) ([www.pbsbiotech.com](http://www.pbsbiotech.com)).

Bioreactors for PSC bioprocessing should accurately control and regulate cellular microenvironment, aiming at supporting cell viability while providing spatial and temporal control of signaling. Different bioreactor types have been used for PSC cultivation such as microfluidic culture systems, rotatory culture systems and stirred tank bioreactors (reviewed in [89]). Stirred tank bioreactors (Figure 1.6B-C) offer efficient gas/nutrient transfer, precise control and monitoring of culture environment (e.g. pH, temperature,  $pO_2$ , gas composition, nutrients) and non-destructive sampling (Figure 1.6B-C). These bioreactors offer enormous engineering prospects, as they are scalable, reproducible, versatile and fully automated. One of the main limitations of stirred tank bioreactors is the hydrodynamic shear stress promoted by stirring. Up to now, the minimal volume required to set up the experiments was very high (approximately 50 mL), which compromised the use of stirred bioreactors for high-throughput applications by demanding higher starting cell numbers and increasing the costs associated to optimization studies. Large efforts have been made towards the development of smaller scale systems (working volume 10–15 mL) and two options are available today including the ambr® systems (from TAP Biosystems) and the low volume spinner flasks (from HexaScreen).

During the last decade, single-use disposable bioreactors have been developed and applied in preclinical, clinical, and production-scale biotechnological facilities [90]. In contrast to reusable bioreactors made from glass or stainless steel, single-use bioreactors are made of FDA-approved (Food and Drug Administration) plastics [91]. Single-use bioreactors offer several advantages such as reduced costs in construction of production facilities, reduced risk of cross-contamination, less cleaning validation needed and rapid changeover of processes [92]. However, these bioreactors also present limitations including lack of instrumentation for single-use sensors, possible secretion of leachables and extractables from the plastic cover and limited number of vendors available [91, 92].

Today, there are different disposable bioreactor types commercially available ([90, 91]). These include spinner vessels, such as the SuperSpinner D 1000 (Sartorius), and stirred tank disposables: Mobius CellReady (Millipore; Figure 1.6C), Univessel SU (Sartorius) and CelliGen BLU (Eppendorf); micro bioreactors are also available, the Ambr bioreactor. Different bioreactor designs have also been developed as single-use disposables. One example is the wave induced bioreactor (WAVE Bioreactor from GE Healthcare and BIOSTAT CultiBag from Sartorius-Stedim). This bioreactor (Figure 1.6D) has a rocking platform capable of inducing a wave motion in the culture media without an impeller or other invasive mixer. This rocking system promotes rapid medium homogeneity and provides the optimal oxygen transfer in the inflated bag [92, 93]. Studies has shown that this bioreactor presents

lower shear stress when compared to the stirred tank bioreactor [94]. In addition, this bioreactor has a simple design, appealing to either biological engineers or medical professionals. Pneumatically mixed bioreactors (e.g. Air-Wheel® Bioreactor Systems from PBS Biotech (Figure 1.6E)) are another example of disposable devices with unique characteristics. This bioreactor provides mixing and optimal oxygen transfer via gas buoyancy (air bubbles), eliminating the need for an external mechanical agitator [92, 95]. This pneumatic mixing type assures low shear stress [95], always an advantage for stem cell bioprocessing.

In order to enhance stem cell metabolism and further improve cell viability, proliferation and differentiation, different operation modes can be adopted, including fed-batch and perfusion [15]. The fed-batch strategy is considered the most adequate for optimizing cell metabolism, enabling a more efficient uptake and consumption of nutrients, resulting in reduced accumulation of metabolites in culture supernatant [96]. Perfusion strategies have been developed in stem cell bioprocesses to ensure continuous renewal of nutrients and growth factors and constant removal of toxic byproducts [70, 96]. Growth factors play an important role in stem cell processes, providing survival, proliferation and differentiation signals. This feature of continuous medium addition and removal has potential to be integrated in expansion, differentiation and/or cell lineage selection steps. Addition of different medium formulations and removal of cell debris are also possible using perfusion strategies.

Optimization of PSC bioprocessing should result in large cell yields through process intensification, specialization and integration, rather than just scale-up technologies [15]. The establishment of platforms capable of integrating isolation and reprogramming, inoculation, expansion, differentiation, purification and harvesting would result in the scale-up of well differentiated cells to clinical relevant numbers [15]. Several bioprocesses combining PSC (human and mouse) expansion and cardiomyocyte differentiation have been reported in recent years. Table 1.2 presents results of recent studies integrating PSC-derived expansion and differentiation in computer controlled bioreactors, operating in batch and perfusion modes.

**Table 1.2:** Studies involving cultivation of mESCs in scalable 3D approaches involving expansion and differentiation into cardiomyocytes.

Stirred Tank Bioreactor	Operating mode	Culture volume (ml)	Initial cell number	Final CM number	CM/ESC ratio	Ref
Standard Spinner vessel	Batch	250	$5 \times 10^7$	$5.86 \times 10^7$	1.2	[97]
DASGIP Cellferm-Pro (DASGIP Tech.)	Perfusion	250	$0.9 \times 10^6$	$3.5 \times 10^6$	3.8	[70]
Biostat MD (Sartorius)	Batch	2000	$2 \times 10^8$	$1.28 \times 10^9$	6.4	[98]
Biostat MD (Sartorius)	Perfusion	2000	$2 \times 10^8$	$4.6 \times 10^9$	23	[99]

### 1.3 Purification of iPSC-derived cardiomyocytes

The use of cardiomyocytes derived from PSCs in cell-based therapy has been hampered by the inability of differentiation protocols to obtain homogenous, pure and functional cardiomyocytes. To prevent unwanted side effects, like tumor formation or inefficient therapies, it is necessary to eliminate the high degree of heterogeneity of the final cell population (reviewed in [3]). Therefore developing effective purification protocols is imperative to obtain populations highly enriched in cardiomyocytes. There are several purification/enrichment strategies, including genetic and non-genetic approaches for selection based on distinct cellular and molecular characteristics of cardiomyocytes.

#### 1.3.1 Genetic selection of cardiomyocytes

Genetic-based purification protocols allow efficient enrichment of cardiomyocytes in mESC cultures (purity >99.6% [100]). In this approach, undifferentiated cells are genetically modified to integrate and stably express a transgene, such as a fluorescent marker (e.g. eGFP, dsRed) or an antibiotic-resistant gene (e.g. resistance against geneticin, puromycin) under control of a specific cardiac promoter. A number of cardiac specific promoters have been used, such as human myosin light chain ventricular isoform (Myl2) [101] and mouse [102] and human [103] cardiac  $\alpha$ -myosin heavy chain ( $\alpha$ -MHC). Since differentiated cardiomyocytes express these selection markers, these cells can be selected from a heterogeneous population by fluorescence-activated cell sorting (FACS) or by addition of antibiotics, if the transgene encodes antibiotic resistance genes (reviewed in [54]). Although this approach results in a highly enriched population, it presents some disadvantages, as genetic modification of cells can promote/induce tumor formation, cell lines have to stably express the transgene, which is a time consuming process, and the enrichment process is highly dependent on cell line [54].

### 1.3.2 Non-genetic purification of cardiomyocytes

Cell lineage purification from heterogeneous populations can also be achieved using non-genetic methods. These strategies range from mechanical to biochemical methods, based on cells physical and structural properties (reviewed in [3]).

Micro dissection and Percoll gradient centrifugation are the most widely used methods for cardiomyocyte enrichment [21]. Micro dissection is based on the isolation of contracting areas, enriched with cardiomyocytes, through the manual dissection of these areas from a cell culture plate [104]. In Percoll separation methods, dissociated cells are loaded onto two layers of Percoll and centrifuged, enabling separation of cardiomyocytes from non cardiac cells, who will reside in a upper layer (lower density than cardiomyocytes) [105]. Both these techniques are simple and inexpensive, however they lack scalability and are time-consuming (reviewed in [40, 54]).

Enrichment of cardiomyocytes can also be carried out by targeting specific surface markers of cardiomyocytes. Using specific antibodies, enrichment is possible by selecting differentiated cardiomyocytes (positive selection) or non-cardiac cells (negative selection), since their surface marker expression is distinct (reviewed in [54]). Three surface markers are associated with stem-cell derived cardiomyocytes: signal-regulatory protein alpha (SIRPA) [106], vascular adhesion molecule 1 (VCAM1) [107] and activated leukocyte cell adhesion molecule (ALCAM) CD166, which is a specific marker for early murine cardiomyocytes [108]. Cell sorting can be achieved with fluorescence-activated cell sorting (FACS) or magnetic-assisted cell separation (MACS) techniques. FACS can simultaneously target multiple markers, while MACS can only target a single marker although presenting higher throughput. These methods can assure enriched populations, containing over 90% of cardiomyocytes [54]. However studies have shown that these approaches result in the loss of some cardiomyocytes, as not all express these markers [106, 107]. Cardiomyocytes have a unique feature of presenting high content of mitochondria. Thus, labeling the mitochondria of cardiomyocytes with fluorescent dyes provides another means of purification. Tetramethylrhodamine methyl ester perchlorate (TMRM) has been used for this purpose, as it is non-toxic to cells and the labeling is reversible [109]; using this method cardiomyocytes can be efficiently selected (99% of purity) using FACS, as they will be part of the high fluorescence intensity fraction [3, 109].

Recently, novel purification methods have been developed based on distinct metabolic flows of cardiomyocytes. Exploiting distinct metabolic flow methods, studies have stated that 99% purity can be achieved using glucose depleted culture medium containing abundant lactate, using either mouse or human PSC-derived cardiomyocytes [110, 111]. This

cardiomyocytes enrichment protocol is achieved without the use of complex devices or labor-intensive steps, being adequate for clinical applications [111].

#### 1.4 Characterization of cardiomyocytes

Structural and functional characterization of differentiated cardiomyocytes is essential to evaluate the outcome of differentiated protocols and quality of cell-based products. For cell-based therapies, characterization of cell-based product or cells to be used in transplantation is important to minimize the risk of host rejection, tumor formation or arrhythmias (reviewed in [3]). In the last few years, extensive characterization of PSC-derived cardiomyocytes have been carried out to evaluate and confirm their cardiac phenotype [40, 112].

The cardiomyocyte differentiation process of PSCs can be monitored by following the temporal gene expression pattern. Pluripotency markers are down-regulated soon after differentiation followed by up-regulation of cardiac mesoderm markers and then cardiomyocyte-associated genes (reviewed in [54]). To confirm the phenotype of the final differentiated population, it is essential to detect the expression of cardiomyocyte-associated genes [113]. Some of these cardiac proteins are described in Table 1.3.

**Table 1.3: Cardiac markers used for the characterization of cardiomyocytes (adapted from [54]).**

<b>Structural proteins</b>	$\alpha$ -Actinin; cTnT; cTnI; $\alpha/\beta$ -MHC; Myl2; Myl7; Desmin; Titin
<b>Transcription factors</b>	NKX2-5; GATA4; MEF2C; TBX5; TBX20
<b>Gap junction proteins</b>	N-cadherin; Connexin 43
<b>Surface proteins and ion channels</b>	$\alpha 1/\beta 1$ -adrenergic receptors; L-type calcium channel, HCN4

\* cTnT – cardiac troponin T; cTnI – cardiac troponin I; MHC – myosin heavy chain; Myl2/Myl7 – myosin light chain (ventricular/atrial); NKX2-5 – NK2 transcription factor related locus 5; Gata4 – Zinc finger transcription factor 4; MEF2C – myocyte enhancer factor; TBX5/TBX20 – T box protein 5/20; HCN4 – Hyperpolarization Activated Cyclic Nucleotide-Gated Potassium Channel 4.

There are some techniques available to ensure a robust and efficient characterization of PSC-derived cardiomyocytes. These techniques enable characterization based on the morphologic, structural and electrophysiological properties of cardiomyocytes. Flow cytometry (Figure 1.7A) provides a quantitative method to evaluate the purity of the differentiated and enriched population, by measuring the number of cells expressing cardiac-specific proteins [3]. Reverse transcription-polymerase chain reaction (RT-PCR, Figure 1.7B) can be used to assess changes in gene expression throughout the differentiation process.



Studies have also shown that changes in cardiomyocyte gene expression can also be characterized with a transcriptional profiling approach, using microarrays analysis [114]. Immunofluorescence microscopy (Figure 1.7C) using specific antibodies is another strategy used for evaluating structural characterization of cardiomyocytes [40].

Cardiomyocytes can also be characterized based on their functional properties. Studies have shown that PSC-derived cardiomyocytes display functional properties of early-stage human heart cells, including atrial, ventricular and pacemaker phenotypes (reviewed in [37]). Functional assays should also demonstrate that cardiomyocytes can generate action potentials (APs) when stimulated by an electric signal, resulting in intracellular  $\text{Ca}^{2+}$  release and, as a consequence, cell/muscle contraction [37, 112]. This characterization is achieved using electrophysiology or calcium indicator assays (e.g. Fluo-3, Rhod-3) (Figures 1.7D-F).

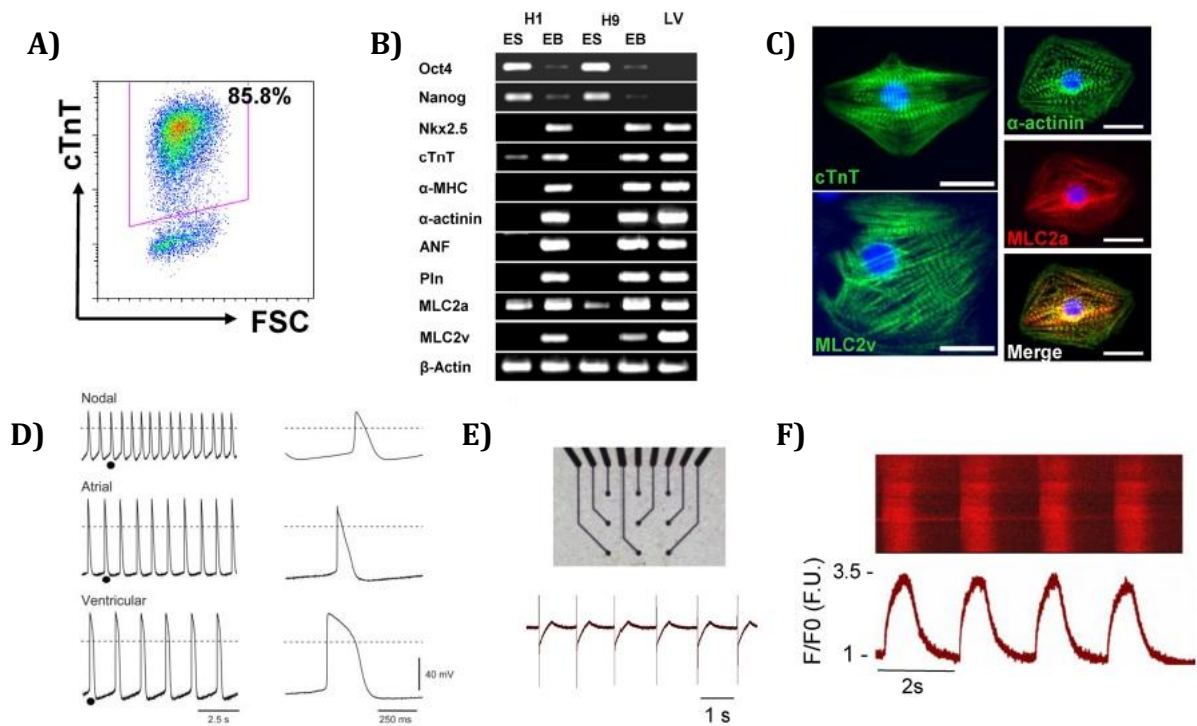


**Figure 1.7: Basic characterization of PSC-derived cardiomyocytes.** **A)** Flow cytometry provides a quantitative method to evaluate relative yield and purity of cardiomyocytes. Measurement of cells expressing cardiac troponin T (cTnT). FSC indicates forward scatter; **B)** Reverse transcription-polymerase chain reaction is used as a first assessment for changes in gene expression typical of cardiogenesis. ES indicates embryonic stem cells, EB embryoid body, H1 and H9 are ESC lines, and LV left ventricular cells; **C)** Immunofluorescence microscopy with antibodies specific for myofilament proteins determines whether cells exhibit organized sarcomeres typical of cardiomyocytes. MLC indicates myosin light chain. **D)** Functional assessment of cardiomyocytes can be provided by cellular electrophysiology measurements to determine whether cardiac action potentials of different cardiomyocyte subtypes are present; **E)** Extracellular field potential measurements by multi-electrode arrays provide a method to detect spontaneous electric activity in cardiomyocyte preparations; **F)** Detection of  $\text{Ca}^{2+}$  transients typical of cardiomyocytes providing another assessment of functional integrity of differentiating cardiomyocytes. Cells loaded with the  $\text{Ca}^{2+}$  indicator Fluo-3 were imaged by

laser scanning confocal microscopy in the line-scan mode with  $\text{Ca}^{2+}$  transients displayed and time versus normalized  $\text{Ca}^{2+}$  transient intensity ( $F/F_0$ ) shown below [40].

## 1.5 Cryopreservation and storage of PSC-derived cardiomyocytes

The therapeutic use of clinical grade cardiomyocytes is also dependent on developing efficient, scalable and integrated methods for storage of cardiomyocytes. Several companies and academic institutes have aimed at establishing good manufacturing practices compatible (GMP), efficient and customized cryopreservation protocols for long term storage of cardiomyocytes derived from PSC bioprocessing (reviewed in [115]). Cryopreservation of cardiomyocytes is considered a critical step in an integrated bioprocess, since it can exert tremendous influence and irreversible effects on cardiomyocyte quality. For successful allogeneic therapies, banking and recovery of stored cells must be accomplished without compromising cell viability or function, promoting adoption of cell-based allogeneic products (reviewed in [115]). Preserving cells also allows the generation of master and working cell banks so that consistent and quality-controlled stocks of cells are available for *in vitro* toxicology studies or drug screening purposes [116].

Cryopreservation-induced events, such as ice crystallization or osmotic shock induced-necrosis, activated apoptosis, disruption of cell-cell and cell-matrix adhesions, affect survival and fate of stored cells during cryopreservation (reviewed in [115]). Thus, developing robust cryopreservation and storage processes that have minimal adverse effects on PSC-derived cardiomyocytes is crucial for successful banking and shipping [117]. Cryopreservation is defined as the maintenance or storage of biological material at temperatures typically below the glass transition of pure water ( $-132^\circ\text{C}$ ), at which biological metabolism is dramatically diminished [118]. As differentiation protocols are complex and lengthy, preserving stocks of PSCs allows time for quality control and safety testing, ensuring the usage of quality and well characterized PSCs, reducing waste and process inefficiency [117].

Suitable storage strategies at low temperatures (hypothermic storage) are also a demand for transport and delivery of cells, for short time periods [117]. Hypothermic storage can be defined as the preservation of cells and tissues at chilled temperatures that often range between  $4$  and  $10^\circ\text{C}$ . Commercial solutions (e.g. Prime-XV™ Hypothermic Preservation Solution, Irvine Science, and HypoThermosol®-FRS, BioLife Solutions Inc.) are available for hypothermic storage of cells and tissues, as cryopreservation can be circumvented when simple transportation is needed using hypothermic solutions.

A cryopreservation procedure involves the steps represented in Figure 1.8. A pre-freezing treatment is necessary to bring cells to the state at which they will be frozen (e.g.

single-cell suspension, cell aggregates, cell monolayers),. Then cells are transferred to the platform where they will be cryopreserved (e.g. cryovials, well-plates). Before the freezing process, samples are loaded with cryoprotective agents (CPA; e.g. DMSO, glycerol) to help minimize cryoinduced damage during the freezing and thawing procedure. Increased attention has been given towards the development of preservation formulations, such as Cryostor, STEM-CELLBANKER or Synth-a-Freeze [115]. The cells are then frozen at the desired cooling rate to the storage temperature at which they will be stored (e.g. -80°C, -196°C) Upon cell thawing, CPAs are removed diluting the sample in medium, after which post-thaw cell recovery is evaluated [119].

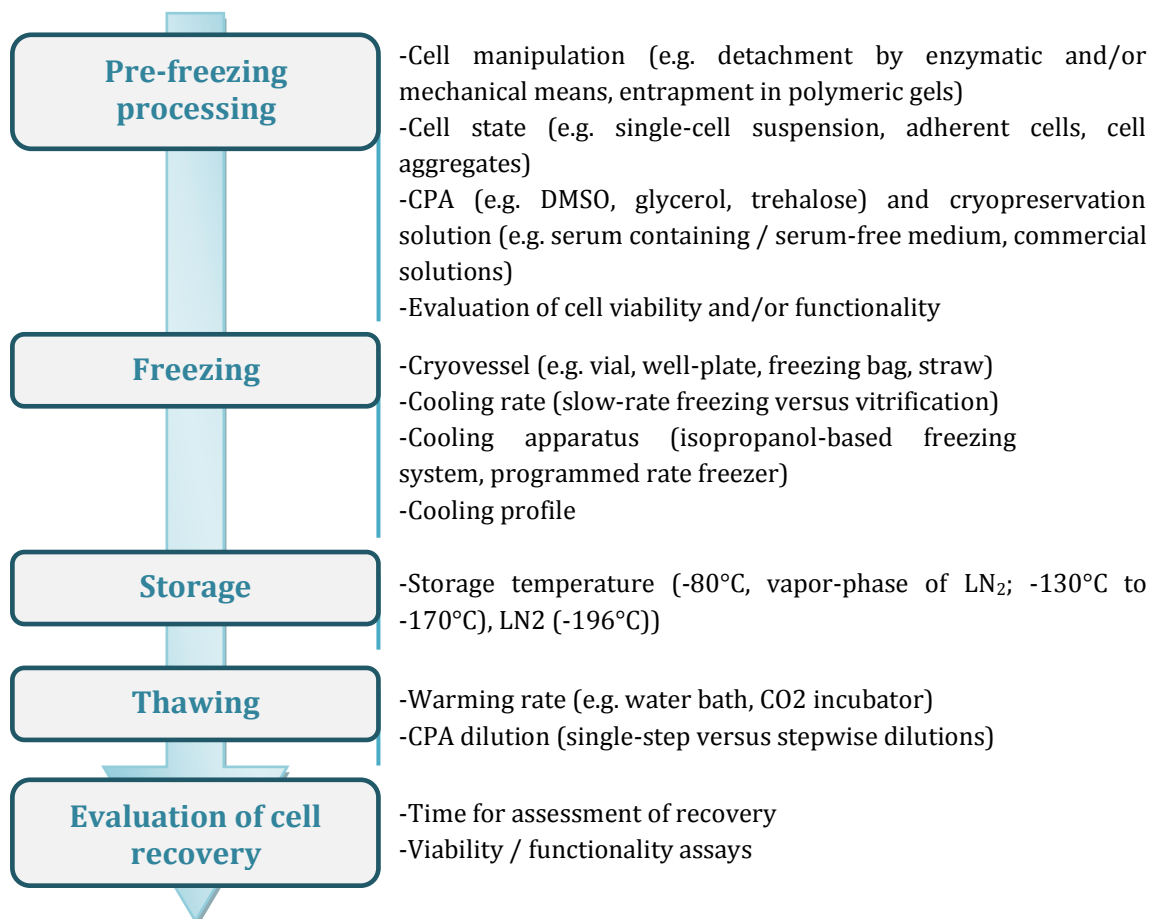


**Figure 1.8: Main steps composing common cryopreservation procedure for mammalian cells.** Important parameters for each step are listed.

Slow-rate freezing is a common approach and is the most appropriate method when dealing with large quantities of cells [120]. Slow-rate freezing consists in freezing samples at a slow cooling rate to minimize the possibility of intracellular ice formation, which is likely to be formed due to the large fraction of water in biological cells and tissues. Slow cooling helps prevent ice formation, by promoting cell dehydration during the freezing step. Basic principles and damaging events underlining slow cooling injury have been well documented. Cells can be damaged due to cryoprotectant toxicity, osmotic damage due to exposure and

removal of cryoprotectants and high solute concentrations to which cells are sometimes exposed during freezing [121]. To avoid cell damage, cells are suspended in specific quantities of cryoprotectant agents (e.g. 5-20% DMSO in medium or serum) and placed in a controlled rate freezer or in an isopropanol bath, able to cool the sample at 1°C/min. CPAs (penetrating and non-penetrating) can protect cells reducing concentration of damaging electrolytes, at given subzero temperatures, and reduce the extent of cell volume change during the freezing and thawing process [122].

Several protocols for cryopreservation of undifferentiated cells have been reported to date [123]. However, there is still a need to develop effective cryopreservation protocols for cardiomyocytes derived from PSCs. Recent studies have shown that cryopreservation of hESCs-derived cardiomyocytes is possible, cryopreserving cells as a single cell suspension and achieving cell recoveries over 80% [124]. Due to the lack of results and information regarding PSC-derived cardiomyocyte cryopreservation, novel 2D and 3D cryopreservation strategies are a demand for efficient storage after bioprocess production of PSC-derived cardiomyocytes.

## **1.6 PSC-derived cardiomyocytes as promising cell models for cardiotoxicity assays**

The pharmaceutical industry currently generates large libraries of new drugs with the aim of selecting those most promising for clinical trials [125]. Drug attrition rates have drastically increased in the past years, resulting in growing costs for the pharmaceutical industry and consumers, as drugs often fail during advanced stages of clinical trials [126]. At an early stage, to improve drug safety and reduce development costs it is crucial to distinguish specific from off-target effects of drugs [125]. In addition to safety and efficacy issues, drugs fail due to the lack of *in vitro* models that correlate with clinical results and poor preclinical toxicity screening assays [127]. Recent withdrawals of prescription drugs that affect the heart have highlighted the need for more reliable cardiac safety pharmacology assays.

PSC-derived cardiomyocytes have potential to be considered as a suitable model for *in vitro* assessment of pharmacological and toxicological studies [128]. Cardiomyocytes from animals been used for these applications however they are inadequate for this purpose as they do not fully translate to results observed in humans and show qualitative differences inter-species [129]. Cardiomyocytes differentiated from PSCs have potential to overcome these limitations, by reducing the burden of animal model use, decreasing time and cost of bringing new drugs to market [127]. These cells also display many characteristics of human

cardiomyocytes, including structural, functional and molecular properties making them suitable for drug discovery applications, disease modeling and cardiotoxicity screening [127].

### **Oxidative stress and cardioprotection**

Heart failure and many of the conditions that predispose to heart failure are associated with oxidative stress. Several drugs that advance to clinical trials are later withdrawn from the market due to cardiotoxicity issues (e.g. Terfenadine, Cisaprine, Grepafloxacin) [130]. Also, many anti-cancer drugs tested in clinical trials (e.g. doxorubicin, paclitaxel and docetaxel) are associated with the generation of reactive oxygen species (ROS), thus leading to oxidative stress and major cell damage [131]. ROS, such as superoxide ( $O_2^-$ ), hydrogen peroxide ( $H_2O_2$ ) or hydroxyl ( $OH^\cdot$ ), are small molecules produced by several enzyme systems in cardiomyocytes, either as a primary product or as a secondary byproduct. When existent in adequate quantities, ROS are involved in the synthesis of energy and in boosting the cells defense mechanism. However, when their production overcomes their removal, the cells experience oxidative stress which may cause adverse effects due to irreversible modification of macromolecules, causing damage on the cells membranes, proteins and DNA [132].

Antioxidant compounds (e.g. catechin, resveratrol, procyanidin, polyphenols) have been shown to present ROS scavenging properties, resulting in protection against cellular damage from oxidative stress [133]. The use of antioxidant compounds has become an attractive intervention in attenuating drug-induced cardiomyopathy. Thus, developing suitable oxidative stress models of PSC-derived cardiomyocytes is imperative for many drug screening, cardiotoxicity and cardioprotection assays.



## 2. Aim of the thesis

The main aim of this thesis was the development of a robust, scalable and integrated strategy for miPSC-derived CM production and selection. This approach should allow the achievement of high CM differentiation yields and CM enrichment at the end of the process, as well as producing relevant numbers of CMs, without compromising their structural quality and functionality. To achieve this goal, different bioreactor systems and strategies were used, including single-use bioreactors with distinct agitation types, stirred tank bioreactors and automated continuous perfusion system.

The second objective was the development of cryopreservation and hypothermic storage strategies to ensure an efficient storage of CMs after mass production in environmentally controlled bioreactors. 2D and 3D approaches were evaluated using different cryopreservation and storage solution formulations.

Finally, bioprocess derived CMs were used to evaluate their potential as promising cell model systems in cardiotoxicity/cardioprotection assays. 2D and 3D approaches were tested during oxidative stress induction and cardioprotective pretreatments. Hydrogen peroxide and catechin were used as cardiotoxic and cardioprotective agent, respectively.

The thesis rational is schematically illustrated in Figure 2.1.

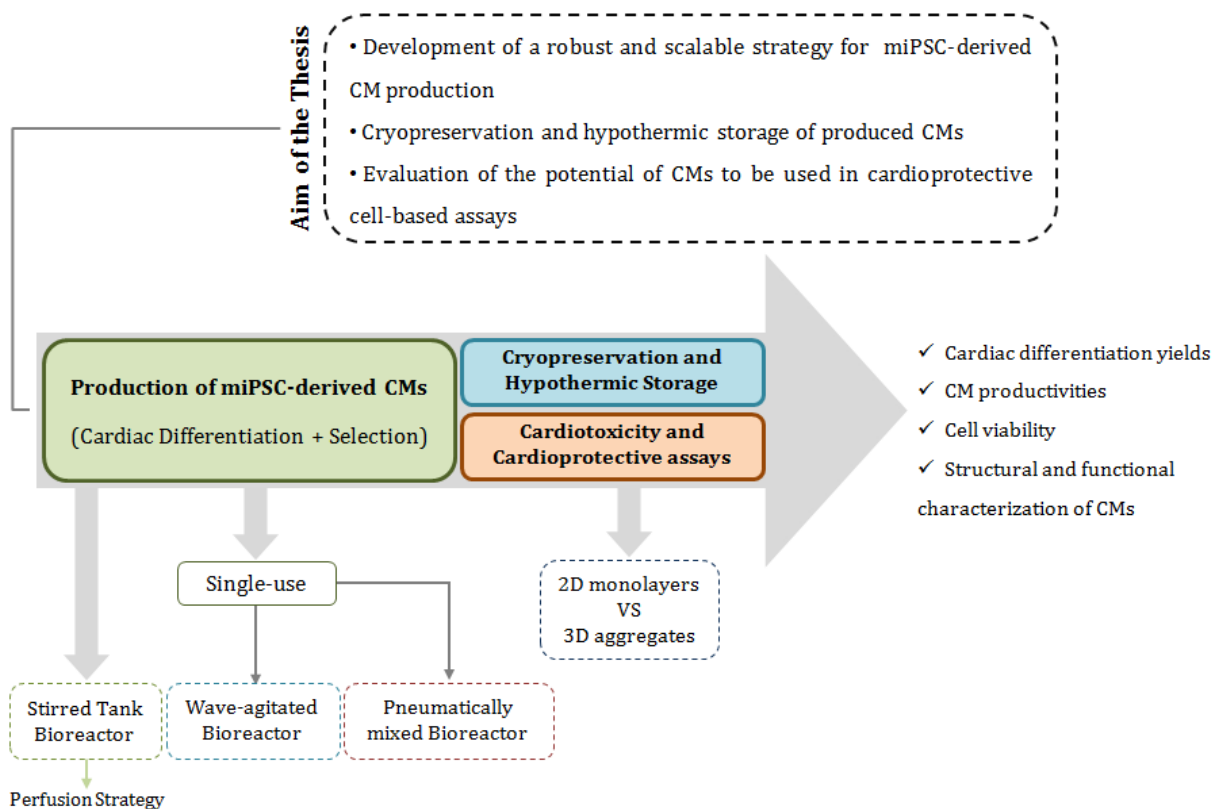


**Figure 2.1: Thesis rational.** Aim of the thesis, strategies outlined and major readouts obtained.





### 3. Materials and Methods

#### 3.1 miPSC culture on feeder layers

In this study, a murine transgenic  $\alpha$ PIG-iPSC line was used [134]. This cell line was genetically modified to integrate and stably express a transgene containing puromycin-N-acetyl transferase and eGFP (enhanced green fluorescent protein) genes, both under control of the cardiac-restricted promoter  $\alpha$ -MHC [134]. Murine iPSCs (miPSCs) were propagated as colonies in static conditions (6-well plates) on a monolayer of mitotically inactivated murine embryonic fibroblasts (MEFs, E14.5) in expansion culture medium (Dulbecco modified Eagle medium (DMEM) supplemented with 15% (v/v) Fetal Bovine Serum (FBS), 1% (v/v) Minimum Essential Medium – Non-Essential Amino Acids (MEM-NEAA), 2mM L-glutamine, 50 $\mu$ M  $\beta$ -mercaptoethanol, 500 $\mu$ g/mL Geneticin (Neomycin sulfate/G418) (all from Invitrogen)) and 100 U/ $\mu$ L Leukemia inhibitory factor (LIF, Milipore). miPSC were cultured at 37°C, in a humidified atmosphere of 5% CO<sub>2</sub>. Every 2-3 days, when miPSC colonies covered about 80% of the culture surface area, colonies were dissociated with 0.05% (w/v) Trypsin/EDTA (Invitrogen) for 5min at 37°C. After dissociation, miPSCs were plated onto MEFs feeders at a density of 0.125 - 0.25x10<sup>6</sup> cell/well.

#### 3.2 miPSC differentiation in fully controlled bioreactors

##### 3.2.1 miPSC differentiation in stirred tank bioreactor

Aggregation Step: miPSC colonies were dissociated with 0.05% Trypsin/EDTA (as described above) and inoculated as single cells at a concentration of 0.7x10<sup>5</sup> cell/mL into an Erlenmeyer, in 100mL of differentiation medium (Iscove's Modified Dulbecco's Medium (IMDM) supplemented with 20% (v/v) FBS, 1% (v/v) MEM- NEAA, 1% (v/v) Penicillin-Streptomycin (Pen/Strep), 50  $\mu$ M  $\beta$ -mercaptoethanol (all from Invitrogen) and 100 $\mu$ M Ascorbic acid (Wako Chemicals GmbH)). miPSC cultures were placed on an orbital shaker, at 80-90 rpm, and cultivated for 2 days at 37°C, in a humidified atmosphere of 5% CO<sub>2</sub>.

Expansion and Differentiation Step: At day 2, cell aggregates were inoculated at a concentration of 150 aggregates/mL in computer-controlled stirred tank bioreactors (DASGIP Technology DS0200TBSC model, Eppendorf), equipped with a trapezoid impeller with arms, and with a working volume of 200mL. The headplate of the bioreactor has ports for pH and pO<sub>2</sub> electrodes, allowing online measurement and control of parameters, ports for sampling tubes and for addition and/or removal of culture medium. The dissolved oxygen (DO) was controlled via surface aeration with Air and N<sub>2</sub> - DO: 4% O<sub>2</sub> (approximately 20% air saturation), surface aeration rate: 0.1vvm and CO<sub>2</sub>: 5%. Temperature was kept at 37°C using a

DASGIP TC4SC4 Control System via Bioblock by heating and cooling cycles. This control system was also used to promote intermittent agitation profiles (agitation rate: 90rpm) in these bioreactor cultures. Data acquisition and process control were performed using DASGIP Control Software 4.0.

At day 9, cell lineage selection of the cultures was induced by performing a partial medium exchange (50% v/v), replacing the culture medium for differentiation medium supplemented with 8 $\mu$ g/mL Puromycin (Invivogen). Two different process approaches for miPSCs-derived CM selection were evaluated and compared: A) semi-continuous (i.e. manual medium exchange) and B) continuous perfusion operation modes.

A) Semi-Continuous system: Medium exchanges were performed, by partially replacing culture medium for fresh differentiation medium supplemented with Puromycin (8 $\mu$ g/mL), at days 12 (70% v/v) and 14 (50% v/v). In addition, at day 12, the bioreactor working volume was reduced to 100mL. Medium exchanges were performed by stopping agitation and allowing CM aggregates to settle (2-3min with no agitation).

B) Continuous Perfusion system: A fully automated continuous perfusion system was incorporated using computer controlled peristaltic pumps. The perfusion apparatus (Figure 3.1) included a DASGIP MP8 Multi Pump module, one port for the inlet and one port for the outlet, one computer, the bioreactor vessel, the inlet and outlet containers and their respective scales. The weight in each scale was continuously monitored to ensure a precise control of perfusion rates throughout the culture. Two perfusion rates were tested as summarized in table 3.1, represented as dilution rates ( $D = F/V$ , where F is the perfusion rate used and V is the working volume).

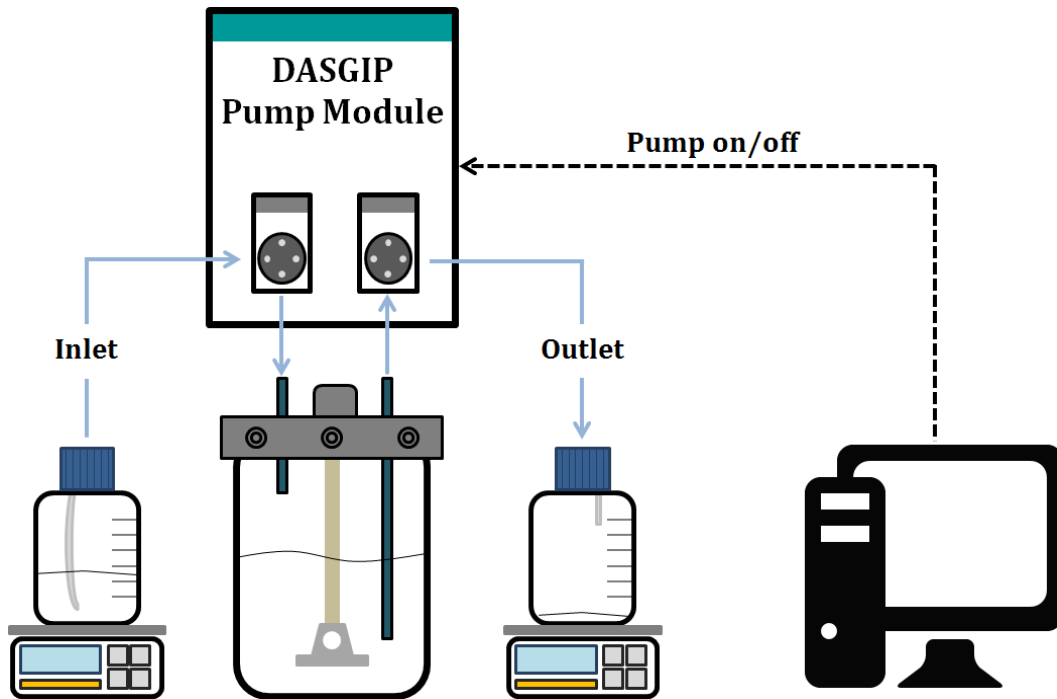


**Figure 3.1: Perfusion apparatus used in continuous perfusion experiments.**

**Table 3.1: Dilution rates tested in the continuous perfusion system approach.**

Strategy	Dilution Rate (D; day <sup>-1</sup> )		
	day 9 - 12	day 12 - 14	day 14 - 16
I) Low Perfusion rate	0.14	0.36	0.24
II) High Perfusion rate	0.70	1.80	1.20

In both strategies evaluated, CM aggregates were harvested from stirred tank bioreactors at day 16. These aggregates were dissociated into single cells by incubation with 0.25% (w/v) Trypsin/EDTA and then transferred to 2D static culture systems (6-, 24- or 48-well plates). CMs were cultured in differentiation medium on surfaces coated with CELLstart CTS (Invitrogen), according to manufacture instructions. Cells were cultivated in incubators at 37°C, in a humidified atmosphere of 5% CO<sub>2</sub>, until further analysis.

### 3.2.2 Disposable single-use bioreactors

CM differentiation of miPSCs was also evaluated in two types of disposable single-use computer controlled bioreactors: 1) wave agitated bioreactor (WAVE Bioreactor™ 20/50 and WAVEPOD™ II; GE Healthcare) and 2) pneumatically mixed bioreactor (Pneumatic Bioreactor System, PBS 3 Air-Wheel Bioreactor System; PBS Biotech).

**1) Wave Bioreactor:** miPSCs were inoculated in the wave Cellbag™ (GE Healthcare) as single cells, at a concentration of  $0.7 \times 10^5$  cell/mL, under defined conditions (temperature: 37°C; DO: 4% O<sub>2</sub>, approximately 20% air saturation; CO<sub>2</sub>: 5%; surface aeration rate: 0.1vvm; rocking angle: 4°; agitation rate: 10-26rpm). Cells were cultured in differentiation medium supplemented with 100µM Ascorbic acid and 0.025% (v/v) Antifoam C emulsion (Sigma-Aldrich). Different starting volumes were evaluated, namely 300mL and 500mL. At day 2, aggregate concentration was adjusted to yield 150 aggregates/mL by increasing the working volume of the culture up to 500mL and 1000mL respectively. At day 9, cell lineage selection was induced by performing a partial medium exchange (50% v/v) by replacing culture medium for fresh differentiation medium supplemented with 8µg/mL Puromycin. At day 11, the produced miPSC-derived CMs were harvested, dissociated and transferred to 2D culture systems, as described above (Section 3.2.1), for cell characterization and functionality tests. Data acquisition and process control were performed using UNICORN DAQ 1.0 Control Software.

**2) Pneumatically mixed Bioreactor:** The aggregation step was performed in Erlenmeyers (shake flasks) as described above (Section 3.2.1). At day 2, miPSC aggregates were inoculated at 150 aggregate/mL in the PBS bioreactor under defined conditions (temperature: 37°C; DO: 4% O<sub>2</sub>, approximately 20% air saturation; CO<sub>2</sub>: 5%; surface aeration rate: 0.1vvm via micro and macrosparger). Cells were cultured in differentiation medium supplemented with 100µM Ascorbic Acid and 0.025% (v/v) Antifoam C emulsion. Stirring rate was kept between 15-32 rpm. At day 9, cells were harvested from the bioreactor. Data acquisition and process control were performed using PBS Biotech Control Software (VxWorks OS).

### **3.3 Cryopreservation and hypothermic storage of CMs derived from miPSC**

CMs derived from miPSCs were cryopreserved using different freezing solutions: Cryopreservation medium (90% FBS and 10% (v/v) Dimethyl Sulfoxide (DMSO; Sigma-Aldrich)), Cryostor™CS10 (Stem Cell Technologies) and PRIME-XV (Irvine Scientific). Before cryopreservation using the FBS+10% DMSO formulation, CMs were pretreated with 10µM of Rho-associated kinase inhibitor (ROCKi; Millipore), diluted in differentiation medium, for 1 hour at 37°C. In addition, a low temperature storage solution (hypothermic storage: 2-8°C) was also tested, HypoThermosol®-FRS (BioLife Solutions Inc.). Cryopreservation and low temperature storage were tested in 2D cell monolayers and 3D aggregate systems.

### 3.3.1 Cryopreservation of 2D monolayers

Freezing: Cells were plated at  $1 \times 10^6$  cell/well in 24-well plates, coated with CELLstart, and maintained for 7 days in culture. At day 7, cells were cryopreserved in 300  $\mu$ L of freezing solution (mentioned above) using a controlled rate freezer, Planer Kryo 560-16 (Cryo), using the following program: 1) Hold temperature at 4°C for 20min; 2) Initiate temperature decrease at a freezing rate of  $-1^\circ/\text{min}$  until  $-80^\circ\text{C}$ .

Thawing: Cryopreserved cells were thawed in a 37°C water bath and a three-step dilution (1:1, 1:2 and 1:4) in differentiation medium was performed in order to dilute the DMSO while reducing the osmotic shock. Post-thaw studies were performed directly in the cell plates.

### 3.3.2 Cryopreservation of 3D aggregates

Freezing: CM aggregates were transferred to cryovials at 300 aggregate/vial and 700  $\mu$ L of freezing solution (mentioned above) was added to each vial. Aggregates were allowed to equilibrate in the freezing solution for 20min at 4°C. Samples were frozen to  $-80^\circ\text{C}$  in an isopropanol-based freezing system ("Mr. Frosty", Nalgene), at a cooling rate very close to  $1^\circ\text{C}$  *per* minute, and stored in the gas phase of liquid nitrogen ( $\text{LN}_2$ ) reservoir until their thawing.

Thawing: Following cryopreservation, cells were quickly thawed placing cryovials in a 37°C water bath. A three-step dilution (1:1, 1:2 and 1:6) in differentiation medium was performed immediately after thawing. Aggregates were then transferred to 12-well plates for post-thaw studies.

### 3.3.3 Hypothermic storage of CMs derived from miPSC

miPSC-derived CMs were stored in HypoThermosol®-FRS as 2D cell monolayers and 3D aggregates. CMs were plated at  $1 \times 10^6$  cell/well, in coated 24-well plates, and aggregates were transferred to cryovials at 300 aggregate/vial. For these approaches, 300  $\mu$ L and 700  $\mu$ L of storage solution was added, respectively. CMs were stored at 4°C during 7 days. After this period, storage solution was removed, CMs were washed once with warm medium and differentiation medium was added. Stored aggregates were transferred to 12-well plates and post-thaw studies were carried out in 2D and 3D stored cells.

### 3.3.4 Assessment of cell recovery of CMs

Cell recovery was assessed with PrestoBlue™ assay (thoroughly explained in Section 3.5) before freezing, after thawing and during days 1, 3 and 7 of the post-thawing process. Results were expressed in terms of percentage of cell recovery in relation to the control (cells before freezing). Medium exchanges were performed at days 1, 3 and 7.

### 3.4 Cardiotoxicity and cardioprotective assays

miPSC-derived CMs were inoculated at  $10^5$  cell/well in 48-well plates coated with CELLstart, for 2D cell monolayers, and approximately 5 Agg/well, for 3D experiments. In both approaches cells were cultured in differentiation medium.

Cardiotoxicity assay: To induce oxidative stress, CMs were incubated with hydrogen peroxide ( $H_2O_2$ ; Sigma-Aldrich) diluted in differentiation medium for 20 hours, using concentrations ranging from 50-900  $\mu$ M. After incubation, cells were washed 3 times with warm Phosphate-buffered saline (PBS; Invitrogen) and cell viability was assessed before and after stress induction with PrestoBlue™ assay (Section 3.5). Results were expressed in terms of percentage of cellular viability in relation to the control (cells incubated with differentiation medium only).

Cardioprotective assay: Cardioprotective evaluation assay was performed using an antioxidant compound, catechin. CMs were pretreated with catechin diluted in differentiation medium for 24 hours, using different concentrations: 150mg/L and 300mg/L. After pretreatment, cells were washed 3 times with warm PBS and oxidative stress was induced with  $H_2O_2$  (400 and 500  $\mu$ M) for 20 hours. Control wells were performed with differentiation medium only and with differentiation medium supplemented with  $H_2O_2$ . Cell viability was assessed three times: i) before catechin pretreatment; ii) after catechin pretreatment and iii) after oxidative stress incubation. Results were expressed in terms of percentage of cellular viability in relation to the control (cells incubated with differentiation medium only).

### 3.5 Cell viability evaluation

Cell Membrane Integrity assay: Culture viability was assessed using 2 enzyme substrates: fluorescein diacetate (FDA; Sigma-Aldrich) and propidium iodide (PI; Sigma-Aldrich). Cells were incubated with 20  $\mu$ g/mL FDA and 10  $\mu$ g/mL PI in PBS for 2-3min and then visualized using fluorescence microscopy (DMI6000, Leica). FDA is a non-polar, non-fluorescent fluorescein analogue which enters all cells freely. In viable cells, FDA is converted by intracellular esterases to highly fluorescent fluorescein and confers cells green fluorescence. PI is a polar, red colored fluorescent compound that only enters cells with lack of membrane integrity, intercalating with DNA and therefore nucleus dying/dead cells stain red [135].

Trypan Blue exclusion method: Total number of viable cells was determined after incubation with 0.1% (v/v) Trypan Blue dye (Invitrogen) in PBS. Using a Fuchs-Rosenthal haemocytometer chamber, cells with damaged membranes (non-viable) stain blue in presence of this compound.

Lactate Dehydrogenase (LDH) activity: LDH activity, from the culture supernatant, was determined following spectrophotometrically (at 340 nm) the rate of oxidation of NADH to NAD<sup>+</sup> coupled with the reduction of pyruvate to lactate. The specific rate of LDH release (qLDH) was calculated for each time interval using the following equation:  $q_{LDH} = \Delta LDH / (\Delta t \times \Delta X_V)$ , where  $\Delta LDH$  is the change in LDH activity over the time period  $\Delta t$ , and  $\Delta X_V$  is the average of the total cell number during the same period. The cumulative value qLDH<sub>cum</sub> was estimated by  $qLDH_{cum\ i+1} = qLDH\ i + qLDH\ i+1$ . This assay is a useful tool to monitor cell lysis since LDH is an intracellular enzyme that is only presented in culture supernatant when the cell membrane is damaged.

PrestoBlue™ assay: Metabolic activity was determined using the metabolic indicator PrestoBlue reagent following the manufacture's recommendation (Invitrogen). Briefly, cells were incubated for 1-2 hours with fresh culture medium containing 10% (v/v) PrestoBlue reagent. Fluorescence was measured (excitation wavelength: 570 nm, emission wavelength: 585 nm) using a microwell plate fluorescence reader FLx800 (Biotek). The active ingredient of prestoBlue (resazurin) is a nontoxic non-fluorescence indicator dye that is converted to red-fluorescent resorufin via the reduction reaction of metabolically active cells. Produced fluorescence is proportional to the number of live and metabolic active cells. Thus, PrestoBlue assay provides a quantitative measure of cell viability and metabolic activity.

### 3.6 Evaluation of aggregate concentration and size

The number of total aggregates and eGFP positive aggregates were counted in 4-6 wells of a 24-well plate, containing 250-400 $\mu$ L of culture samples, using a phase contrast and fluorescence inverted-microscope (Leica Microsystems GmbH). Using this microscope and ImageJ software, aggregate size was determined by measuring two perpendicular diameters of each aggregate, from a minimum of 30 aggregates. These measures were used to calculate the average diameter of each aggregate. Aggregates with less than 20 $\mu$ m diameter, generally duplets or triplets, were not considered.

### 3.7 Culture yields determination

Expansion Fold (Cells/miPSCs): Fold increase (FI) in cell concentration was determined based on the ratio  $Cells_{day9} / input\ miPSCs$ , where  $Cells_{day9}$  is the total cell number at day 9 and input miPSCs is total cell number at day 0 (i.e. cell inoculum).

Differentiation Yield (CMs/miPSCs): Differentiation yield was determined based on the ratio  $CMs_{day16} / input\ miPSCs$ , where  $CMs_{day16}$  is the total number of GFP positive cells on day 16 and input miPSCs is total cell number at day 0 (i.e. cell inoculum).

CMs generated per liter of culture medium throughput (CMs/L): CMs generated per liter of culture medium throughput was determined based on the ratio  $CMs_{day16}/V_{total}$ , where  $CMs_{day16}$  is the total number of GFP positive cells on day 16 and  $V_{total}$  is the total volume of differentiation medium used in the bioprocess.

Cell recovery (%): Cell recovery was determined based on the ratio  $CMs_{d16}/Cells_{d9}$  (in terms of percentage), where  $CMs_{day16}$  is the total number of GFP positive cells on day 16 and  $Cells_{d9}$  is the total cell number at day 9 (before CM selection)

### **3.8 Characterization of miPSCs and miPSC-derived CMs**

Alkaline Phosphatase (AP) Staining: Undifferentiated PSCs are characterized by high expression levels of alkaline phosphatase (AP). Cultures were stained using an AP activity detection kit (Millipore) according to the manufacturer's instructions and observed under phase contrast microscopy. Positively stained miPSCs (purple) were considered undifferentiated cells.

#### **3.8.1 Structural characterization**

Immunocytochemistry: miPSCs cultures were fixed in 4% (w/v) paraformaldehyde (PFA, Sigma-Aldrich) in PBS for 20min, permeabilized for 15min with 0.1% (w/v) Triton X-100 solution (Sigma-Aldrich), for Oct-4, and incubated with primary antibody overnight at 4°C in 0.125% (w/v) fish skin gelatin (FSG, Sigma-Aldrich) in PBS. Primary antibodies used were: Oct-4, SSEA-1 (1:200, all Santa Cruz Biotechnology) and SOX2 (1:500, Millipore). Cells were washed three times in PBS and the secondary antibodies were applied to the cells for 60min at room temperature in the dark. After three washes with PBS, cell nuclei were counterstained with Hoechst 33432 (Sigma-Aldrich). Secondary antibodies used were: AlexaFluor 488 goat anti-mouse IgG and AlexaFluor 488 goat anti-mouse IgM (1:200 dilution in 0.125% (w/v) FSG in PBS; both antibodies from Invitrogen).

CM cultures were fixed in 4% (w/v) PFA in PBS for 20min, permeabilized for 10min with 0.5M Ammonium chloride (Sigma-Aldrich), 0.25% Triton X-100 in PBS at room temperature and blocked with 5% FBS in PBS for 60min at room temperature. Cells were incubated with primary antibody overnight at 4°C in 0.8% (w/v) bovine serum albumin (BSA, Sigma-Aldrich) in PBS. Primary antibodies used were:  $\alpha$ -sarcomeric actinin (1:200, Sigma-Aldrich), titin (1:100, Santa Cruz Biotechnology), troponin I (TnI, 1:100, Millipore) and anti-atrial natriuretic peptide (ANP, 1:200, Millipore). Cells were washed in PBS and secondary antibodies were applied for 60min at room temperature in the dark. Secondary antibodies



used were: AlexaFluor 594 goat anti-mouse IgG (1:200 dilution in 0.8% (w/v) BSA (Sigma-Aldrich) in PBS, from Invitrogen). Nuclei staining was assessed using Hoechst.

Flow Cytometry analysis: For SSEA-1 (stage-specific embryonic antigen-1) positive cell analysis, miPSC colonies were dissociated into single cells with 0.05% (w/v) EDTA/Trypsin and afterwards resuspended in washing buffer (WB) solution (5% (v/v) FBS in PBS). After two washing steps, cells were incubated with the primary antibody, SSEA-1 (1:10 in PBS), for 1 hour at 4°C, washed three times in WB and then incubated with the secondary antibody, AlexaFluor 488 goat anti-mouse IgM (1:200), for additional 30min at 4°C. After two washing steps with WB, cells were resuspended in WB and analyzed in a flow cytometry instrument (CyFlow space, Partec). Ten thousand events were registered *per sample*.

For eGFP positive cell analysis, cell aggregates were dissociated into single cells with 0.25% (w/v) Trypsin/EDTA and afterwards resuspended in WB solution. Cells were incubated for 2min with PI (1:1000) and analyzed in the flow cytometry instrument. The percentage of eGFP positive cells reflects culture purity throughout the differentiation process. Ten thousand events were registered *per sample*.

Semiquantitative and quantitative RT-PCR: Aggregates were sedimented, washed with PBS and centrifuge at 300 x *g* for 5min. The pellet was snap-frozen by immersion in liquid nitrogen. Total RNA was extracted using the High Pure RNA Isolation Kit (Roche), and reverse transcription was performed with High Fidelity cDNA Synthesis Kit (Roche), following manufacturer's instructions. Gene expression profiles of various markers during cardiac differentiation were analyzed by RT-PCR using the DreamTaq Green PCR Master Mix (Thermo Scientific). In 20µL reactions with final primer (Table 7.1 – Section 7, Page 77) concentrations of 0.5µM, 1µL of cDNA template was used. After RT-PCR, 10µL of the reaction were loaded on a 1.5% agarose (Invitrogen) gel. Bands were detected with a CCD camera using Intas UV-System and Intas GDS application (Intas). Relative quantification of gene expression was performed using SYBR Advantage qPCR Premix (Clontech) in 10µL reactions with a 1:25 diluted cDNA template and 0.2µM final primer concentrations. The reactions were performed in 384-well plates using AB 7900HT Fast Real Time PCR System (Applied Biosystems). Cycle threshold (Ct's) and melting curves were determined by SDS 2.1 Software. All data was analyzed using the comparative CT method ( $2^{-\Delta\Delta Ct}$  method) for relative gene expression analysis. Changes in gene expression were normalized to GAPDH gene expression as internal control.

### **3.8.2 Functional characterization**

Electrophysiological Characterization: Purified CMs were washed twice with PBS (Invitrogen) and dissociated using 0.05% Trypsin/EDTA (Invitrogen) 2 days before measurement. Single CMs were plated on glass cover slips coated with 0.1 % gelatin. Patch clamp-experiments were performed as described previously [136]. Briefly, the cover slips were placed into a recording chamber (37°C) and cells were continuously perfused with extracellular solution (as described in [136]). Cell membrane capacitance was determined online using Pulse software (Heka Elektronik). Action potential (AP) recordings of spontaneously beating CMs were performed utilizing the whole-cell current-clamp technique with an EPC-9 amplifier (HEKA Elektronik) and operated through the Pulse acquisition software. Response to hormonal regulation was analyzed by administering 1  $\mu$ M isoproterenol and 1  $\mu$ M carbachol (both from Sigma-Aldrich).

Detection of Ca<sup>2+</sup> Transients: Ca<sup>2+</sup> imaging was performed according to the standard protocol provided in Rhod-3- Calcium Imaging kit (Invitrogen). Briefly, cells were labeled with Rhod-3 for 1h at 37°C, washed twice in PBS, incubated for 1h with a water-soluble reagent to reduce baseline signal and washed again in PBS. Cells were imaged live using a spinning disk confocal microscope (Nikon Eclipse Ti-E; System: Andor Revolution XD; Confocal Scanner: Yokogawa CSU-x1) and Calcium transients were determined using Micro-Manager 1.4 and ImageJ softwares.

### **3.9 Statistical analysis**

Statistical analysis was determined with a single-factor analysis of variance (ANOVA), using Microsoft Excel's data-analysis toolpack (Microsoft Corporation). Three independent experiments were performed. A 95% confidence level was considered to be statistically significant.

## 4. Results and Discussion

### 4.1 Bioprocess engineering of miPSCs

#### 4.1.1 Production of miPSC-derived CMs in fully controlled bioreactors

The first task of this thesis was the development of a robust, scalable and integrated strategy for the production and selection of CMs derived from miPS cells. For this purpose, a murine transgenic  $\alpha$ PIG-iPS cell line was used. This cell line was genetically modified to integrate and stably express a transgene containing puromycin-N-acetyl transferase and eGFP genes, both under control of the cardiac-restricted promoter alpha myosin heavy chain ( $\alpha$ -MHC). This characteristic enables an easy monitoring of the cardiac differentiation process, by assessing GFP expression over time (by fluorescence microscopy and/or flow cytometer analyses), and CM selection upon addition of puromycin in the culture media. Some studies have shown that this cell enrichment approach is highly efficient, capable of obtaining pure populations of PSC-derived CMs [102, 103].

miPSCs were propagated as colonies on monolayers of inactivated feeder cells (mouse embryonic fibroblast; MEFs). These feeder cells support the growth of pluripotent stem cells by producing growth factors and providing adhesion molecules and ECM components for cell attachment [46]. Medium is supplemented with LIF to further maintain the cells pluripotent state throughout propagation [137]. Before initiating the differentiation and CM production procedure, the undifferentiated state and pluripotency of miPSCs was evaluated by immunofluorescence microscopy, flow cytometry analysis and by alkaline phosphatase activity test (Figure 4.1).

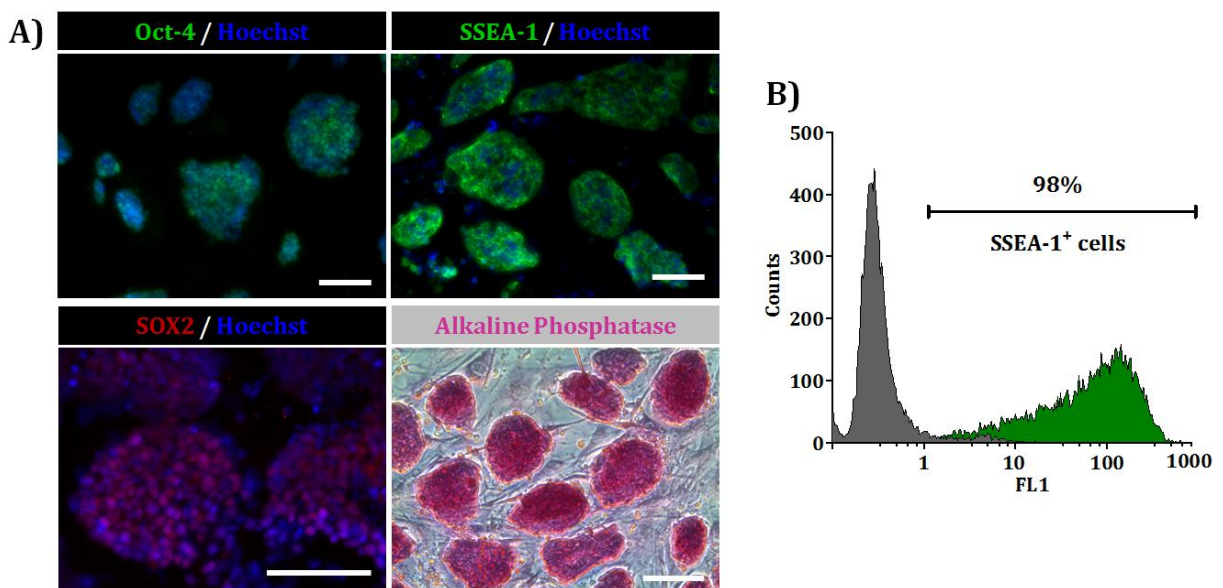


**Figure 4.1: Characterization of miPSCs.** A) Immunofluorescence images of Oct-4, SSEA-1 and SOX2 labeling, and phase contrast picture of alkaline phosphatase activity. Nuclei were labeled with Hoechst

33432 (blue). Scale bars: 100  $\mu\text{m}$ . **B)** Histogram obtained in flow cytometry analysis of SSEA-1 positive cells before bioprocess initiation.

Figure 4.1A shows that miPSCs stained positive for specific stem cell markers (OCT-4, SSEA-1 and SOX2) and presented alkaline phosphatase activity. The percentage of SSEA-1 positive cells was high (98%, Figure 4.1B), indicating that almost the entire population had an undifferentiated and pluripotent phenotype.

Different bioreactor designs were evaluated and compared in terms of their ability to support miPSC growth and CM differentiation namely, stirred tank bioreactor (Stirred Tank BR), Wave bioreactor (Wave BR) and a pneumatically mixed bioreactor (PBS BR). All these bioreactor systems are capable of an automated process control, online measurement and adjustment of the culture parameters. Stirred tank BRs have been widely used in the pharmaceutical industry and more recently in stem cell biomanufacturing [15]. Wave and PBS BR are single-use technologies that offer unique advantages for the bioprocessing of stem cells, such as a low shear stress environment, improved mass and oxygen transfer, rapid medium homogeneity and unique agitation types (as previously mentioned in Section 1.2.6).

In these experiments, miPSCs were cultivated in 4% dissolved oxygen (hypoxia conditions). Our group and others have shown that low oxygen tensions/concentrations (2-5%) enhance PSC proliferation [67, 68] and CM differentiation [69, 70]. In fact, during cardiomyogenesis, many cues and processes are influenced by hypoxia conditions (reviewed in [138]). Therefore, hypoxia conditions were used in all tested bioreactors aiming to favor cell expansion and CM-lineage differentiation.

Recent evidences suggest that mechanical stimulation enhances CM differentiation of PSCs, contractile function and up-regulates cardiac gene expression [139, 140]. Thus our strategy consisted in varying the agitation type and profile on each bioreactor system to promote cyclic mechanical stimuli to the cells and ultimately potentiate their differentiation towards CMs.

miPSCs were cultured in bioreactors as 3D aggregates, as this approach has been shown to enhance cell differentiation and functionality [79]. Cell aggregation step was performed in Erlenmeyer flasks for 2 days. At day 2, miPSC aggregates presented high viability and an average size of 155 $\mu\text{m}$ , ranging from 70 to 270 $\mu\text{m}$  (Figure 4.2); these aggregates were transferred to Stirred Tank and PBS BR at a final concentration of 150 aggregates/mL in a working volume of 200mL and 2L, respectively. The Wave BRs were inoculated with single cells and cell aggregation step was promoted inside the Cellbag™. By day 2, cell aggregates presented high cell viability and similar size distribution as the ones produced in Erlenmeyer flasks (Figure 4.2). Aggregate concentration was adjusted in the

Wave BR to yield 150 aggregates/mL, by addition of differentiation medium (Materials and Methods, section 3.2.2).

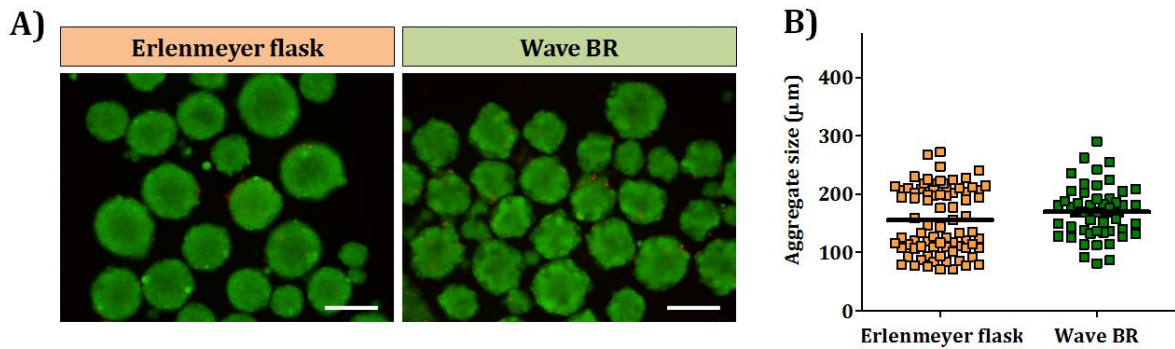


**Figure 4.2: miPSCs aggregation step.** Cell aggregation was evaluated in Erlenmeyer flasks and in the Wave BR. **A)** Viability analysis of miPSCs aggregates at day 2 using FDA (live cells, green) and PI (dead cells, red). Scale bars: 200 µm. **B)** Comparison of aggregate size at day 2.

Two working volumes were tested in Wave BRs: 0.5L and 1L. In all culture systems, cell aggregates were cultured in the presence of ascorbic acid for additional 7 days. At day 9, CM lineage selection was promoted by addition of puromycin to the culture medium. Cardiospheres (pure CM aggregates) were harvested at day 11, in Wave BRs, and at day 16, in Stirred Tank BRs. Figure 4.3 presents an overview of the differentiation process.

### miPSC Expansion & Differentiation

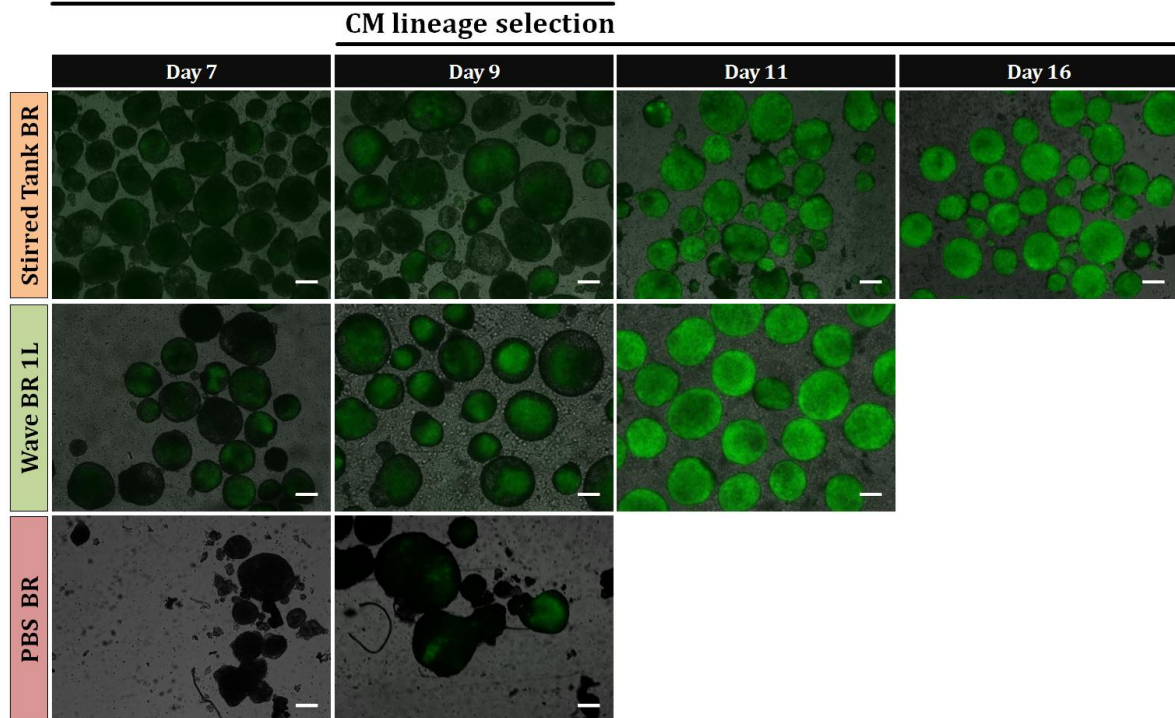


**Figure 4.3: miPSC differentiation into CMs using different bioreactor systems.** Different bioreactor systems were tested for their capacity to support expansion and cardiomyocyte differentiation of miPSC: stirred tank bioreactor (Stirred Tank BR); wave-induced bioreactor (Wave BR); pneumatically mixed bioreactor (PBS BR). Phase contrast and fluorescence images showing cell aggregates with eGFP<sup>+</sup> cells (green) at days 7, 9, 11 and 16 of the cultures. Scale bars: 200 µm.

The results show that Stirred Tank and Wave BRs were the most suitable culture systems for miPSC-derived CM production. miPSCs cultivated in both bioreactors were able to proliferate and differentiate into CMs (Figure 4.3 and 4.4A). By the end of both processes pure populations of eGFP positive and beating aggregates were achieved (>96% eGFP positive cells, Table 4.1).

On the other hand, the PBS BR revealed to be an unsuitable culture system for miPSC differentiation. Aggregate concentration in PBS BR decreased rapidly until day 9 (Figure 4.4B) and the presence of eGFP positive cells was rarely observed until day 9 of culture (Figure 4.3). In addition, during culture time cell deposition on the bioreactor vessel was observed (Annex 2; Section 7 Figure 7.1). According to the manufacturer's instructions, the used PBS BR model (PBS3) is appropriate for cultivating cells in working volumes from 1.5 to 3L. In our experiments, PBS BR started with a 2L working volume. However, to monitor the culture, extensive sampling was collected throughout culture time, leading to a reduction in the working volume (below 1.8L). This resulted in unexpected foam formation due to the air-wheel mixing above the gas-liquid interface (Annex 2; Section 7 Figure 7.1). In addition, the air-wheel mixing mechanism captures rising bubbles, from macro sparging, and converts them into rotational mixing power. Bioreactor sparging is used as a method to efficiently supply oxygen to cells [141]. However, bioreactor sparging and foam formation are responsible for bubble-associated damage [141] (e.g. bubble formation at sparger, bubble burst at fluid surface) which presents major damage to animal cells that lack a protective cell wall [142]. Although an antifoam emulsion was added, adverse effects from foam formation occurred. These results suggest that higher concentrations of this antifoam agent should be tested, as antifoam must be supplied in sufficient quantity to prevent foam formation during air-wheel mixing of the bioreactor.

Figure 4.4 presents the main results obtain from the previous BR processes.

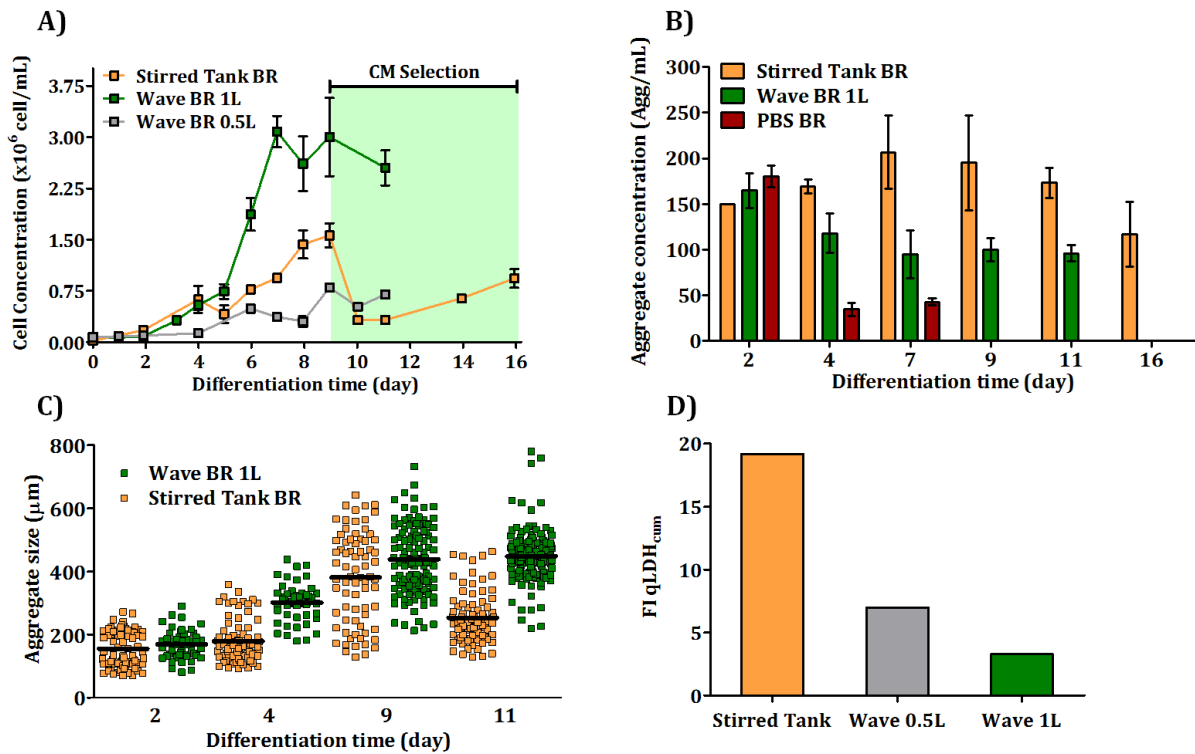


**Figure 4.4: Production of miPSC-derived CMs using fully controlled bioreactors.** Main results obtained from miPSC bioprocessing using different environmentally controlled bioreactor systems. Profiles of cell concentration **(A)**, aggregate concentration **(B)** and aggregate size **(C)** during culture time. **D)** Fold increase in LDH release cumulative values until culture day 9.

As mentioned before, two different working volumes were tested in Wave BR, namely 0.5 and 1L. Figure 4.4A shows that 1L is the most suitable working volume for expansion and differentiation of miPSCs into CMs, since higher cell numbers were achieved throughout the culture. In addition, Wave BR 1L resulted in an overall bioprocess improvement, achieving a 3.8-fold increase in miPSC expansion (72.9 Cells<sub>day9</sub>/input miPSCs) and a 5.3-fold higher differentiation yield (60.1 CMs/input miPSCs) over the Wave BR 0.5L. Nonetheless, the Wave BR 0.5L was also able to produce highly pure CMs (97%; Table 4.1). On the other hand, when a working volume of 0.5L was used with the Wave BR, cell/aggregate deposition on the sides of the Cellbag™ was observed (Annexes 2; Section 7 Figure 7.1), resulting in a 2-fold higher cell lysis until day 9 (Figure 4.4D). Fold increase in LDH release was calculated until day 9, since from this timepoint onwards antibiotic selection was induced, and cell death also resulted from antibiotic-based selection. According to the manufacturer's instructions, the used Cellbag™ is appropriate for cultivating cells with working volumes between 0.1 and 1L. However, our results showed that for the cultivation of miPSCs as cell aggregates, 0.5L is not appropriate and higher working volumes should be used.

The results show that both, Stirred Tank and Wave BRs, enhanced cell proliferation. Although higher cell concentrations were observed in the Wave BR 1L (Figure 4.4A), similar expansion folds were obtained on both bioreactors (Table 4.1 - Stirred Tank BR: 72.4

Cells<sub>day9</sub>/input miPSCs; Wave BR 1L: 72.9 Cells<sub>day9</sub>/input miPSCs). However, the Stirred Tank BR presented a higher fold increase in LDH accumulation, achieving a 5.8-fold increase when compared to the Wave BR 1L, which is in fact the highest LDH release obtained from the compared bioprocesses (Figure 4.4D). This difference in LDH release may be related to shear stress issues. Wave BRs have been shown to promote a lower shear stress environment when compared to standard Stirred Tank BRs, due to its gentle rocking motion [94]. Since a wave-induced agitation presents less shear damage to cells/aggregates, higher cell viabilities may be obtained in Wave BR than in Stirred Tank BR cultures. In contrast to the Stirred Tank BR, higher cell concentration and lower aggregate concentration was observed in Wave BR 1L during differentiation time (Figure 4.4A-B). The Wave BR 1L presented higher aggregate sizes (around 450µm on days 9 and 11, Figure 4.4C), and consequently higher number of cells per aggregate. For example, by day 9, aggregates from Wave BR 1L were composed by  $3 \times 10^4$  cell/agg, as for aggregates from Stirred Tank BR were only composed by  $8 \times 10^3$  cell/agg. The higher aggregate sizes (600/800µm) observed in Wave BR, may be due to some aggregate fusion promoted by the gentle wave-induced agitation characteristic of these bioreactors. Nevertheless, no harmful cell clumping or necrotic centers were observed in Wave BR 1L culture (Figure 4.4A).

To analyze the effect of different agitation types on miPSCs differentiation towards CM lineage, differentiating cells were characterized based on their gene expression and levels of eGFP positive cells, throughout the process. RT-PCR and flow cytometry analyses were performed to compare/evaluate cardiomyocyte differentiation throughout culture time in both Stirred Tank and Wave BRs. RT-PCR analysis confirmed that miPSCs differentiated earlier into CMs in the Wave BR, as an earlier and enhanced expression of mesoderm and cardiac specific genes was observed, when compared to the Stirred Tank BR (Figure 4.5A). The expression of the pluripotent gene Oct-4 decreased more rapidly, reaching very low levels on day 6 of differentiation and undetectable levels from day 8-9 onwards (Figure 4.5A). In contrast, Oct-4 is still highly expressed at this stage of differentiation in the Stirred Tank BR and was only undetectable in the purified CMs. T-Brachyury, a mesodermal marker, reached a peak of expression earlier in the Wave BR (day 4). Also, the expression of the cardiac specific markers (cTnT, Nkx2.5, HCN4, Myl2 and Myl7) was detected earlier in Wave cultures. These findings are in agreement with the results obtained in flow cytometry analysis. In Wave bioreactor cultures, eGFP positive cells were detected from day 5 onwards. For example, by day 7, 46% of the cells were eGFP positive whereas in Stirred Tank BR, at the same timepoint, only few cells were eGFP positive (Figure 4.5B). In addition to earlier expression of cardiac specific markers in Wave cultures, greater band intensities were also observed before CM selection (day 9), indicating a substantial enhancement in the expression



of the cardiac specific markers in Wave cultures when compared to Stirred Tank cultures. At this timepoint, RT-qPCR also confirmed that cTnT and Myl7 were highly expressed in Wave BRs than in Stirred Tank BR (Figure 4.5C). These results corroborate with the percentage of eGFP positive cells determined at day 9. Before CM selection, the percentage of eGFP positive cells in the Wave BR (82%) was 2.5-fold higher when compared to the Stirred Tank BR (32%; Figure 4.5B). Consequently, only 2 days of antibiotic treatment were sufficient to obtain a pure CM population (>97% eGFP positive cells) in Wave bioreactors whereas 7 days were required to reach the same purity in the Stirred Tank BR (Figure 4.5B). At the end of both bioprocesses, expression of cTnT reached similar levels, whereas Myl7, a marker of atrial-like CMs, presented higher expression in Wave cultures (Figure 4.5C).

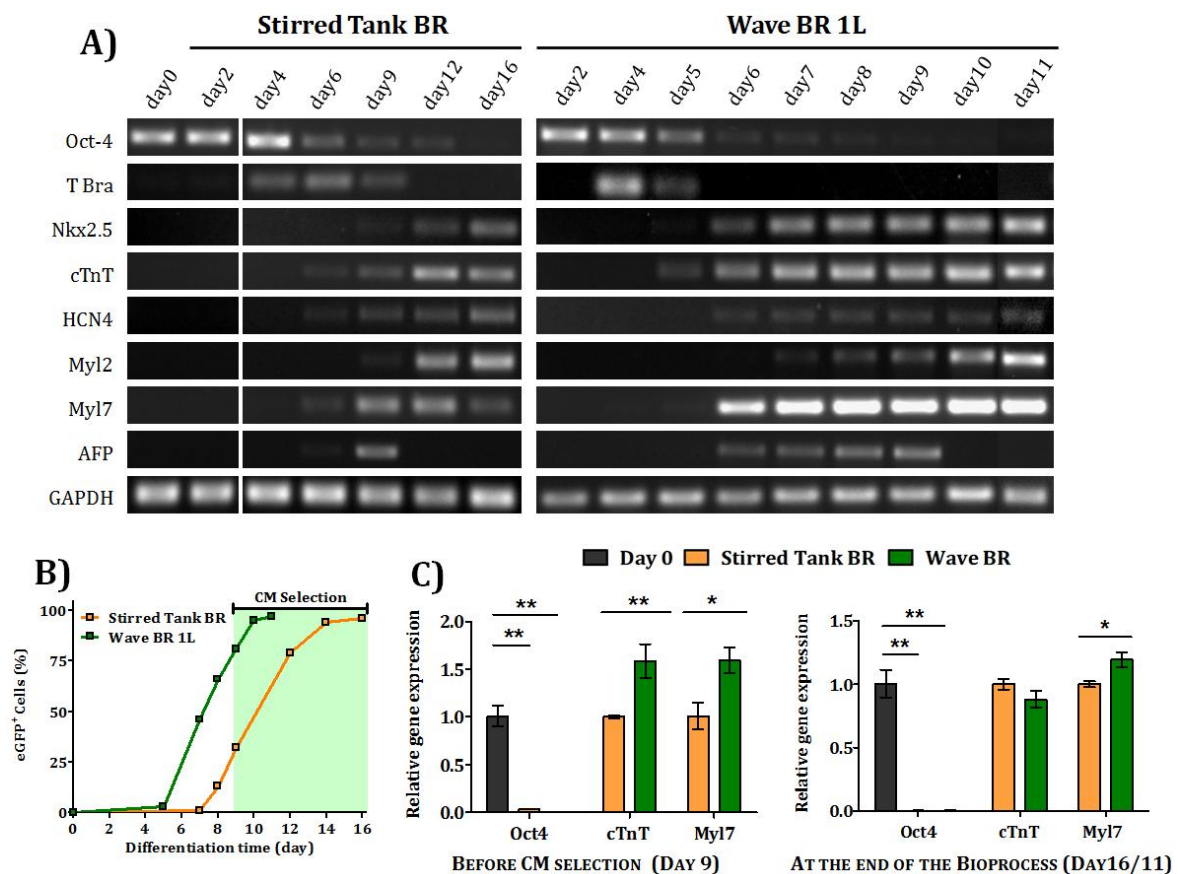


**Figure 4.5: Evaluation of gene expression and levels of eGFP positive cells during CM production in Stirred Tank and Wave BRs.** RT-PCR was used to assess changes in gene expression during miPSC expansion and differentiation into CMs. Flow cytometry was assessed to quantify the levels of eGFP positive cells during culture time. **A)** Semiquantitative RT-PCR analyses demonstrating the expression of pluripotency (Oct-4), endoderm (AFP), mesoderm (T-Bra) and CM-specific (Nkx2.5, cTnT, HCN4, Myl2, Myl7) genes during the time course of differentiation process in Stirred Tank and Wave BRs. **B)** Percentage of eGFP<sup>+</sup> cells during culture time, determined by flow cytometry analysis. **C)** Quantitative RT-PCR analysis of cells cultured in both Stirred Tank and Wave BRs, before CM selection (day 9) and at the end of the process (day 16 and 11 for Stirred Tank and Wave bioreactor cultures, respectively). Data was analyzed using the comparative CT method (Stirred Tank, operating under continuous stirring, was used as a control). Significantly different results: P<0.05 (\*) and P<0.01 (\*\*).

The differences observed in Stirred Tank and Wave culture outcomes, including temporal gene expression patterns and eGFP positive cell levels, may be related with the specific agitation type of both BRs, and consequently with the frequency of stretch applied in both systems. In these experiments, miPSCs were subjected to distinct cyclic strains by varying the agitation type and profile used in BRs. In the Stirred Tank BR, using an intermittent stirring, cyclic tensions at frequencies close to 0.033Hz were promoted, whereas with a Wave-induced agitation higher frequencies were reached (0.43-0.45Hz). Cardiac cells experience mechanical strains with every heartbeat, i.e., at a pulsatile frequency close to 1Hz [143]. Therefore, inducing cyclic tensions at higher frequencies (closer to 1Hz) may favor cardiomyogenesis by better mimicking the physiological environment.

miPSCs were successfully differentiated into CMs using environmentally controlled bioreactors. The Stirred Tank and Wave BR processes developed herein showed promising results in the development of robust and scalable strategies for the production and purification/selection of CMs. Table 4.1 presents a quantitative characterization of the Stirred Tank and Wave BR processes.

**Table 4.1: Quantitative characterization of CM production derived from miPSCs using environmentally controlled bioreactors.**

Strategy	Stirred Tank BR	Wave BR 0.5L	Wave BR 1L
Cell inoculum ( $\times 10^6$ cell)	4.3	20.9	38.9
Expansion Fold ( $\text{Cells}_{\text{day}9}/\text{input miPSCs}$ )	72.4	19.2	72.9
Differentiation Yield ( $\text{CMs}_{\text{d}16}/\text{input miPSCs}$ )	29.7	11.5	60.2
Total Cell Number ( $\times 10^6$ cell)	133.2	248.0	2420.0
Final CM Purity (%)	96.0	97.0	97.0
Total CM Number ( $\times 10^6$ cell)	127.9	240.6	2347.4
Final CM number per Liter ( $\times 10^8$ CMs/L)	3.0	3.2	16.5

The high degree of heterogeneity observed in the differentiated population derived from PSCs represents a considerable hurdle towards the application of these cells in clinical applications. The transgenic enrichment strategy used in this thesis presents a possible solution for this issue, capable of producing highly pure CMs (96-97%). Genetic-based selection strategies have been shown to enrich stem cell derived populations (reviewed in [54]). However, these methods are not ideal for clinical applications, requiring genetic manipulations and the use of costly and time consuming processes (previously stated in the Introduction, Section 1.3.1). Non-genetic purification of CMs should be tested over the use of a transgenic enrichment strategy. For instance, an interesting approach could be to exploit the distinct metabolic requirements of CMs and non-CM cell types. Previous studies have

stated that it is possible to achieve a CM purity of 99% when using a glucose depleted culture medium containing abundant lactate [110]. As the Wave BR strategy achieves purity levels of 81% before CM enrichment, this strategy could prove promising in the development of a non-genetic purification step in the bioprocess developed herein.

As previously discussed, in the Stirred Tank BR lower differentiation yields were obtained when compared to the Wave BR, possibly due to the lower cyclic strain frequencies (0.033Hz) applied in this BR. Nonetheless, it should be noted that Stirred Tank and Wave BR strategies developed herein presented higher differentiation yields when compared to the ones reported in literature: 3.77 CM/PSC [70], using a 0.25L DASGIP model; 6.4 [98] and 23 CM/PSC [99], using a 2L Biostat Sartorius BR (see Table 1.2, Section 1.2.6).

The number of CMs generated per liter of culture medium throughput (CMs/L) is a common parameter used to measure the cost-effectiveness and scale-up potential of a stem cell bioprocess [99], in which expensive medium and growth factors are used. Thus, this value can be used to compare CM productivity of different stem cell bioprocesses. The Stirred Tank BR system showed the lowest CM productivity,  $3.0 \times 10^8$  CMs/L. On the other hand, the Wave BR 1L, resulted in a 5.4-fold increase in CM productivity ( $16.5 \times 10^8$  CMs/L) over the Stirred Tank and in a 3.2-fold improvement over the highest productivity stated in the literature for mPSC-derived CMs production ( $5.1 \times 10^8$  CMs/L [99]).

All together, these results suggest that Wave BRs are preferable platforms for mass production of CMs since they allow to reach clinically relevant CM productivities in just one liter bioreactor run, present promising capacity to boost CM differentiation and importantly result in a 5 days shorter differentiation protocol .

#### **4.1.2 Development of a perfusion strategy in a stirred tank bioreactor**

The Stirred Tank BR was able to successfully produce pure CMs from miPSCs, nonetheless this BR strategy showed potential to be improved. Perfusion strategies have been developed and integrated in Stirred Tank BRs, ensuring constant media renewal of culture medium and removal of metabolic byproducts [70, 96]. In addition, continuous perfusion-feeding ensures optimal process uniformity with respect to temperature, pH and dissolved oxygen, avoiding the fluctuation in pH and gas composition that normally occurs upon manual medium exchanges [99]. This approach also presents potential for the development of more robust purification/selection protocols, ensuring a culture free of cell debris at the end of the bioprocess. Perfusion strategies have also been developed for single-use disposable bioreactors. However these technologies are still emerging and therefore present high costs and complex devices [144, 145].

With the objective of developing an integrated stirred tank bioreactor approach, with a continuous and automated perfusion system, computer controlled peristaltic pumps with gravimetric control were used. This strategy was integrated during the selection step of the process (i.e. from day 9 onwards). Perfusion rates are an important factor when developing perfusion strategies. Two different perfusion rates were tested: 1) Perfusion rates reproducing the medium exchanges of the semi-continuous Stirred Tank BR process ( $D=0.14-0.36\text{day}^{-1}$ ); 2) Perfusion rates 5 times higher ( $D=0.7-1.8\text{day}^{-1}$ ). Figure 4.6 presents the main results obtained from these experiments.

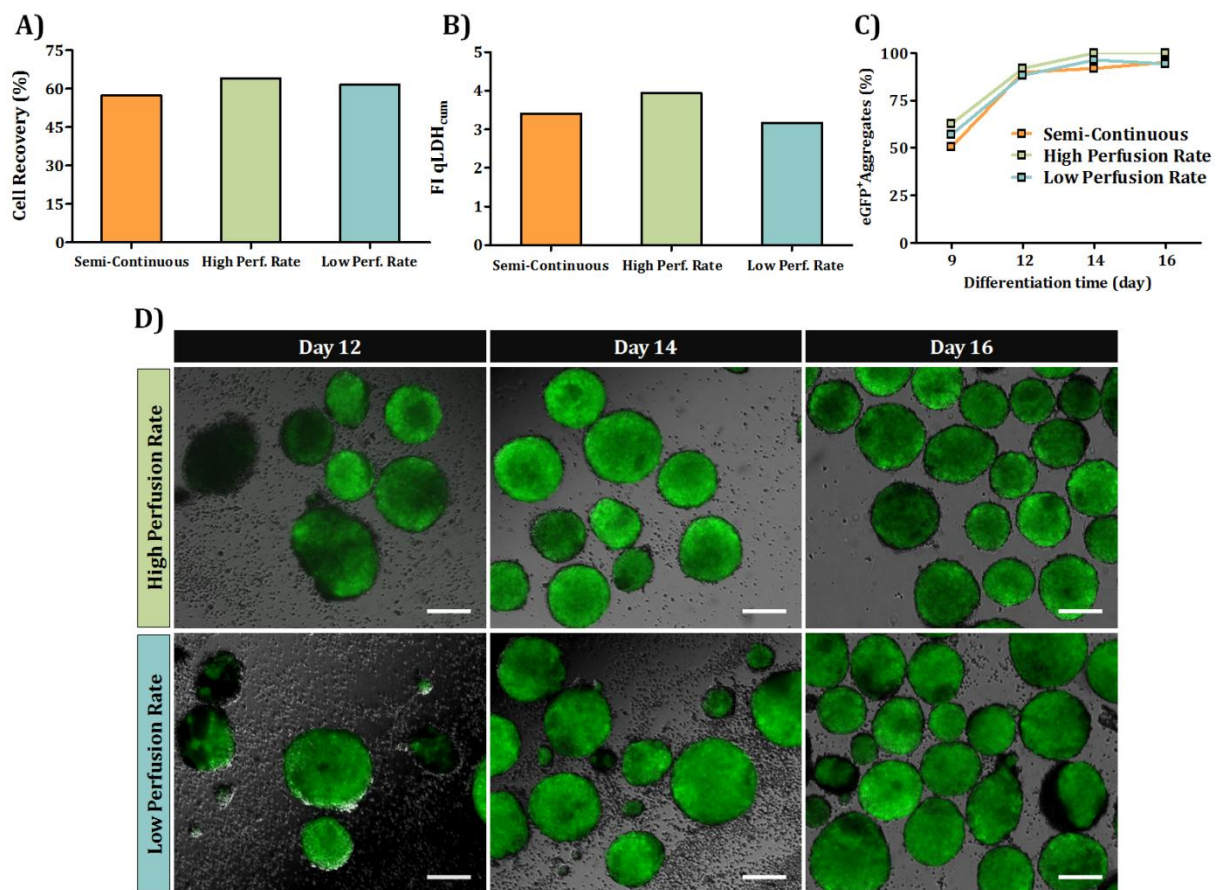


**Figure 4.6: Production of miPSC-derived CMs using a continuous perfusion strategy.** Different perfusion rates were tested: Low perfusion rate (mimics Stirred Tank BR medium exchanges) and high perfusion rate (5 times the rates used for the low perfusion rate). Continuous perfusion and the previous Stirred Tank strategy were compared from day 9 until the end of the process. **A)** Cell recovery at day 16. **B)** Fold increase in LDH release cumulative values during CM selection. **C)** Percentage of eGFP<sup>+</sup> aggregates during selection. **D)** Phase contrast and fluorescence images showing eGFP<sup>+</sup> cells (green) and single cells/cell debris present in the culture supernatant at different time points of the selection process. Scale bar: 200  $\mu\text{m}$ .

The results show that using a continuous perfusion strategy during the selection step presents no adverse effects on culture outcome. Cell recovery during selection was similar using both perfused and manual medium exchange approaches, reflecting no meaningful cell loss due to the perfusion strategy (Figure 4.6A). Also, the continuous addition of fresh

medium with puromycin did not compromise cell viability during antibiotic selection, as no relevant differences were observed in LDH release in perfused and non-perfused bioreactors (Figure 4.6B). Similar profiles of eGFP positive aggregates were achieved in all the tested strategies (Figure 4.6C), showing that the developed perfusion approaches did not compromise cardiac differentiation potential in relation to the previous developed semi-continuous process. In addition, the perfusion rates used in this work did not affect culture purity and CM differentiation yields.

Despite similar culture outcomes, using a higher perfusion rate strategy, a clean culture with no cell debris was obtained at day 16 (Figure 4.6D). In contrary, the lower perfusion strategy was not able to effectively remove cell debris during the selection step. By day 16 single cells and cell debris were observed in higher extend in culture supernatant. This is a major drawback in continuous integrated industrial processes, as this bioprocess would need an additional separation step (e.g. Filtration or Sedimentation) to remove single cells and cell debris from the supernatant.

Although ensuring a culture free of cell debris, the higher perfusion strategy is not suitable from an economical perspective. As previously stated, the number of CMs generated per liter of culture medium throughput (CMs/L) can be used to measure the cost-effectiveness of a stem cell bioprocess. At the end of the bioprocess with the higher perfusion strategy,  $1.7 \times 10^8$  CMs/L were obtained, whereas with a lower perfusion strategy achieved  $3.8 \times 10^8$  CMs/L. Five times more medium was used in the high perfusion strategy during CM selection, resulting in higher overall costs of the bioprocess when compared to the lower perfusion strategy. The values obtained are lower than the highest result stated in the literature for CM production using perfusion-based strategies,  $5.1 \times 10^8$  CMs/L [99], which reflects the high quantity of medium used in these experiments.

In this work, an automated continuous perfusion strategy was implemented in the bioprocessing of miPSCs. This implementation is a step towards obtaining a fully automated and integrated bioprocess, capable of generating miPSC-derived CMs. Also, the perfusion strategy developed in this thesis provides a straightforward approach, requiring less culture manipulation and with scale-up potential for large-scale production of CMs. In order to obtain improved results, a perfusion strategy could also be used during the expansion/differentiation phase. During this culture period, cell retention devices (e.g. ceramic membrane or spin filters) could be used over computer controlled pumps, aiming to enhance cell densities during culture possibly resulting in higher CM productivities.

### 4.1.3 Structural and functional characterization of miPSC-derived CMs

At the end of the bioprocess it is essential to confirm the quality (phenotype, potency and functionality) of the final differentiated product. Cardiospheres obtained from Stirred Tank and Wave 1L BRs were dissociated, plated into 2D static plates and cultured for a few additional days. CMs were characterized based on their structural features using immunocytochemistry tools.

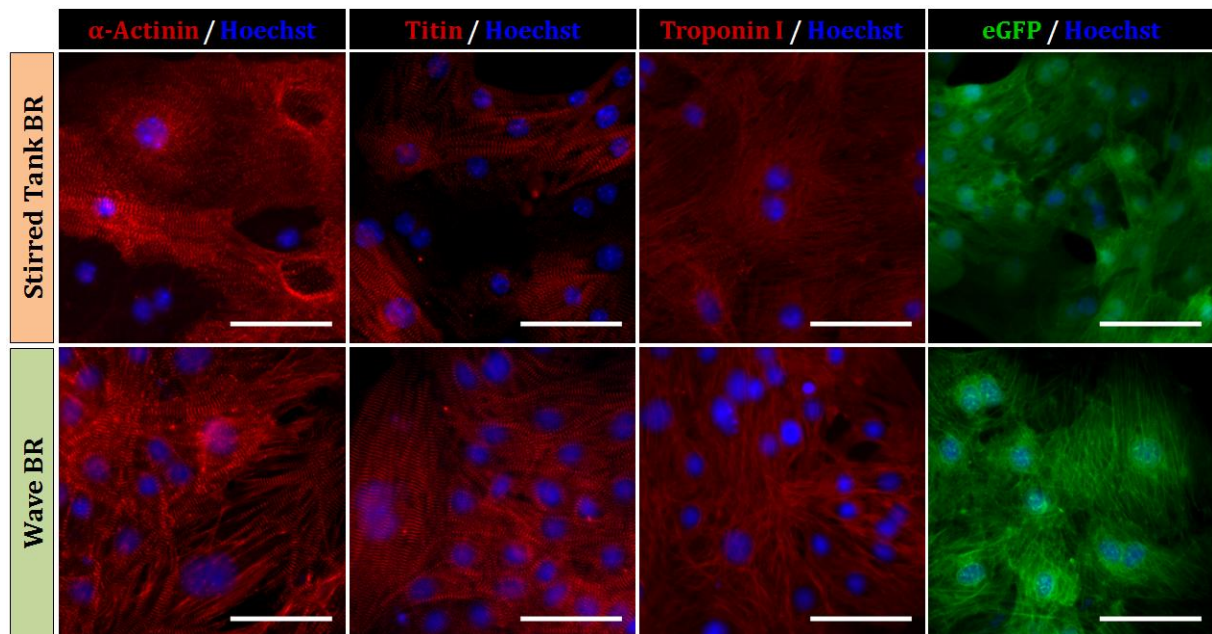


**Figure 4.7: Structural characterization of miPSC-derived CMs produced in Stirred Tank and Wave BRs.** CM aggregates were dissociated into single cells, plated on 2D plates and cultured for additional days before analyses. Immunofluorescence labeling of CMs (from both bioreactor systems) using sarcomeric  $\alpha$ -actinin, titin and troponin I antibodies (red). Expression of eGFP was also detected on differentiated CMs (green). Nuclei were labeled with Hoescht 33432 (blue). Scale bars: 50  $\mu$ m.

Figure 4.7 shows that CMs produced in both bioreactor systems exhibited a typical cardiac morphology, with highly organized  $\alpha$ -actinin, titin and cardiac troponin I structures, while still expressing eGFP. CMs were also characterized based on their functional properties using cellular electrophysiology.

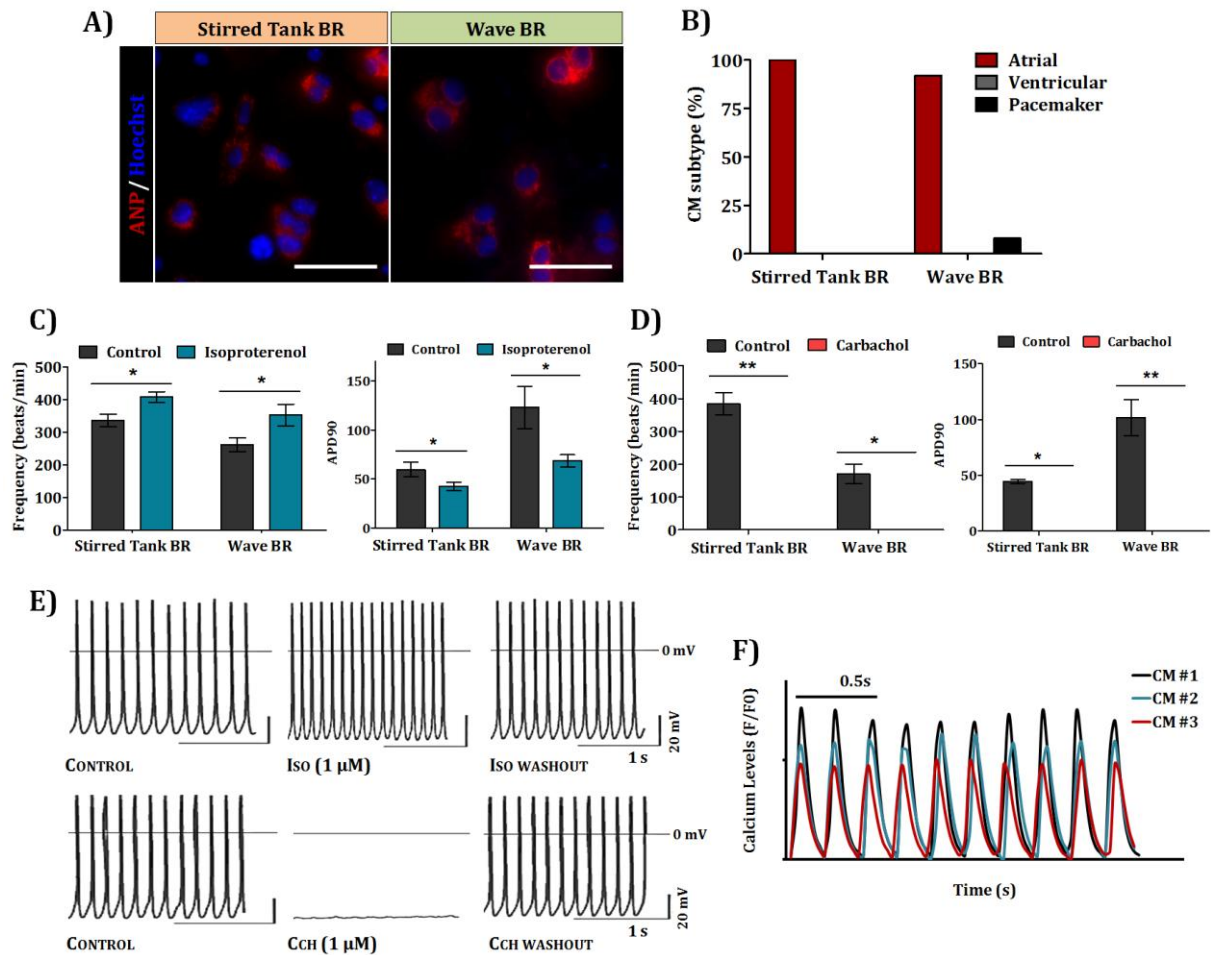


**Figure 4.8: Functional characterization of miPSC-derived CMs produced in Stirred Tank and Wave BRs.** CM aggregates were dissociated into single cells, plated on 2D plates and cultured for additional days before analyses. **A)** Immunofluorescence labeling of CMs (from both bioreactor systems) using atrial natriuretic peptide (ANP) antibody (red). Nuclei were labeled with Hoescht 33432 (blue). Scale bars: 50  $\mu\text{m}$ . **B)** Percentage of each CM subtype (Atrial, Ventricular and Pacemaker) in the final differentiated population from both bioreactors. **C-E)** Pharmacological response of CMs. **C)** Effects of 1  $\mu\text{M}$  Isoproterenol (Iso) on beating frequency and on action potential duration at 90% repolarization (APD90) in miPSC-derived CMs. **D)** Effects of 1  $\mu\text{M}$  Carbachol (Cch) on beating frequency and on action potential duration at 90% repolarization in miPSC-derived CMs. **E)** Representative recording of wave-derived CM action potentials. APs were recorded before the application of the drug (Control) in the presence of the drug (Iso/Cch), and after washout of the drug (washout). **F)** Graphical representation of calcium level cycling contractions determined by confocal imaging of the calcium dependent dye Rhod-3. Three independent cells were analyzed (CM #1-3). Significantly different results:  $P < 0.05$  (\*) and  $P < 0.01$  (\*\*) vs control.

Action potential (AP) recording on single CMs was performed by our collaboration at University of Cologne (UKK). The results are presented in Figures 4.8B-E and Table 4.2. APs are generated as a result of opening and closing of voltage-gated ion channels in the sarcolemmal membrane. APs occur when positively charged ions (i.e.  $\text{K}^+$ ,  $\text{Na}^+$ ,  $\text{Ca}^{2+}$ ) diffuse through the cells membrane, inducing changes in membrane potential. These diffusions cause

membrane depolarization and repolarization. The frequency is a direct measurement of action potentials, as higher frequencies results in more action potentials occurring.

The results show that CMs from both bioprocesses exhibited mainly an atrial-like phenotype. Figure 4.8A shows that most CMs presented cytoplasmic (ANP)-granules, a peptide that is synthesized and stored by atrial-like CMs [41]. The APs characteristic of atrial-like phenotype can be identified by the absence of a distinct plateau during the repolarization phase [82] (Figure 4.8E). These results are in agreement with the ones obtained in RT-PCR analysis, which showed a reduced expression of HCN4 and Myl2 markers (characteristic of pacemaker and ventricular-like phenotypes, respectively) in the final differentiated population (Figure 4.5A/C, Page 41), when compared to the Myl7 marker (atrial-like phenotype). These results were expected due to the use of the  $\alpha$ -MHC promoter that becomes restricted to atrial regions throughout early fetal development [146].

**Table 4.2: Action potential parameters for CMs obtained from Stirred Tank and Wave BRs.** MDP - Maximum Diastolic Potential; Vmax – maximum velocity of depolarization; Vdd – velocity of diastolic depolarization; APD90 – action potential duration at 90% repolarization; APD50 - action potential duration at 90% repolarization.

Bioreactor	Stirred Tank BR	Wave BR 1L
MDP (mV)	-59.81±1.01	-57.97±1.15
Frequency (beats/min)	321.92±23.27	296.42±25.08
Vmax (dE/dt) (V/s)	26.52±1.78	20.59±2.38
Vdd (V/s)	0.10±0.01	0.12±0.01
APD90	84.40±16.41	83.65±7.29
APD50*	18.14±1.07	23.01±1.89
APD90/APD50	5.25±1.27	4.07±0.47
Cells (n)	22	25

\*Significantly different result: P<0.05

According to Table 4.2, AP parameters obtained for CMs derived from both bioreactors were very similar, presenting no statistical difference (except ADP50), showing that CMs produced in both developed strategies present similar functional properties. In addition, the obtained results were in agreement with the values described in literature for atrial-like CMs derived from murine ESCs and iPSCs [136]. Moreover, the produced CMs exhibited AP parameters similar to the ones described for atrial-like late development stage (LDS) fetal CMs (differentiation day 16-19), such as MDP (-63.3±1.3 mV), Frequency (234±19 beats/min), Vmax (27.9±0.7 V/s) and Vdd (0.115±0.017 V/s) [136]. In addition, the response of miPSC-derived CMs to  $\beta$ -adrenergic regulation with Isoproterenol and muscarinic signaling with Carbachol were tested. When 1 $\mu$ M of Isoproterenol, a vasodilator that increases heart rate [147], was administered to CMs, significant increase of AP frequency was



observed (Figure 4.8C/E). Also, the increase in frequency resulted in rapid membrane repolarization and lower AP duration, hence lower APD<sub>90</sub> (Figure 4.8C). Positive chronotropic effects of Isoproterenol were reversible on washout. When administering 1 $\mu$ M of Carbachol, a synthetic acetylcholine analog known to decrease heart rate [148], a decrease in AP frequency was expected. However, an absence of AP was observed (Figure 4.8D-E). This effect could possibly be justified by the use of an excessive dose/concentration of Carbachol that could completely restrain ion diffusion through the cells membrane. Lower concentrations of Carbachol should be tested to verify this hypothesis. Also, it should be noted that positive chronotropic effects of Carbachol were reversible on washout.

To establish that calcium signaling drives excitation-contraction coupling of miPSC-derived CMs, changes in intracellular calcium were imaged across the contraction cycle using confocal microscopy. CMs exhibited a synchronized calcium transient profile (Figure 4.8F). Also, as expected, calcium traces accompanied contraction of the cells, indicating normal calcium homeostasis (results not shown).

In summary, CMs obtained at the end of both bioprocesses present molecular, structural and functional properties typical of CMs, as proved by immunocytochemistry and electrophysiology analysis.

## 4.2 Cryopreservation and hypothermic storage of miPSC-derived CMs

The bioprocesses developed in this thesis, using fully controlled Stirred Tank and Wave BRs, were able to produce quality miPSC-derived CMs. Cryopreservation of CMs is a critical step in integrated bioprocesses. Thus, efficient long term storage of these cells is needed, without compromising their viability and/or functionality. Cryopreserving CMs allows the generation of master and working cells banks, which is a prerequisite for clinical or industrial applications, where quality and consistent stocks of cells are a demand. In addition, suitable hypothermic storage is also needed for appropriate transport of bioprocess developed CMs, avoiding the need of cryopreservation during short term delivery of these cells.

This task aimed at developing efficient protocols for cryopreservation and hypothermic storage of miPSC-derived CMs. This approach consisted on designing 2D and 3D cryopreservation procedures, using different cryopreservation medium formulations: FBS+10% DMSO, CryoStor™CS10 and PRIME-XV (solution still not commercially available). FBS+10% DMSO is a common formulation used in cryopreservation strategies. Previous data from our lab has shown that cryopreservation with this formulation is capable of suitable post thaw recovery, using neuroblastoma N2a and colon adenocarcinoma Caco-2 cell lines [149]. This formulation has also been used with ESC-derived CMs, however low cell survival was observed [150]. CryoStor™CS10 (CS10) is an animal protein-free, serum-free and defined cryopreservation medium containing 10% (DMSO). This solution has been shown to effectively cryopreserved ESC-derived CMs as single cells [151]. PRIME-XV is a new variant of Irvine Scientific cryopreservation solutions, with the feature of being DMSO-free (according to manufacturer's information). Hypothermic storage, at 4°C, was also tested using 2D and 3D approaches. For this purpose, a commercial solution was tested, HypoThermosol®-FRS (referred to as HTS from now on), which is a serum-, protein- and DMSO-free solution that enables improved and extended preservation of cells.

During the last few years, different serum-containing medium formulations have been tested for the cryopreservation of stem cells. However, despite being economically appealing, most of the used serums contain undefined proteins and show batch-batch variation which ultimately lead to unpredictable cell survival. Recently, the use of Rho-associated kinase inhibitor (ROCKi) has been reported to improve cell viability after thawing, in both human ESCs [152] and human ESC-derived CMs [150]. Thus, the effect of pretreatment with ROCK inhibitor on CM viability after thawing was also evaluated, using the FBS + 10% DMSO formulation.

### 4.2.1 Cryopreservation of CMs as monolayers and aggregates

miPSC-derived CMs were cryopreserved as confluent 2D monolayers. As previously indicated cells were plated at  $1 \times 10^6$  cell/well, maintained for 7 days and cryopreserved in the tested cryopreservation solutions (Materials and Methods 3.3.1). After thawing at  $37^\circ\text{C}$ , CM post-thaw recovery was evaluated during a 7 day period. Figure 4.9 presents the main results obtained from post-thaw evaluation of CMs.

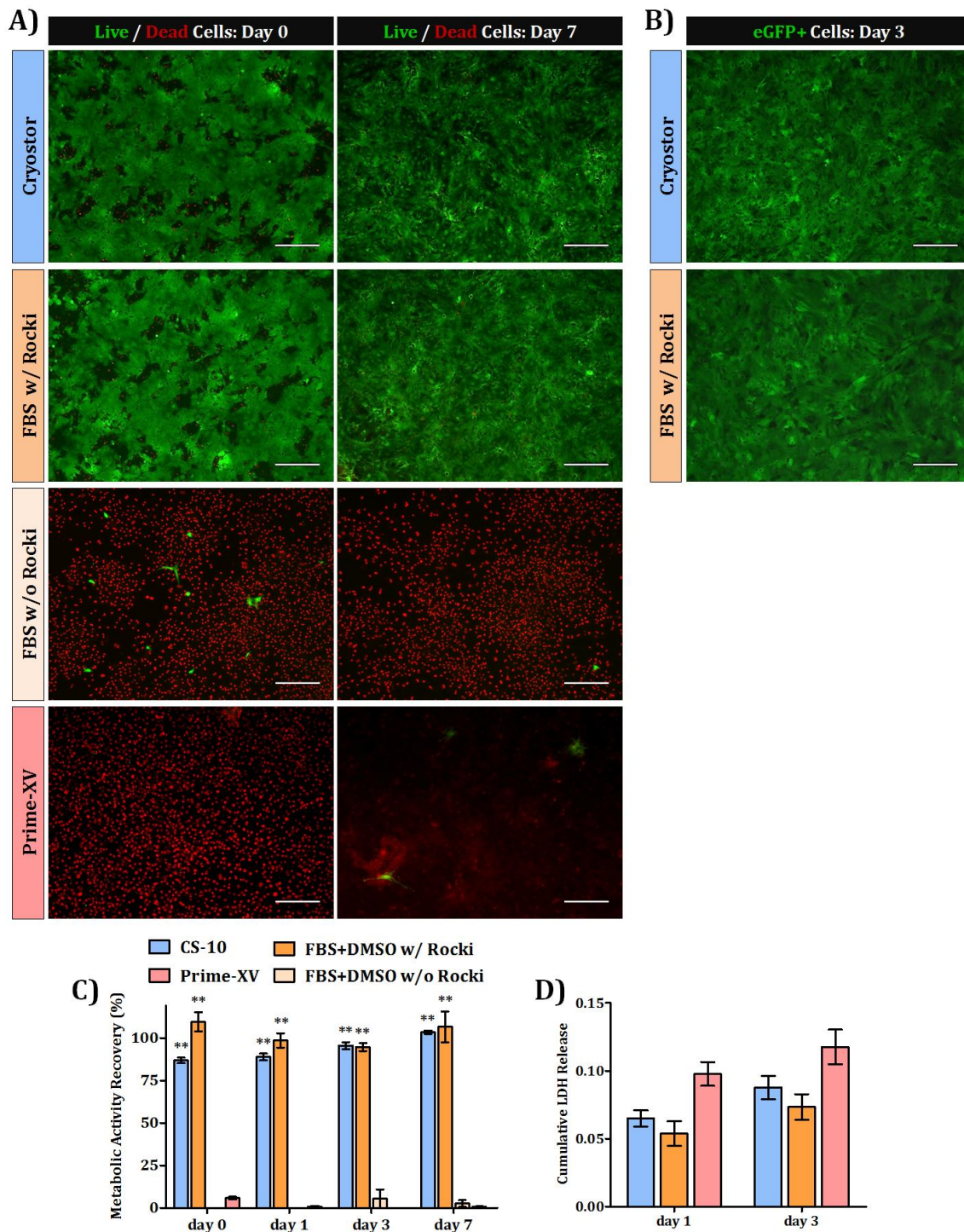


**Figure 4.9:** Effect of cryopreservation medium on miPSC-derived CM viability after cryopreservation of CM monolayers. Different cryopreservation medium formulations were tested:

FBS+10%DMSO (with and without ROCK inhibitor pretreatment), CryoStor™CS10 and PRIME-XV. Post-thaw recovery of CMs was evaluated during 7 days. **A)** Cell viability was assessed using FDA (live cells, green) and PI (dead cells, red) at days 0 and 7. **B)** Phase contrast and fluorescence imaging showing eGFP positive cells (green) at day 3. Scale bars: 200µm. **C)** Evaluation of metabolic activity recovery during the 7-day post-thaw evaluation period. **D)** Cumulative values of LDH release during post-thaw evaluation period. Significantly different results:  $P < 0.01$  (\*\*); CS10 and FBS+DMSO w/ ROCKi vs FBS+DMSO w/o ROCKi and PRIME-XV.

The results obtained show that CS10 and FBS+10% DMSO, with ROCK inhibitor pretreatment (FBS+DMSO w/ ROCKi), were suitable solutions for miPSC-derived CM cryopreservation as 2D monolayers. Most of the CM monolayer remained viable and maintained eGFP expression immediately after thawing and during the 7-day post-thaw evaluation period (Figure 4.9A-B). In addition, beating CMs were observed 1-2 days after thawing (results not shown). On the other hand, FBS+10% DMSO, without ROCK inhibitor pretreatment (FBS+DMSO w/o ROCKi), and PRIME-XV proved to be unsuitable for the cryopreservation of CM monolayers, as extensive cell death was observed immediately after cell thawing (Figure 4.9A). These fluorescence imaging results are in line with the ones obtained with the PrestoBlue assay (Figure 4.9C). CS10 and FBS+DMSO w/ ROCKi show significant differences in metabolic activity recovery over FBS+DMSO w/o ROCKi and PRIME-XV, presenting recoveries over 87% and 94% (respectively) during the 7-day evaluation period. No significant differences in metabolic activity recovery were observed between CS10 and FBS+DMSO w/ ROCKi. At day 7, both solutions presented a 100% metabolic activity recovery. Also, a significant increase in cell viability and metabolic activity recoveries was observed when cells were pretreated with ROCKi, using the FBS+DMSO formulation (Figure 4.9A/C). In fact, very low metabolic activity recoveries were obtained when cryopreserving CMs with FBS+DMSO w/o ROCKi and PRIME-XV solutions (<2% at day 7) (Figure 4.9C). In addition, cryopreservation using PRIME-XV resulted in increased LDH release during post-thaw recovery, presenting a 1.5-fold and 1.8-fold increase over CS10 and FBS+DMSO w/ ROCKi (respectively) at day 1 (Figure 4.9D).

CM applications in research and therapy would greatly benefit from the development of 3D based cryopreservation procedures as cardiospheres express a tissue-like structure, more resembling of the *in-vivo* environment that enhances cell functionality. Efficient cryopreservation of cardiospheres would present a step forward towards the application of these cells, as 3D aggregates can be useful tools in drug screening, toxicology studies and regenerative medicine applications (reviewed in [153]). As previously described, cardiospheres were transferred to cryovials at 300 aggregate/vial and cryopreserved in the various cryopreservation solutions (Materials and Methods 3.3.2). After thawing, cardiospheres were transferred to well plates and cultured in static conditions for 7 days.

Post-thaw recovery was evaluated during time period. Figure 4.10 presents the main results obtained from post-thaw evaluation of cardiospheres.

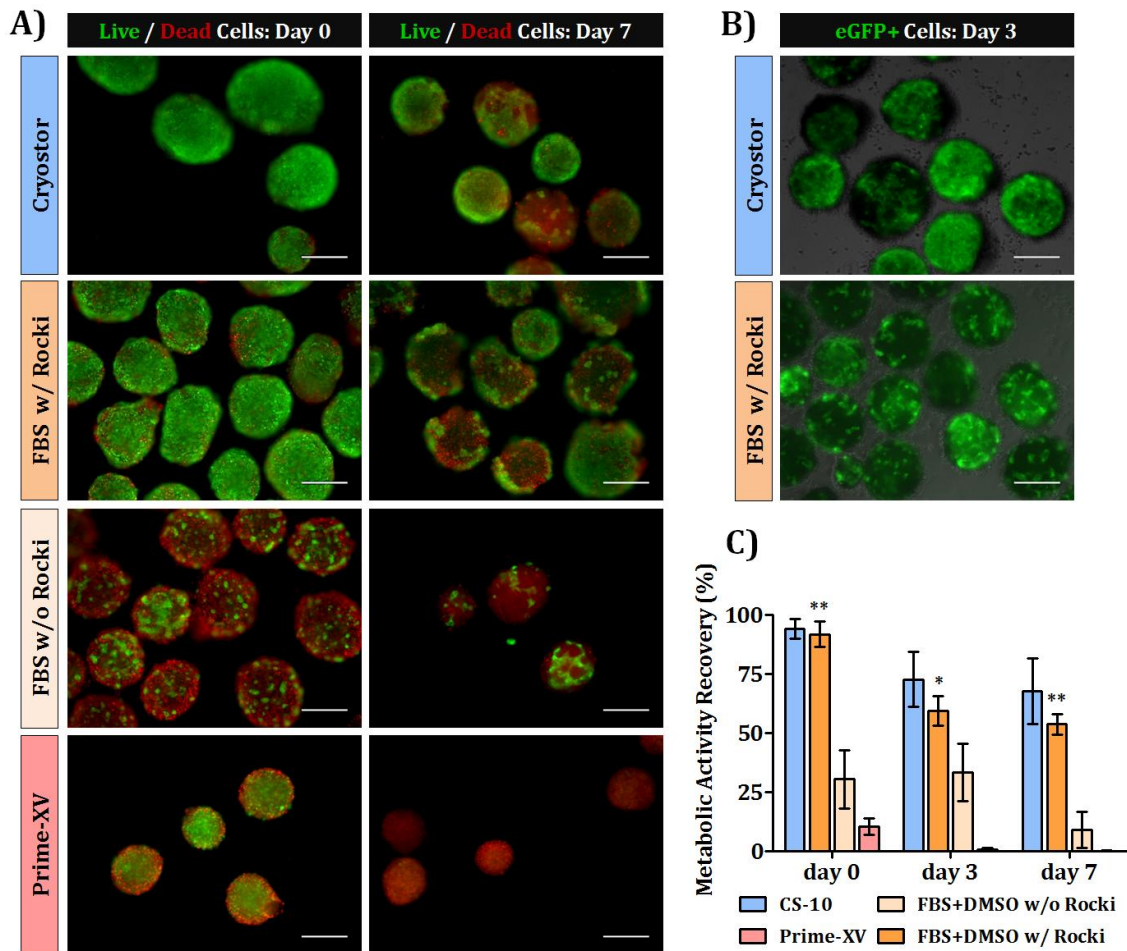


**Figure 4.10: Effect of cryopreservation medium on miPSC-derived CM viability after cryopreservation of cardiospheres.** Different cryopreservation medium formulations were tested: FBS+10%DMSO (with and without ROCK inhibitor pretreatment), CryoStor™CS10 and PRIME-XV. Post-thaw recovery of CMs was evaluated during 7 days. **A)** Cell viability was assessed using FDA (live cells, green) and PI (dead cells, red) at days 0 and 7. **B)** Phase contrast and fluorescence imaging showing eGFP positive cells (green) at day 3. Scale bars: 200µm. **C)** Evaluation of metabolic activity recovery during the 7-day post-thaw evaluation period. Significantly different results:  $P < 0.05$  (\*)  $P < 0.01$  (\*\*) vs FBS+DMSO w/o ROCKi.

The results obtained show that CS10 and FBS+DMSO w/ ROCKi, were the best solutions for cryopreservation of CMs cultured as cardiospheres. Immediately after thawing, high cardiosphere viability was observed using these solutions (Figure 4.10A). In addition, beating of cardiospheres was observed 2-3 days after thawing (results not shown). However, during the 7-day post-thaw evaluation period, some cell death was observed. Nonetheless, some cardiospheres were able to fully maintain their viability, when using CS10 (Figure 4.10A; day 7). Despite some apparent cell death, cardiospheres still showed considerable eGFP expression after cryopreservation using these solutions (Figure 4.10B). Similar to the results observed in monolayer cryopreservation, FBS+DMSO w/o ROCKi and PRIME-XV were

inappropriate for cardiosphere cryopreservation. Cryopreservation using these solutions resulted in extensive cell death after thawing (Figure 4.10A) and consequent no eGFP expression (results not shown).

Figure 4.10C shows the metabolic activity recovery of cardiospheres. Cardiospheres cryopreserved with CS10 and FBS+DMSO w/ ROCKi presented the highest recoveries achieving values of 94% and 91% at day 0, respectively. The decrease in cell viability observed in Figure 4.10A was in line with a decrease in metabolic activity recovery, as a 27% (CS10) and 38% (FBS+DMSO w/ ROCKi) decrease in metabolic activity recovery was observed by day 7. On the other hand, cryopreservation of CMs using FBS+DMSO w/o ROCKi and PRIME-XV, show reduced metabolic activity recoveries during the post-thaw period. In addition, FBS+DMSO w/o ROCKi presented an initial value of 30%, which reduced to 9% at day 7. It should be noted that a significant difference in metabolic activity recovery is observed at the end of the 7-day recovery period, as the results obtained with FBS+DMSO w/ ROCKi present an increase of 45% in metabolic activity recovery over the ones obtained with FBS+DMSO w/o ROCKi (Figure 4.10C)

The results obtained from cryopreservation of miPSC-derived CMs as monolayers and cardiospheres showed that CS10 and FBS+DMSO w/ ROCKi were the most suitable solutions for the strategies evaluated in this work. CS10 is supplemented with components to reduce generation of free radicals or energy deprivation during cryopreservation and inhibit apoptosis [154]. The improvement in cell survival is related to a direct reduction in the level of both apoptosis and necrosis by inhibition of cellular stress during cryopreservation [154, 155]. In addition, CS10 contains 10% DMSO which is a penetrating cryoprotectant agent (CPA). Penetrating CPAs have been suggested to act by reducing the concentration of damaging electrolytes at a given subzero temperature [156] and reducing the extent of cell volume change during slow-rate freezing and thawing [157]. On the other hand, PRIME-XV had no DMSO addition (according to manufacturer's information) which could help justify the extended cell death observed in these experiments. However, it should be noted that no information regarding the added CPA and concentration of CPA used in this solution is known. Although these solutions presented the most promising results, some qualitative differences were observed when comparing the results obtained from post-thaw evaluation of monolayers and cardiospheres. The slight decrease in cell viability and metabolic activity recoveries observed in cardiospheres could be related to heat and mass diffusion restrictions in cardiospheres [158], which could eventually restrict the diffusion of CPAs to the center of the aggregate. Also, ice crystals can intercalate the tissue and mechanically deform cells, and intracellular ice may be formed between the intercellular interactions needed to maintain the

functional 3D architecture [158]. In a future perspective, it could be interesting to evaluate the impact of the size and shape of cardiospheres on the results obtained.

The ROCK inhibitor pretreatment on the FBS+DMSO formulation showed promising results. An improvement of 100% (CM monolayers) and 44% (cardiospheres) on metabolic activity recovery was observed when ROCK inhibitor pretreatment was performed using this medium formulation. Previous work has stated that ROCK inhibitor enhances cell–cell adhesion and cell aggregation by modulating gap junctions, thereby blocking the pathway to apoptosis (reviewed in [159]). In addition, the improvement observed with ROCK inhibitor pretreatment may also be related to the ability to avoid anoikis, which is a subtype of apoptosis induced by the loss of cell adhesion, e.g. the loss of anchorage to the extracellular matrix, as adhesion to the extracellular matrix been shown to prevent caspase activity, thus preventing apoptosis [160]. Despite the improvement observed in cell recovery yields and viability with ROCK inhibitor pretreatment, some difference was observed when comparing the results obtained from 2D and 3D cryopreservation using FBS+DMSO w/o ROCKi, as the 2D approach presented lower metabolic activity recoveries. The presence of cell–cell and cell–surface interactions on monolayers has been shown to render cells more susceptible to freezing injury [161, 162]. These interactions are likely sites for monolayer damage by the osmotic stresses and phase changes in cryopreservation, and have been associated with enhanced susceptibility to intracellular ice formation [163]. The cells extended morphology may also create conditions for cryopreservation-induced damage to the cells structure (cytoskeleton or gap junctions) due to mechanical forces, such as extracellular ice [161]. DMSO was the only compound added to prevent cryopreservation damage unlike CS10, which contains numerous high quality cryo-protecting components. These features may explain the difference observed between cryopreservation of monolayers and cardiospheres using this solution. Despite this fact, from an economical perspective, the FBS+DMSO formulation is less costly and easy to prepare in any stem cell lab, as most of its components exist for common lab procedures.

Cryopreservation has already been accomplished successfully with some cells such as human PSCs (ESCs and iPSCs) [164], neuronal cells [165] and Caco-2 cells [149], using single cell, 2D or 3D approaches. CMs derived from ESCs have been cryopreserved, using single cell approaches [150, 151]. The results obtained in this work show, for the first time, the successful cryopreservation of miPSC-derived CMs using both monolayer and cardiosphere approaches.

#### 4.2.2 Hypothermic storage of CMs as monolayers and aggregates

CMs were also stored at hypothermic temperatures with the aim of developing efficient procedures for short-term transport/shipping. CMs were stored as monolayers ( $1 \times 10^6$  cell/well) and cardiospheres (300 aggregates/vial) at  $4^\circ\text{C}$  for 7 days. After the storage period, cell recovery was evaluated for 7 days. Figure 4.11 presents the main results obtained from hypothermic storage of CMs.

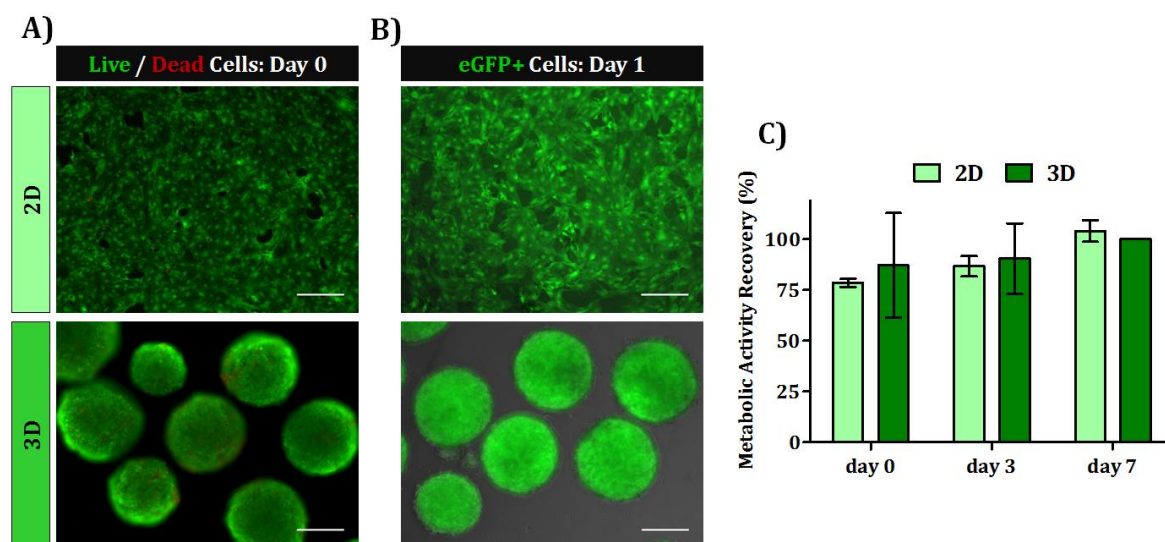


**Figure 4.11: Hypothermic storage of miPSC-derived CMs as monolayers and cardiospheres.** Hypothermic storage was tested using HTS as a storage solution. Cell recovery was evaluated for 7 days. **A)** Cell viability was assessed using FDA (live cells, green) and PI (dead cells, red) after cell recovery. **B)** Phase contrast and fluorescence imaging showing eGFP positive cells (green) at day 1. Scale bars:  $200\mu\text{m}$ . **C)** Evaluation of metabolic activity recovery during 7 days after storage.

The results obtained show that HTS is a suitable solution for hypothermic storage of CMs cultured as 2D monolayers and 3D cardiospheres, during a 7-day storage period. CM monolayers and cardiospheres remained viable after storage (Figure 4.11A) and maintained eGFP expression in both approaches (Figure 4.11B). Also, beating of CMs as monolayers and cardiospheres was observed immediately after storage recovery (results not shown). Metabolic activity recovery results show an increase in metabolic activity until day 7 (Figure 4.11C). The reduced metabolic activity observed at day 0 is a result of storage at hypothermic temperatures using HTS, which reduces cell metabolism during storage [166]. Together with CS10, both solutions are part of a number of preservation solutions currently available in the field of regenerative medicine [167]. These solutions have been carefully formulated to maintain the ionic and hydraulic balances of cells at low temperatures. This feature facilitates preservation of cell homeostasis and control of ionic environment, not achievable using traditional preservation formulations consisting of basal culture medium with serum protein and DMSO supplementation [167]. This solution has been tested using mesenchymal stem cells, achieving cell recoveries of 85% after 4 days storage at hypothermic temperature [168].



Previous studies have shown the successful hypothermic storage of neonatal CMs, during a 2-day storage period [169]. However, no previous studies have been shown regarding hypothermic storage of miPSC-derived CMs.

#### 4.2.3 Characterization of cryopreserved and hypothermically stored CM monolayers

To confirm CM quality after cryopreserved and hypothermic storage, CM monolayers were characterized based on their structure. For this analysis, CM monolayers cryopreserved using CS10 and stored in hypothermal conditions using HTS were used. Figure 4.12 presents the structural characterization of these cells using immunocytochemistry.

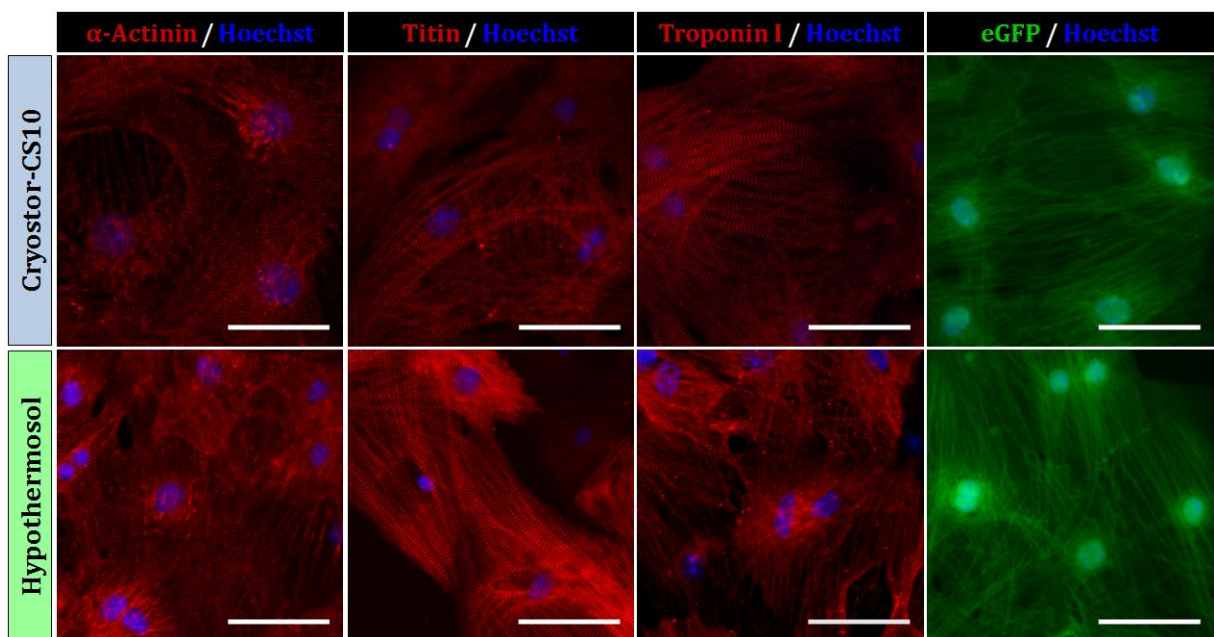


**Figure 4.12: Structural characterization of cryopreserved and hypothermically stored CM monolayers.** Immunofluorescence labeling of CM monolayers, obtained at day 7 of the post-thaw recovery period, using sarcomeric  $\alpha$ -actinin, titin and troponin I antibodies (red). Expression of eGFP was also detected on cryopreserved and stored CMs. Nuclei were labeled with Hoescht 33432 (blue). Scale bars: 50  $\mu$ m.

Immunocytochemistry was performed to confirm the quality, detecting the presence of cardiac-specific proteins, on cryopreserved and stored CMs. Figure 4.12 shows that CMs cryopreserved in CS10 and hypothermically stored exhibited a typical cardiac morphology, with highly organized  $\alpha$ -actinin, titin and cardiac troponin I structures, while still expressing eGFP. These results confirm that cryopreserved CMs, using CS10 solution, and hypothermic storage using HTS maintained their structural features. This confirms that the preserved CMs maintained their structural quality and ultimately proves that the strategies developed in this thesis efficiently cryopreserved and stored miPSC-derived CMs.

### 4.3 Evaluation of the potential of miPSC-derived CMs to be used in the development of cardioprotective cell-based assays

CMs derived from PSCs have been used for various toxicology applications, such as drug screening assays or cardiotoxicity screening [170]. This task aimed at evaluating the potential of miPSC-derived CMs to be used in the development of cardioprotective strategies. For this purpose, CMs were evaluated as monolayers and cardiospheres. On a preliminary approach, CM monolayers were exposed to 50-900 $\mu$ M H<sub>2</sub>O<sub>2</sub> for 20 hours. Figure 4.13 presents the results from this experiment.

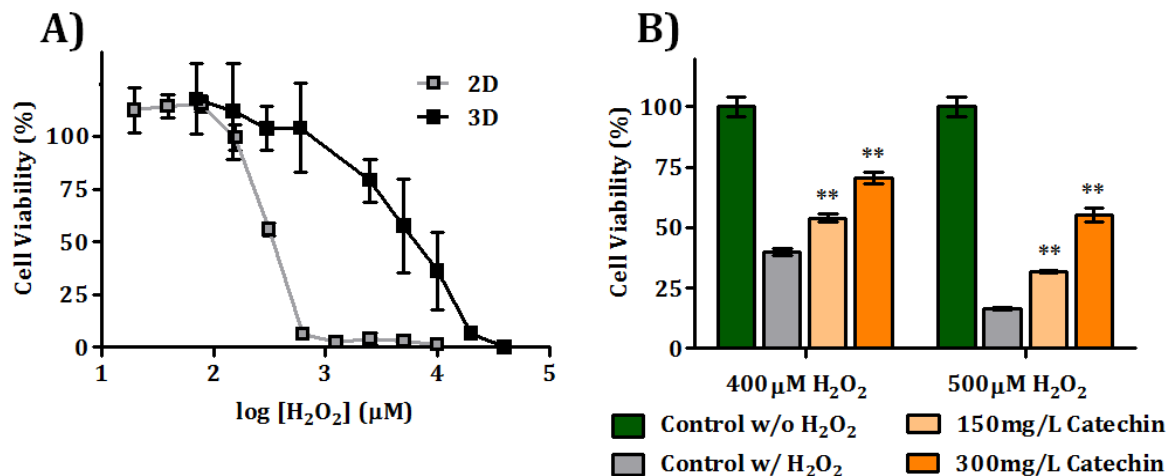


**Figure 4.13: Effect of oxidative stress and antioxidant pretreatment on CMs.** H<sub>2</sub>O<sub>2</sub> oxidative stress was induced exposing cells to concentrations between 50-900 $\mu$ M, during 20 hours. For cardioprotective effect evaluation, Cells were treated before H<sub>2</sub>O<sub>2</sub> exposure with 150 and 300mg/L of catechin, during 24 hours. Cell viability was measured before and after oxidative stress. **A)** Evaluation of oxidative stress on cell viability. CM monolayers and cardiospheres were tested. **B)** Cardioprotective effect of catechin during oxidative stress, using CM monolayers, when exposed to 400 $\mu$ M and 500 $\mu$ M H<sub>2</sub>O<sub>2</sub>. Significantly different results: P<0.01 (\*\*) vs Control w/ H<sub>2</sub>O<sub>2</sub>.

The preliminary results obtained from the monolayer approach show a decrease in cell viability when CMs were exposed to concentrations higher than 150 $\mu$ M H<sub>2</sub>O<sub>2</sub> (Figure 4.13A). To evaluate the cardioprotective effect of an antioxidant compound, IC<sub>50</sub> and IC<sub>80</sub> of H<sub>2</sub>O<sub>2</sub> were estimated. These measures are commonly used to determine the concentration of an inhibitor where the viability is reduced by 50 and 80%, respectively. The results show that IC<sub>50</sub> and IC<sub>80</sub> presented values of approximately 400 and 500 $\mu$ M, respectively. These concentrations were chosen and used to evaluate the cardioprotective effect of catechin, an antioxidant compound already reported to show cardioprotective effect on rat heart cell lines [171]. With this objective, CM monolayers were pretreated with different concentrations of catechin for 24 hours - 150 and 300mg/L, before exposure to H<sub>2</sub>O<sub>2</sub>. The results obtained show that catechin pretreatment resulted in a significant increase in cell viability when compared to untreated cells subjected to oxidative stress (Figure 4.13B). In addition,

pretreatment with 300mg/L proved to be the most promising concentration for this natural compound, as an increase of 31% (400 $\mu$ M H<sub>2</sub>O<sub>2</sub>) and 39% (500 $\mu$ M H<sub>2</sub>O<sub>2</sub>) in CM viability was observed when compared to the viability of untreated CMs. These results show that catechin was able to protect CMs against cellular damage from oxidative stress induction, in a dose dependent manner.

The cardiotoxicity of H<sub>2</sub>O<sub>2</sub> was also evaluated on CMs cultured as 3D cardiospheres. The results obtained show that cardiospheres display inherent higher resistance to H<sub>2</sub>O<sub>2</sub> when compared to CMs cultured as monolayers (Figure 4.13A). As a consequence, estimated values of IC<sub>50</sub> and IC<sub>80</sub> increased to 5 and 15mM, respectively. Cell monolayers present extended morphologies which makes cell-cell and cell-matrix contacts more exposed to oxidative damage. However, cell aggregates contain extensive cell-cell contacts, intercellular adhesion structures and well distributed extracellular matrixes [39], allowing them to express a tissue-like structure, which may confer more resistance to ROS damage, hence explaining the obtained results.

According to our knowledge, no previous studies have used miPSC-derived CMs for the evaluation of the cardioprotective effect of antioxidant compounds. The preliminary results obtained in this work suggest that CMs derived from miPSC are promising tools to be used in the establishment of cardiotoxicity and cardioprotective cell-based assays. Future studies should be carried out to evaluate the cardioprotective effect of other compounds, not only at the level of cell viability but also on functionality, in both 2D and 3D culturing approaches. Also, miPSC-derived CMs should be compared to well established cell model systems that have been used for cardiotoxicity evaluation in CMs, including H9C2 [172] and AC16 [173] cell lines or adult rat CMs [174].



## 5. Conclusion

In this work, a robust, scalable and integrated strategy for the production and selection of miPSC-derived CMs using environmentally controlled bioreactors was developed. From the different bioreactor systems tested, the wave bioreactor was the most suitable system for CM production, allowing high differentiation yields (60 CM/input of miPSC) and CM productivities ( $16.5 \times 10^8$  CM/L), simultaneously reducing bioprocess duration in 5 days, when compared to a stirred tank bioreactor systems. In addition, the wave bioreactor was able to produce  $2.3 \times 10^9$  CMs which is an adequate quantity of CMs to regenerate an infarcted area after a heart attack. Extensive characterization revealed that the produced CMs present a typical cardiac morphology, structure and functionality. Moreover, an automated continuous perfusion system was implemented and integrated in stirred tank bioreactors. The perfusion rates tested enabled efficient removal of cell debris and did not compromise cardiac differentiation potential and CM yields

Furthermore, efficient protocols for the cryopreservation of miPSC-derived CMs as 2D monolayers and as 3D aggregates were developed. CryoStor™CS10 and FBS+10% DMSO (with ROCKi pretreatment) revealed to be suitable solutions for cryopreservation of CM-derived from miPSC, assuring high cell recoveries after thawing. In addition, HypoThermosol®-FRS enabled hypothermic storage of CMs for up to 7 days, without compromising cell viability, metabolic activity or cardiac morphology. The integration of the differentiation and cryopreservation steps herein described constitutes an important breakthrough towards the production, banking and shipping of high quality CMs, in a scalable and straightforward manner.

Finally, it was shown that miPSC-derived CMs present potential to be used in the development of cardioprotective cell-based assays. The antioxidant compound catechin, which was shown to present cardioprotective effect with other cell lines, was able to protect miPSC-derived CMs from oxidative stress induced by  $H_2O_2$ .

Hopefully, the robust and integrated bioprocess here developed presents a relevant step forward in the transfer of iPSC to clinical and industrial applications. Furthermore, the knowledge acquired in this work could be translated to human iPSCs, boosting the application of human CMs in various areas, such as regenerative medicine, drug screening or cardiotoxicity assays.



## 6. References

1. Laslett LJ, Alagona P, Clark B a, Drozda JP, Saldivar F, Wilson SR, Poe C, Hart M: The worldwide environment of cardiovascular disease: prevalence, diagnosis, therapy, and policy issues: a report from the American College of Cardiology. *Journal of the American College of Cardiology* 2012, 60:1–49.
2. Allender S, Scarborough P, Peto V: European cardiovascular disease statistics. *European Heart Network and European Society of Cardiology* 2012.
3. Dierickx P, Doevendans P a, Geijsen N, van Laake LW: Embryonic template-based generation and purification of pluripotent stem cell-derived cardiomyocytes for heart repair. *Journal of cardiovascular translational research* 2012, 5:566–80.
4. Zwi-Dantsis L, Gepstein L: Induced pluripotent stem cells for cardiac repair. *Cellular and molecular life sciences : CMLS* 2012, 69:3285–99.
5. Krishna K A, Krishna K S, Berrocal R, Rao K S RK: Myocardial infarction and stem cells. *Journal of pharmacy & bioallied sciences* 2011, 3:182–188.
6. Mignone JL, Kreutziger KL, Paige SL, Murry CE: Cardiogenesis From Human Embryonic Stem Cells. *Circulation Journal* 2010, 74:2517–2526.
7. Egashira T, Yuasa S, Fukuda K: Induced pluripotent stem cells in cardiovascular medicine. *Stem cells international* 2011, 2011(Article ID 348960):1–7.
8. Bollini S, Smart N, Riley PR: Resident cardiac progenitor cells: at the heart of regeneration. *Journal of molecular and cellular cardiology* 2011, 50:296–303.
9. Steinhauser ML, Lee RT: Regeneration of the heart. *EMBO molecular medicine* 2011, 3:701–12.
10. Gonzales C, Pedrazzini T: Progenitor cell therapy for heart disease. *Experimental cell research* 2009, 315:3077–85.
11. Sheridan C: Cardiac stem cell therapies inch toward clinical litmus test. *Nature Biotechnology* 2013, 31:5–6.
12. M. J. Evans MHK: Establishment in culture of pluripotent cells from mouse embryos. *Nature* 1981, 292:154 – 156.
13. James A. Thomson, Joseph Itskovitz-Eldor SSS, Michelle A. Waknitz, Jennifer J. Swiergiel VSM, Jones JM: Embryonic Stem Cell Lines Derived from Human Blastocysts. *Science* 1998, 282:1145–1147.
14. Thomson JA, Kalishman J, Golos TG, Durning M, Harris CP, Becker RA, Hearn JP: Isolation of a primate embryonic stem cell line. *Proceedings of the National Academy of Sciences of the United States of America* 1995, 92:7844–7848.
15. Serra M, Brito C, Correia C, Alves PM: Process engineering of human pluripotent stem cells for clinical application. *Trends in biotechnology* 2012, 30:350–9.
16. Takahashi K, Yamanaka S: Induction of pluripotent stem cells from mouse embryonic and adult fibroblast cultures by defined factors. *Cell* 2006, 126:663–76.
17. Yoshida Y, Yamanaka S: iPS cells: a source of cardiac regeneration. *Journal of molecular and cellular cardiology* 2011, 50:327–32.

18. Okita K, Ichisaka T, Yamanaka S: Generation of germline-competent induced pluripotent stem cells. *Nature* 2007, 448:313–7.
19. Yu J, Vodyanik M a, Smuga-Otto K, Antosiewicz-Bourget J, Frane JL, Tian S, Nie J, Jonsdottir G a, Ruotti V, Stewart R, Slukvin II, Thomson J a: Induced pluripotent stem cell lines derived from human somatic cells. *Science (New York, NY)* 2007, 318:1917–20.
20. De Peppo GM, Marolt D: State of the Art in Stem Cell Research: Human Embryonic Stem Cells, Induced Pluripotent Stem Cells, and Transdifferentiation. *Journal of Blood Transfusion* 2012, 2012:1–10.
21. Thorrez L, Sampaolesi M: The future of induced pluripotent stem cells for cardiac therapy and drug development. *Current pharmaceutical design* 2011, 17:3258–70.
22. Takahashi K, Tanabe K, Ohnuki M, Narita M, Ichisaka T, Tomoda K, Yamanaka S: Induction of pluripotent stem cells from adult human fibroblasts by defined factors. *Cell* 2007, 131:861–72.
23. Vannucci L, Lai M, Chiuppesi F, Ceccherini-Nelli L, Pistello M: Viral vectors: a look back and ahead on gene transfer technology. *The new microbiologica* 2013, 36:1–22.
24. Lai MI, Wendy-Yeo WY, Ramasamy R, Nordin N, Rosli R, Veerakumarasivam A, Abdullah S: Advancements in reprogramming strategies for the generation of induced pluripotent stem cells. *Journal of assisted reproduction and genetics* 2011, 28:291–301.
25. Rais Y, Zviran A, Geula S, Gafni O, Chomsky E, Viukov S, Mansour AA, Caspi I, Krupalnik V, Zerbib M, Maza I, Mor N, Baran D, Weinberger L, Jaitin D a, Lara-Astiaso D, Blecher-Gonen R, Shipony Z, Mukamel Z, Hagai T, Gilad S, Amann-Zalcenstein D, Tanay A, Amit I, Novershtern N, Hanna JH: Deterministic direct reprogramming of somatic cells to pluripotency. *Nature* 2013, 502:65–70.
26. Araki R, Uda M, Hoki Y, Sunayama M, Nakamura M, Ando S, Sugiura M, Ideno H, Shimada A, Nifuji A, Abe M: Negligible immunogenicity of terminally differentiated cells derived from induced pluripotent or embryonic stem cells. *Nature* 2013, 494:100–4.
27. Mercola M, Ruiz-lozano P, Schneider MD: Cardiac muscle regeneration : lessons from development. *GENES & DEVELOPMENT* 2011, 25:299–309.
28. BurrIDGE PW, Keller G, Gold JD, Wu JC: Production of de novo cardiomyocytes: human pluripotent stem cell differentiation and direct reprogramming. *Cell stem cell* 2012, 10:16–28.
29. Mauritz C, Schwanke K, Reppel M, Neef S, Katsirntaki K, Maier LS, Nguemo F, Menke S, Hausteim M, Hescheler J, Hasenfuss G, Martin U: Generation of functional murine cardiac myocytes from induced pluripotent stem cells. *Circulation* 2008, 118:507–17.
30. Lawson K a, Meneses JJ, Pedersen R a: Clonal analysis of epiblast fate during germ layer formation in the mouse embryo. *Development (Cambridge, England)* 1991, 113:891–911.
31. Willems E, Bushway PJ, Mercola M: Natural and synthetic regulators of embryonic stem cell cardiogenesis. *Pediatric cardiology* 2009, 30:635–42.
32. Marvin MJ, Di Rocco G, Gardiner a, Bush SM, Lassar a B: Inhibition of Wnt activity induces heart formation from posterior mesoderm. *Genes & development* 2001, 15:316–27.
33. Brennan J, Lu CC, Norris DP, Rodriguez T a, Beddington RS, Robertson EJ: Nodal signalling in the epiblast patterns the early mouse embryo. *Nature* 2001, 411:965–9.



34. Winnier G, Blessing M, Labosky P a, Hogan BL: Bone morphogenetic protein-4 is required for mesoderm formation and patterning in the mouse. *Genes & development* 1995, 9:2105–16.
35. Mima T, Ueno H, Fischman D a, Williams LT, Mikawa T: Fibroblast growth factor receptor is required for in vivo cardiac myocyte proliferation at early embryonic stages of heart development. *Proceedings of the National Academy of Sciences of the United States of America* 1995, 92:467–71.
36. Murry CE, Keller G: Differentiation of embryonic stem cells to clinically relevant populations: lessons from embryonic development. *Cell* 2008, 132:661–80.
37. Rajala K, Pekkanen-Mattila M, Aalto-Setälä K: Cardiac differentiation of pluripotent stem cells. *Stem cells international* 2011, 2011:1–12.
38. Zhang J, Klos M, Wilson GF, Herman AM, Lian X, Raval KK, Barron MR, Hou L, Soerens AG, Yu J, Palecek SP, Lyons GE, Thomson J a, Herron TJ, Jalife J, Kamp TJ: Extracellular matrix promotes highly efficient cardiac differentiation of human pluripotent stem cells: the matrix sandwich method. *Circulation research* 2012, 111:1125–36.
39. Soares CP, Midlej V, De Oliveira MEW, Benchimol M, Costa ML, Mermelstein C: 2D and 3D-Organized Cardiac Cells Shows Differences in Cellular Morphology, Adhesion Junctions, Presence of Myofibrils and Protein Expression. *PLoS ONE* 2012, 7:e38147.
40. Mummery CL, Zhang J, Ng ES, Elliott D a, Elefanty AG, Kamp TJ: Differentiation of human embryonic stem cells and induced pluripotent stem cells to cardiomyocytes: a methods overview. *Circulation research* 2012, 111:344–58.
41. Kehat I, Kenyagin-karsenti D, Snir M, Segev H, Amit M, Gepstein A, Livne E, Binah O, Itskovitz-eldor J, Gepstein L: Human embryonic stem cells can differentiate into myocytes with structural and functional properties of cardiomyocytes. *The Journal of Clinical Investigation* 2001, 108:363–364.
42. Desbaillets I, Ziegler U, Groscurth P, Gassmann M: Embryoid bodies: an in vitro model of mouse embryogenesis. *Experimental Physiology* 2000, 85.6:645–651.
43. Doetschman TC, Eistetter H, Katz M, Schmidt W, Kemler R: The in vitro development of blastocyst-derived embryonic stem cell lines: formation of visceral yolk sac, blood islands and myocardium. *Journal of embryology and experimental morphology* 1985, 87:27–45.
44. Tran TH, Wang X, Browne C, Zhang Y, Schinke M, Izumo S, Burcin M: Wnt3a-induced mesoderm formation and cardiomyogenesis in human embryonic stem cells. *Stem cells* 2009, 27:1869–78.
45. Boheler KR, Czyn J, Tweedie D, Yang HT, Anisimov SV WA: Differentiation of Pluripotent Embryonic Stem Cells Into Cardiomyocytes. *Circulation Research* 2002, 91:189–201.
46. Pekkanen-mattila M, Ojala M, Kerkel E, Rajala K, Skottman H, Aalto-set K: The Effect of Human and Mouse Fibroblast Feeder Cells on Cardiac Differentiation of Human Pluripotent Stem Cells. *Stem Cells International* 2012, 2012:1–10.
47. Bauwens CL, Peerani R, Niebruegge S, Woodhouse K a, Kumacheva E, Husain M, Zandstra PW: Control of human embryonic stem cell colony and aggregate size heterogeneity influences differentiation trajectories. *Stem cells* 2008, 26:2300–10.
48. Ng ES, Davis RP, Azzola L, Stanley EG, Elefanty AG: Forced aggregation of defined numbers of human embryonic stem cells into embryoid bodies fosters robust, reproducible hematopoietic differentiation. *Blood* 2005, 106:1601–3.

49. BurrIDGE PW, Anderson D, Priddle H, Barbadillo Muñoz MD, Chamberlain S, Allegrucci C, Young LE, Denning C: Improved human embryonic stem cell embryoid body homogeneity and cardiomyocyte differentiation from a novel V-96 plate aggregation system highlights interline variability. *Stem cells* 2007, 25:929–38.
50. Mohr JC, de Pablo JJ, Palecek SP: 3-D microwell culture of human embryonic stem cells. *Biomaterials* 2006, 27:6032–42.
51. Mohr JC, Zhang J, Azarin SM, Soerens AG, de Pablo JJ, Thomson J a, Lyons GE, Palecek SP, Kamp TJ: The microwell control of embryoid body size in order to regulate cardiac differentiation of human embryonic stem cells. *Biomaterials* 2010, 31:1885–93.
52. Peerani R, Rao BM, Bauwens C, Yin T, Wood G a, Nagy A, Kumacheva E, Zandstra PW: Niche-mediated control of human embryonic stem cell self-renewal and differentiation. *The EMBO journal* 2007, 26:4744–55.
53. Mummery C, Ward-van Oostwaard D, Doevendans P, Spijker R, van den Brink S, Hassink R, van der Heyden M, Ophhof T, Pera M, de la Riviere AB, Passier R, Tertoolen L: Differentiation of human embryonic stem cells to cardiomyocytes: role of coculture with visceral endoderm-like cells. *Circulation* 2003, 107:2733–40.
54. Xu C: Differentiation and enrichment of cardiomyocytes from human pluripotent stem cells. *Journal of molecular and cellular cardiology* 2012, 52:1203–12.
55. Graichen R, Xu X, Braam SR, Balakrishnan T, Norfiza S, Sieh S, Soo SY, Tham SC, Mummery C, Colman A, Zweigerdt R, Davidson BP: Enhanced cardiomyogenesis of human embryonic stem cells by a small molecular inhibitor of p38 MAPK. *Differentiation* 2008, 76:357–70.
56. Xu XQ, Graichen R, Soo SY, Balakrishnan T, Rahmat SNB, Sieh S, Tham SC, Freund C, Moore J, Mummery C, Colman A, Zweigerdt R, Davidson BP: Chemically defined medium supporting cardiomyocyte differentiation of human embryonic stem cells. *Differentiation* 2008, 76:958–70.
57. Habib M, Caspi O, Gepstein L: Human embryonic stem cells for cardiomyogenesis. *Journal of molecular and cellular cardiology* 2008, 45:462–74.
58. Filipczyk a a, Passier R, Rochat A, Mummery CL: Regulation of cardiomyocyte differentiation of embryonic stem cells by extracellular signalling. *Cellular and molecular life sciences* 2007, 64:704–18.
59. Laflamme M a, Chen KY, Naumova A V, Muskheli V, Fugate J a, Dupras SK, Reinecke H, Xu C, Hassanipour M, Police S, O'Sullivan C, Collins L, Chen Y, Minami E, Gill E a, Ueno S, Yuan C, Gold J, Murry CE: Cardiomyocytes derived from human embryonic stem cells in pro-survival factors enhance function of infarcted rat hearts. *Nature biotechnology* 2007, 25:1015–24.
60. Paige SL, Osugi T, Afanasiev OK, Pabon L, Reinecke H, Murry CE: Endogenous Wnt/beta-catenin signaling is required for cardiac differentiation in human embryonic stem cells. *PloS one* 2010, 5:1–8.
61. Barron M, Gao M, Lough J: Requirement for BMP and FGF signaling during cardiogenic induction in non-precardiac mesoderm is specific, transient, and cooperative. *Developmental dynamics* 2000, 218:383–93.
62. Kattman SJ, Witty AD, Gagliardi M, Dubois NC, Niapour M, Hotta A, Ellis J, Keller G: Stage-specific optimization of activin/nodal and BMP signaling promotes cardiac differentiation of mouse and human pluripotent stem cell lines. *Cell stem cell* 2011, 8:228–40.

63. Yang L, Soonpaa MH, Adler ED, Roepke TK, Kattman SJ, Kennedy M, Henckaerts E, Bonham K, Abbott GW, Linden RM, Field LJ, Keller GM: Human cardiovascular progenitor cells develop from a KDR+ embryonic-stem-cell-derived population. *Nature* 2008, 453:524–8.
64. Wang H, Hao J, Hong CC: Cardiac Induction of Embryonic Stem Cells by a Small Molecule. *ACS chemical biology* 2011:192–197.
65. Cao N, Liu Z, Chen Z, Wang J, Chen T, Zhao X, Ma Y, Qin L, Kang J, Wei B, Wang L, Jin Y, Yang H-T: Ascorbic acid enhances the cardiac differentiation of induced pluripotent stem cells through promoting the proliferation of cardiac progenitor cells. *Cell research* 2012, 22:219–36.
66. Takahashi T, Lord B, Schulze PC, Fryer RM, Sarang SS, Gullans SR, Lee RT: Ascorbic acid enhances differentiation of embryonic stem cells into cardiac myocytes. *Circulation* 2003, 107:1912–6.
67. Serra M, Brito C, Sousa MFQ, Jensen J, Tostões R, Clemente J, Strehl R, Hyllner J, Carrondo MJT, Alves PM: Improving expansion of pluripotent human embryonic stem cells in perfused bioreactors through oxygen control. *Journal of biotechnology* 2010, 148:208–215.
68. Gibbons J, Hewitt E, Gardner DK: Effects of oxygen tension on the establishment and lactate dehydrogenase activity of murine embryonic stem cells. *Cloning and stem cells* 2006, 8:117–122.
69. Niebruegge S, Bauwens CL, Peerani R, Thavandiran N, Masse S, Sevaptisidis E, Nanthakumar K, Woodhouse K, Husain M, Kumacheva E, Zandstra PW: Generation of human embryonic stem cell-derived mesoderm and cardiac cells using size-specified aggregates in an oxygen-controlled bioreactor. *Biotechnology and bioengineering* 2009, 102:493–507.
70. Bauwens C, Yin T, Dang S, Peerani R, Zandstra PW: Development of a perfusion fed bioreactor for embryonic stem cell-derived cardiomyocyte generation: oxygen-mediated enhancement of cardiomyocyte output. *Biotechnology and bioengineering* 2005, 90:452–61.
71. Nava MM, Pietrabissa R, Raimondi MT: Controlling Self-Renewal and Differentiation of Stem Cells via Mechanical Cues. *Journal of Biomedicine and Biotechnology* 2012:1–12.
72. Shimizu N, Yamamoto K, Obi S, Kumagaya S, Masumura T, Shimano Y, Naruse K, Yamashita JK, Igarashi T, Ando J: Cyclic strain induces mouse embryonic stem cell differentiation into vascular smooth muscle cells by activating PDGF receptor beta. *Journal of applied physiology (Bethesda, Md: 1985)* 2008, 104:766–772.
73. Matsumoto T, Yung YC, Fischbach C, Kong HJ, Nakaoka R, Mooney DJ: Mechanical strain regulates endothelial cell patterning in vitro. *Tissue engineering* 2007, 13:207–217.
74. Gwak S-J, Bhang SH, Kim I-K, Kim S-S, Cho S-W, Jeon O, Yoo KJ, Putnam AJ, Kim B-S: The effect of cyclic strain on embryonic stem cell-derived cardiomyocytes. *Biomaterials* 2008, 29:844–56.
75. Elder SH, Goldstein SA, Kimura JH, Soslowsky LJ, Spengler DM: Chondrocyte differentiation is modulated by frequency and duration of cyclic compressive loading. *Annals of biomedical engineering* 2001, 29:476–482.
76. Serra M: Process Engineering of Stem Cells for Clinical Application. Universidade Nova de Lisboa; 2011:1–214.
77. Pampaloni F, Reynaud EG, Stelzer EHK: The third dimension bridges the gap between cell culture and live tissue. *Nature reviews Molecular cell biology* 2007, 8:839–45.
78. Yamada KM, Cukierman E: Modeling tissue morphogenesis and cancer in 3D. *Cell* 2007, 130:601–10.

79. Lund AW, Yener B, Stegemann JP, Plopper GE: The natural and engineered 3D microenvironment as a regulatory cue during stem cell fate determination. *Tissue engineering* 2009, 15:371–80.
80. Burdick J a, Vunjak-Novakovic G: Engineered microenvironments for controlled stem cell differentiation. *Tissue engineering* 2009, 15:205–19.
81. Kehoe DE, Jing D, Lock LT, Tzanakakis ES, Ph D: Scalable Stirred-Suspension Bioreactor Culture. *Tissue engineering* 2010, 16:405–21.
82. Zhang J, Wilson GF, Soerens AG, Koonce CH, Yu J, Palecek SP, Thomson J a, Kamp TJ: Functional cardiomyocytes derived from human induced pluripotent stem cells. *Circulation research* 2009, 104:e30–41.
83. Serra M, Correia C, Malpique R, Brito C, Jensen J, Bjorquist P, Carrondo MJT, Alves PM: Microencapsulation technology: a powerful tool for integrating expansion and cryopreservation of human embryonic stem cells. *PloS one* 2011, 6:e23212.
84. Oh SKW, Chen AK, Mok Y, Chen X, Lim U-M, Chin A, Choo ABH, Reuveny S: Long-term microcarrier suspension cultures of human embryonic stem cells. *Stem cell research* 2009, 2:219–30.
85. Lecina M, Ting S, Choo A, Reuveny S, Oh S: Scalable platform for human embryonic stem cell differentiation to cardiomyocytes in suspended microcarrier cultures. *Tissue engineering Part C, Methods* 2010, 16:1609–1619.
86. Donghui Jing, Abhirath Parikh and EST: Cardiac Cell Generation From Encapsulated Embryonic Stem Cells in Static and Scalable Culture Systems. *Cell Transplant* 2011, 19:1397–1412.
87. Zwi-dantsis L, Sc B, Mizrahi I, Ph D, Arbel G, Sc M, Gepstein A, Gepstein L: Scalable Production of Cardiomyocytes Derived from c-Myc Free Induced Pluripotent Stem Cells. *TISSUE ENGINEERING: Part A* 2011, 17:1027–1037.
88. Fries S, Glazomitsky K, Woods A, Forrest G, Hsu A, Olewinski R, Robinson D, Chartrain M: Evaluation of Disposable Bioreactors. *Bioprocess Analysis* 2005:36–44.
89. Placzek MR, Chung I-M, Macedo HM, Ismail S, Mortera Blanco T, Lim M, Cha JM, Fauzi I, Kang Y, Yeo DCL, Ma CYJ, Polak JM, Panoskaltis N, Mantalaris A: Stem cell bioprocessing: fundamentals and principles. *Journal of the Royal Society* 2009, 6:209–32.
90. Eibl R, Kaiser S, Lombriser R, Eibl D: Disposable bioreactors: the current state-of-the-art and recommended applications in biotechnology. *Applied microbiology and biotechnology* 2010, 86:41–9.
91. Löffelholz C, Husemann U, Greller G, Meusel W, Kauling J, Ay P, Kraume M, Eibl R, Eibl D: Bioengineering Parameters for Single-Use Bioreactors: Overview and Evaluation of Suitable Methods. *Chemie Ingenieur Technik* 2013, 85:40–56.
92. Shukla A a, Gottschalk U: Single-use disposable technologies for biopharmaceutical manufacturing. *Trends in biotechnology* 2013, 31:147–54.
93. Singh V: Disposable bioreactor for cell culture using wave-induced agitation. *Cytotechnology* 1999, 30:149–58.
94. Oncül A a, Kalmbach A, Genzel Y, Reichl U, Thévenin D: Characterization of flow conditions in 2 L and 20 L wave bioreactors using computational fluid dynamics. *Biotechnology progress* 2009, 26:101–10.

95. Lee B, Fang D, Croughan M, Carrondo M, Paik S-H: Characterization of novel pneumatic mixing for single-use bioreactor application. *BMC proceedings* 2011, 5(Suppl 8):1–2.
96. Serra M, Brito C, Costa EM, Sousa MFQ, Alves PM: Integrating human stem cell expansion and neuronal differentiation in bioreactors. *BMC biotechnology* 2009, 9:82.
97. He W, Ye L, Li S, Liu H, Wang Q, Fu X, Han W, Chen Z: Stirred Suspension Culture Improves Embryoid Body Formation and Cardiogenic Differentiation of Genetically Modified Embryonic Stem Cells. *Biological & Pharmaceutical Bulletin* 2012, 35:308–316.
98. Schroeder M, Niebruegge S, Werner A, Willbold E, Burg M, Ruediger M, Field LJ, Lehmann J, Zweigerdt R: Differentiation and lineage selection of mouse embryonic stem cells in a stirred bench scale bioreactor with automated process control. *Biotechnology and bioengineering* 2005, 92:920–33.
99. Niebruegge S, Nehring A, Bär H, Schroeder M, Zweigerdt R, Lehmann J: Cardiomyocyte production in mass suspension culture: embryonic stem cells as a source for great amounts of functional cardiomyocytes. *Tissue engineering Part A* 2008, 14:1591–601.
100. Klug MG, Soonpaa MH, Koh GY, Field LJ: Genetically Selected Cardiomyocytes from Differentiating Embryonic Stem Cells Form Stable Intracardiac Grafts. *Journal of Clinical Investigation* 1996, 98:216–224.
101. Huber I, Itzhaki I, Caspi O, Arbel G, Tzukerman M, Gepstein A, Habib M, Yankelson L, Kehat I, Gepstein L: Identification and selection of cardiomyocytes during human embryonic stem cell differentiation. *The FASEB journal* 2007, 21:2551–63.
102. Xu XQ, Zweigerdt R, Soo SY, Ngoh ZX, Tham SC, Wang ST, Graichen R, Davidson B, Colman a, Sun W: Highly enriched cardiomyocytes from human embryonic stem cells. *Cytotherapy* 2008, 10:376–89.
103. Anderson D, Self T, Mellor IR, Goh G, Hill SJ, Denning C: Transgenic enrichment of cardiomyocytes from human embryonic stem cells. *Molecular therapy* 2007, 15:2027–36.
104. Caspi O, Huber I, Kehat I, Habib M, Arbel G, Gepstein A, Yankelson L, Aronson D, Beyar R, Gepstein L: Transplantation of human embryonic stem cell-derived cardiomyocytes improves myocardial performance in infarcted rat hearts. *Journal of the American College of Cardiology* 2007, 50:1884–93.
105. Chunhui Xu, Shailaja Police, Namitha Rao MKC: Characterization and Enrichment of Cardiomyocytes Derived From Human Embryonic Stem Cells. *Circulation Research* 2002, 91:501–508.
106. Dubois NC, Craft AM, Sharma P, Elliott D a, Stanley EG, Elefanty AG, Gramolini A, Keller G: SIRPA is a specific cell-surface marker for isolating cardiomyocytes derived from human pluripotent stem cells. *Nature biotechnology* 2011, 29:1011–18.
107. Uosaki H, Fukushima H, Takeuchi A, Matsuoka S, Nakatsuji N, Yamanaka S, Yamashita JK: Efficient and scalable purification of cardiomyocytes from human embryonic and induced pluripotent stem cells by VCAM1 surface expression. *PLoS one* 2011, 6:1–9.
108. Hirokazu Hirata, Yoshinobu Murakami, Yoshiaki Miyamoto, Mako Tosaka, Kayoko Inoue, Ayako Nagahashi, Lars Martin Jakt, Takayuki Asahara, Hiroo Iwata, Yoshiki Sawa SK: ALCAM (CD166) is a surface marker for early murine cardiomyocytes. *Cells Tissues Organs* 2006, 184:172–180.
109. Hattori F, Chen H, Yamashita H, Tohyama S, Satoh Y-S, Yuasa S, Li W, Yamakawa H, Tanaka T, Onitsuka T, Shimoji K, Ohno Y, Egashira T, Kaneda R, Murata M, Hidaka K, Morisaki T, Sasaki E, Suzuki T, Sano M, Makino S, Oikawa S, Fukuda K: Nongenetic method for purifying stem cell-derived cardiomyocytes. *Nature methods* 2010, 7:61–6.

110. Tohyama S, Hattori F, Sano M, Hishiki T, Nagahata Y, Matsuura T, Hashimoto H, Suzuki T, Yamashita H, Satoh Y, Egashira T, Seki T, Muraoka N, Yamakawa H, Ohgino Y, Tanaka T, Yoichi M, Yuasa S, Murata M, Suematsu M, Fukuda K: Distinct metabolic flow enables large-scale purification of mouse and human pluripotent stem cell-derived cardiomyocytes. *Cell stem cell* 2013, 12:127–37.
111. Park S-J, Bae D, Moon S-H, Chung H-M: Modification of a purification and expansion method for human embryonic stem cell-derived cardiomyocytes. *Cardiology* 2013, 124:139–50.
112. Vidarsson H, Hyllner J, Sartipy P: Differentiation of human embryonic stem cells to cardiomyocytes for in vitro and in vivo applications. *Stem cell reviews* 2010, 6:108–20.
113. Reinecke H, Minami E, Zhu W-Z, Laflamme M a: Cardiogenic differentiation and transdifferentiation of progenitor cells. *Circulation research* 2008, 103:1058–71.
114. Cao F, Wagner R a, Wilson KD, Xie X, Fu J-D, Drukker M, Lee A, Li R a, Gambhir SS, Weissman IL, Robbins RC, Wu JC: Transcriptional and functional profiling of human embryonic stem cell-derived cardiomyocytes. *PLoS one* 2008, 3:e3474.
115. Abbasalizadeh S, Baharvand H: Technological progress and challenges towards cGMP manufacturing of human pluripotent stem cells based therapeutic products for allogeneic and autologous cell therapies. *Biotechnology advances* 2013, In press.
116. Hunt CJ: Cryopreservation of Human Stem Cells for Clinical Application: A Review. *Transfusion medicine and hemotherapy* 2011, 38:107–123.
117. Coopman K: Large-scale compatible methods for the preservation of human embryonic stem cells: Current perspectives. *Biotechnology Progress* 2011, 27:1511–1521.
118. Baust JG and JMB: Viability and Functional Assays Used to Assess Preservation Efficacy. In *Advances in Biopreservation*. CRC Press - Taylor and Francis Publishing New York; 2006:123–141.
119. Malpique R: Novel Cryopreservation Strategies for Cell-Therapies and Pre-Clinical Research. Universidade Nova de Lisboa; 2010(February):1–230.
120. Holm F, Ström S, Inzunza J, Baker D, Strömberg A-M, Rozell B, Feki A, Bergström R, Hovatta O: An effective serum- and xeno-free chemically defined freezing procedure for human embryonic and induced pluripotent stem cells. *Human reproduction* 2010, 25:1271–9.
121. Meryman HT: Cryopreservation of living cells: principles and practice. *Transfusion* 2007, 47:935–45.
122. Lovelock JE, Hill M: The mechanism of the protective action of glycerol against haemolysis by freezing and thawing. *Biochimica et Biophysica Acta* 1953, 11:28–36.
123. Li Y, Tan J-C, Li L-S: Comparison of three methods for cryopreservation of human embryonic stem cells. *Fertility and sterility* 2010, 93:999–1005.
124. Xu C, Police S, Hassanipour M, Li Y, Chen Y, Priest C, Sullivan CO, Laflamme MA, Zhu W, Biber V, Hegerova L, Yang J, Delavan-boorsma K, Davies A, Lebkowski J, Gold JD, Corporation G, Drive C, Park M: Efficient generation and cryopreservation of cardiomyocytes derived from human embryonic stem cells. *Regenerative Medicine* 2011, 6:53–66.
125. Braam SR, Tertoolen L, van de Stolpe A, Meyer T, Passier R, Mummery CL: Prediction of drug-induced cardiotoxicity using human embryonic stem cell-derived cardiomyocytes. *Stem cell research* 2010, 4:107–16.

126. Kola I, Landis J: Can the pharmaceutical industry reduce attrition rates? *Nature reviews Drug discovery* 2004, 3:711–5.
127. Mordwinkin NM, Burridge PW, Wu JC: A review of human pluripotent stem cell-derived cardiomyocytes for high-throughput drug discovery, cardiotoxicity screening, and publication standards. *Journal of cardiovascular translational research* 2013, 6:22–30.
128. Farokhpour M, Karbalaie K, Tanhaei S, Nematollahi M, Etebari M, Sadeghi HM, Nasr-Esfahani MH, Baharvand H: Embryonic stem cell-derived cardiomyocytes as a model system to study cardioprotective effects of dexamethasone in doxorubicin cardiotoxicity. *Toxicology in vitro: an international journal published in association with BIBRA* 2009, 23:1422–8.
129. Khan JM, Lyon AR, Harding SE: The case for induced pluripotent stem cell-derived cardiomyocytes in pharmacological screening. *British journal of pharmacology* 2013, 169:304–17.
130. Braam SR, Passier R, Mummery CL: Cardiomyocytes from human pluripotent stem cells in regenerative medicine and drug discovery. *Trends in pharmacological sciences* 2009, 30:536–45.
131. Pieniążek a, Czepas J, Piasecka-Zelga J, Gwoździński K, Koceva-Chyła a: Oxidative stress induced in rat liver by anticancer drugs doxorubicin, paclitaxel and docetaxel. *Advances in medical sciences* 2013, 58:104–11.
132. Hafstad AD, Nabeebaccus A a, Shah AM: Novel aspects of ROS signalling in heart failure. *Basic research in cardiology* 2013, 108:359.
133. Zheng J, Lee HCM, Bin Sattar MM, Huang Y, Bian J-S: Cardioprotective effects of epigallocatechin-3-gallate against doxorubicin-induced cardiomyocyte injury. *European journal of pharmacology* 2011, 652:82–8.
134. Halbach M, Peinkofer G, Baumgartner S, Maass M, Wiedey M, Neef K, Krausgrill B, Ladage D, Fatima A, Saric T, Hescheler J, Müller-Ehmsen J: Electrophysiological integration and action potential properties of transplanted cardiomyocytes derived from induced pluripotent stem cells. *Cardiovascular research* 2013:1–9.
135. Ross DD, Joneckis CC, Ordóñez J V, Sisk AM, Wu RK, Hamburger AW Nora RE, Nora RE: Estimation of cell survival by flow cytometric quantification of fluorescein diacetate/propidium iodide viable cell number. *Cancer research* 1989, 49:3776–3782.
136. Kuzmenkin A, Liang H, Xu G, Pfannkuche K, Eichhorn H, Fatima A, Luo H, Saric T, Wernig M, Jaenisch R, Hescheler J: Functional characterization of cardiomyocytes derived from murine induced pluripotent stem cells in vitro. *FASEB journal* 2009, 23:4168–80.
137. R L Williams, D J Hilton, S Pease, T A Willson, C L Stewart, D P Gearing, E F Wagner, D Metcalf, N A Nicola NMG: Myeloid leukaemia inhibitory factor maintains the developmental potential of embryonic stem cells. *Nature* 1988, 336:684–87.
138. Zhang AJP and L: Hypoxia and Fetal Heart Development. *Current Molecular Medicine* 2011, 10:653–666.
139. Geuss LR, Suggs LJ: Making cardiomyocytes: How mechanical stimulation can influence differentiation of pluripotent stem cells. *Biotechnology progress* 2013, In press.
140. Wan C, Chung S, Kamm RD: Differentiation of embryonic stem cells into cardiomyocytes in a compliant microfluidic system. *Annals of biomedical engineering* 2011, 39:1840–7.
141. Chisti Y: Animal-cell damage in sparged bioreactors. *Trends in biotechnology* 2000, 18:420–32.

142. Wu J: Mechanisms of animal cell damage associated with gas bubbles and cell protection by medium additives. *Journal of biotechnology* 1995, 43:81–94.
143. Gupta V, Grande-Allen KJ: Effects of static and cyclic loading in regulating extracellular matrix synthesis by cardiovascular cells. *Cardiovascular research* 2006, 72:375–83.
144. Somerville RPT, Devillier L, Parkhurst MR, Rosenberg S a, Dudley ME: Clinical scale rapid expansion of lymphocytes for adoptive cell transfer therapy in the WAVE® bioreactor. *Journal of translational medicine* 2012, 10:69.
145. Clincke M-F, Mölleryd C, Zhang Y, Lindskog E, Walsh K, Chotteau V: Study of a recombinant CHO cell line producing a monoclonal antibody by ATF or TFF external filter perfusion in a WAVE Bioreactor™. *BMC proceedings* 2011, 5(Suppl 8):P105.
146. Boheler KR, Joodi RN, Qiao H, Juhasz O, Urick AL, Chuppa SL, Gundry RL, Wersto RP, Zhou R: Embryonic stem cell-derived cardiomyocyte heterogeneity and the isolation of immature and committed cells for cardiac remodeling and regeneration. *Stem cells international* 2011, 2011:1–10.
147. Manuscript A, Embryonic H, Exhibit C, Rate B: Human Embryonic and Induced Pluripotent Stem Cell-Derived Cardiomyocytes Exhibit Beat Rate Variability and Power-Law Behavior. *Circulation* 2012, 125:883–893.
148. Billman E: Effect of carbachol and cyclic to ventricular GMP on susceptibility fibrillation. *Faseb* 1990, 4:1668–73.
149. Malpique R, Ehrhart F, Katsen-Globa A, Zimmermann H, Alves PM: Cryopreservation of adherent cells: strategies to improve cell viability and function after thawing. *Tissue engineering Part C* 2009, 15:373–86.
150. Kim YY, Ku S-Y, Liu H-C, Cho H-J, Oh SK, Moon SY, Choi YM: Cryopreservation of human embryonic stem cells derived-cardiomyocytes induced by BMP2 in serum-free condition. *Reproductive sciences* 2011, 18:252–60.
151. Xu C, Police S, Hassanipour M, Li Y, Chen Y, Priest C, Sullivan CO, Laflamme MA, Zhu W, Biber V, Hegerova L, Yang J, Delavan-boorsma K, Davies A, Lebkowski J, Gold JD, Corporation G, Drive C, Park M: Efficient generation and cryopreservation of cardiomyocytes derived from human embryonic stem cells. *Regenerative Medicine* 2011, 6:53–66.
152. Li X, Meng G, Krawetz R, Liu S, Rancourt DE: The ROCK inhibitor Y-27632 enhances the survival rate of human embryonic stem cells following cryopreservation. *Stem cells and development* 2008, 17:1079–1085.
153. Egami M, Haraguchi Y, Shimizu T, Yamato M, Okano T: Latest status of the clinical and industrial applications of cell sheet engineering and regenerative medicine. *Archives of pharmacal research* 2013.
154. Baust JM, Van Buskirk, Baust JG: Cell viability improves following inhibition of cryopreservation-induced apoptosis. *In vitro cellular developmental biology Animal* 2000, 36:262–270.
155. Baust JM, Van Buskirk R, Baust JG: Modulation of the cryopreservation cap: elevated survival with reduced dimethyl sulfoxide concentration. *Cryobiology* 2002, 45:97–108.
156. Lovelock JE: The mechanism of the protective action of glycerol against haemolysis by freezing and thawing. *Biochim Biophys Acta* 1953, 11:28–36.
157. Pegg DE: The current status of tissue cryopreservation. *Cryo Letters* 2001, 22:105–114.



158. Karlsson JO, Toner M: Long-term storage of tissues by cryopreservation: critical issues. *Biomaterials* 1996, 17:243–256.
159. Li Y, Ma T: Bioprocessing of cryopreservation for large-scale banking of human pluripotent stem cells. *BioResearch open access* 2012, 1:205–14.
160. Grossmann J: Molecular mechanisms of “detachment-induced apoptosis - Anoikis.” *Apoptosis* 2002, 7:247–260.
161. Acker JP, Larese A, Yang H, Petrenko A, McGann LE: Intracellular ice formation is affected by cell interactions. *Cryobiology* 1999, 38:363–371.
162. Yang, H., Xia, X.M., Ebertz, S.L., and McGann LE: Cell junctions are targets for freezing injury. *Cryobiology* 1996, 33:672.
163. Acker JP, Elliott JA, McGann LE: Intercellular ice propagation: experimental evidence for ice growth through membrane pores. *Biophysical Journal* 2001, 81:1389–1397.
164. Mollamohammadi S, Taei A, Pakzad M, Totonchi M, Seifinejad A, Masoudi N, Baharvand H: A simple and efficient cryopreservation method for feeder-free dissociated human induced pluripotent stem cells and human embryonic stem cells. *Human reproduction Oxford England* 2009, 24:2468–2476.
165. Malpique R, Osório LM, Ferreira DS, Ehrhart F, Brito C, Zimmermann H, Alves PM: Alginate encapsulation as a novel strategy for the cryopreservation of neurospheres. *Tissue engineering Part C* 2010, 16:965–77.
166. Buskirk RG Van, Baust JM, Snyder KK, Mathew AJ, Baust JG: Successful Short- and Long-Term Preservation of Cells and Tissues. *BioProcess International* 2004, November:42–49.
167. Baust, J.M., Baust, J.G., and van Buskirk R: Cryopreservation outcome is enhanced by intracellular-type medium and inhibition of apoptosis. *Cryobiology* 1998, 37:410.
168. Ginis I, Ph D, Grinblat B, Shirvan MH: Evaluation of Bone Marrow-Derived Mesenchymal Stem Cells After Cryopreservation and Hypothermic Storage in Clinically Safe Medium. *Tissue engineering Part C* 2012, 18:453–463.
169. Kristi K. Snyder, John M. Baust, Robert G. Van Buskirk and JGB: Enhanced Hypothermic Storage of Neonatal Cardiomyocytes. *Cell Preservation Technology* 2005, 3:61–74.
170. Sartipy P, Björquist P: Concise review: Human pluripotent stem cell-based models for cardiac and hepatic toxicity assessment. *Stem cells* 2011, 29:744–8.
171. Du Y, Lou H: Catechin and proanthocyanidin B4 from grape seeds prevent doxorubicin-induced toxicity in cardiomyocytes. *European Journal of Pharmacology* 2008, 591:96–101.
172. Zordoky BNM, El-Kadi AOS: H9c2 cell line is a valuable in vitro model to study the drug metabolizing enzymes in the heart. *Journal of pharmacological and toxicological methods* 2007, 56:317–22.
173. Davidson MM, Nesti C, Palenzuela L, Walker WF, Hernandez E, Protas L, Hirano M, Isaac ND: Novel cell lines derived from adult human ventricular cardiomyocytes. *Journal of molecular and cellular cardiology* 2005, 39:133–147.
174. Zhang Y, Nuglozeh E, Touré F, Schmidt AM, Vunjak-Novakovic G: Controllable expansion of primary cardiomyocytes by reversible immortalization. *Human gene therapy* 2009, 20:1687–1696.



## 7. Annexes

### Annex 1 - Supplementary table: RT-PCR primers

**Table 7.1:** List of primers used for semiquantitative and quantitative RT-PCR analysis.

Marker	For/Rev	Sequence 5'-3'	Product length
<i>GAPDH</i>	for	ACCTTGCCACAGCCTTG	142
	rev	GGCTCATGACCACAGTCCAT	
<i>CTNT</i>	for	GGTGCCACCCAAGATCCCCG	199
	rev	AATACGCTGCTGCTCGGCC	
<i>NKX2.5</i>	for	CAGCCAAAGACCCTCGGGCG	142
	rev	TGCGCCTGCGAGAAGAGCAC	
<i>HCN4</i>	For	TGCTGTGCATTGGGTATGGA	337
	rev	TTTCGGCAGTTAAAGTTGATG	
<i>MYL2</i>	for	TGCCAAGAAGCGGATAGA	328
	rev	CAGTGACCCTTTGCCCTC	
<i>MYL7</i>	for	AGTAGGAAGGCTGGGACCCG	306
	rev	CTCGGGGTCCGTCCCATTGA	
<i>T-BRACHYURY</i>	for	CTGCGTTCAAGGAGCTAAC	91
	rev	CCAGGCCTGACACATTTACC	
<i>AFP</i>	for	CCCACTTCCAGCACTGCCTGC	374
	rev	GGCTGCAGCAGCCTGAGAGT	
<i>OCT-4</i>	for	CATGTGTAAGCTGCGGCC	268
	rev	GCCCTTCTGGCGCCGGTTAC	

## Annex 2 – Adverse effect of different bioreactor designs

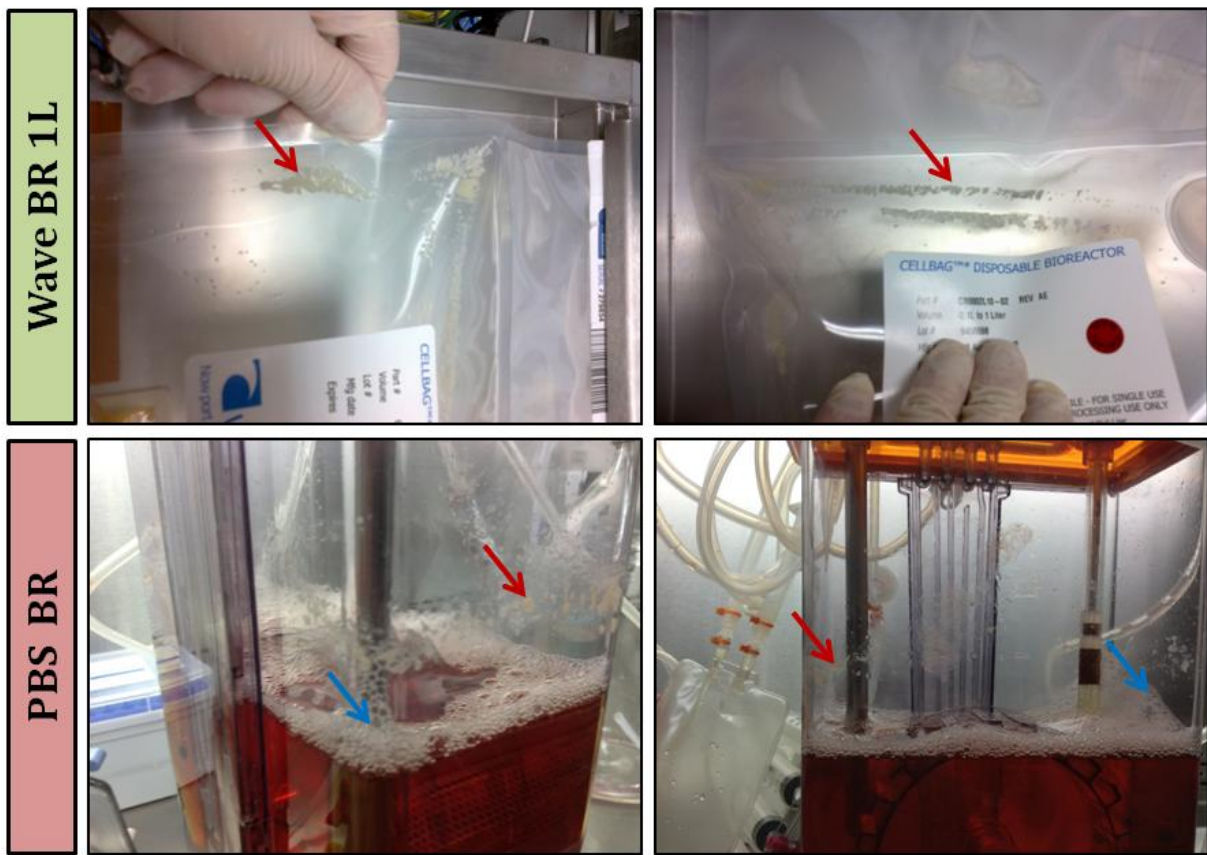


**Figure 7.1: Bioreactor design adverse effects of miPSC aggregate culture. A)** Cell/aggregate deposition occurred on the sides of the Cellbag™ during miPSC culture in the Wave BR. Red arrows indicate cell deposition sites. **B)** Cell/aggregate deposition and excessive foam formation occurred during miPSC culture in the PBS BR. Red arrows indicate cell deposition sites. Blue arrows indicate excessive foam formation.